Real-Time Analysis of an Active Distribution Network - Coordinated Frequency Control for Islanding Operation

Cha, Seung-Tae; Østergaard, Jacob; Wu, Qiuwei

Publication date:
2012

Document Version
Publisher's PDF, also known as Version of record

Technical University of Denmark

Seung Tae Cha

Real-Time Analysis of an Active Distribution Network

- Coordinated Frequency Control for Islanding Operation

PhD Thesis, July 2012

DTU Electrical Engineering
Department of Electrical Engineering

Seung Tae Cha

Real-Time Analysis of an Active Distribution Network

- Coordinated Frequency Control for Islanding Operation

PhD Thesis, July 2012

Real-Time Analysis of an Active Distribution Network – Coordinated Frequency Control for Islanding Operation

Author(s):
Seung Tae Cha

Supervisor(s):
Professor, Jacob Østergaard, Technical University of Denmark
Assistant Professor, Qiuwei Wu, Technical University of Denmark

Department of Electrical Engineering
Centre for Electric Power and Energy (CEE)
Technical University of Denmark
Elektrovej 325
DK-2800 Kgs. Lyngby
Denmark

www.elektro.dtu.dk/cee
Tel: (+45) 45 25 35 00
Fax: (+45) 45 88 61 11
E-mail: cet@elektro.dtu.dk

Release date:	July 2012
Class:	public
Edition:	2
Comments:	A dissertation submitted in partial fulfillment of the requirements for the degree of Doctor of Philosophy at Technical University of Denmark.

Abstract

The increasing penetration of distributed generation (DG) and distributed energy resources (DERs), and the consequential requirement to accommodate and integrate them within distribution networks brings both challenges and opportunities to the distribution system operator (DSO). This will enable and require a transition from today's passive distribution networks to future active distribution networks (ADNs) which utilizes advanced operation and control strategies in order to improve power supply reliability, and realize the potential of DG to provide system support.

The presence of DERs within distribution networks makes it possible to operate the distribution networks independently which is called islanding operation. However, it is a challenge to ensure secure and reliable operation of the islanded system due to a number of reasons, e.g. low inertia in the islanded system, intermittency of some of the DERs, etc. Particularly during islanding operation, with relatively few DG units, the frequency and voltage control of the islanded system is not straightforward. DG units, specially based on renewable energy sources (RESs), i.e. wind and solar, have an intermittent nature and intrinsic characteristics, they can't ensure the constant power supply required by loads. Furthermore, the DG units with relatively slow response have insufficient dynamic performance in terms of load following.

In order to meet the challenges, coordinated control strategies are needed to ensure smooth transition to the islanding operation and reliable operation of the islanded system. The goal of this Ph.D project is to develop effective frequency control strategies for the islanding operation of ADNs. The developed control strategies are comprised of a primary frequency control scenario with a battery energy storage system (BESS) and two secondary frequency control scenarios with BESS and DG units. During the islanding transition, the frequency is regulated by the fast-acting primary control of the BESS. The secondary control of the main management system (MMS) detects the status of the BESS and tries to return the power output of the BESS to reference value by assigning the total power difference to the dispatchable DG units. Hence, the dispatchable DG units can be coordinated to share the load following burden of the BESS.

To that end, firstly, a reliable real-time model of the Bornholm distribution system is constructed using the real-time digital simulator (RTDS). The resulting model is capable

of performing dynamic simulations of the islanded Bornholm distribution system to investigate the frequency regulation performance. In addition, a generic model of Bornholm distribution system is constructed, which can be used as a benchmark model for smart grid testing purposes. In both cases, the simulation results are compared and provided a desirable performance with very high degree of accuracy.

Secondly, the simplified battery model is adopted and has been modeled in the RTDS in order to investigate the role of the BESS as a primary frequency regulator during islanding transition. The effectiveness of proposed primary frequency control strategy is illustrated by using two test cases (i.e. IEEE 9-bus and Bornholm). In both cases, the frequency regulation performance is highly improved without degrading the proposed control performance.

Thirdly, a new fuzzy logic based secondary frequency control strategy between a BESS and dispatchable DG units is proposed for further improving the system frequency performance as well as reducing output power fluctuations. The simulation results show that the frequency regulation performance is highly improved with fuzzy logic control (FLC) when the system enters into islanding operation.

Lastly, an intelligent multi-agent based secondary frequency control strategy for the islanding operation of ADN is proposed. A complete software-in-the-loop (SIL) simulation is carried out and optimization of the parameters of the secondary controller is achieved in a simple manner through the effective application of particle swarm optimization (PSO) technique. Simulation results show that the proposed multi-agent based secondary frequency control strategy performs well, in comparison to the performance of proportional integral (PI) control design.

Resumé

Den stigende udbredelse af decentral produktion (GD) og distribuerede energiressourcer (DER), og det deraf følgende krav om at facilitere og integrere dem i distributionsnettet medfører både udfordringer og muligheder for distributionssystemoperatøren. Dette vil både kræve og muligøre en overgang fra dagens passive distributionsnet til et fremtidigt aktivt distributionsnet (ADN), der udnytter avancerede drift og kontrolstrategier for at forbedre forsyningenspålideligheden, og samtidig udnytte DGs potentiale i forhold til systemydelser.

Tilstedeværelsen af DER-enheder i distributionsnettet gør det muligt at drive dele af nettet i såkalt ødrift. Det er imidlertid en udfordring at opretholde en sikker og pålidelig forsyning under ødrift af en række årsager, for eksempel på grund af lav inerti og stokastisk adfærd for visse energiressourcer. Især under ødrift med forholdsvis få distribuerede energiressourcer, kan frekvensen og spændingsregulering være problematisk. DER-enheder baseret på vedvarende energikilder, som vindkraft og solenergi, har egenskaber som gør at de ikke altid vil kunne imødekomme den konstante strømforsyning krævet af et lokalt forbrug. Endvidere har DER-enheder med en længere reaktionstid ikke de dynamiske kvaliteter som kræves af et fluktuerende forbrug.

For at imødegå de udfordringer, er det nødvendigt at benytte koordinerende styringsstrategier for at sikre en gnidningsløs overgang til, og drift af, et distributionssytem i ødrift. Dette Ph.D.-projekt har til formål at udvikle effektive frekvensstyringsstrategier for ødrift af aktive distributionsnet. De udviklede kontrolstrategier består af et primært frekvenskontrol scenarie med et batteri energilager system (BESS) og to sekundære frekvensstyrede scenarier med BESS og DER-enheder. Under overgangen til ødrift bruges BESS-enheder til hurtig primær frekvensregulering. Den sekundære kontrol udføres ved at det primære control system (MMS) registrerer status for BESS-enhederne og forsøger at returnere udgangseffekten af BESS-enhederne til en reference-værdi ved at kompensere for den total effekt-difference ved hjælp af de kontrolerbare GD-enheder. Herved kan de kontrolerbare GD-enheder koordineres således at de hjælper BESS-enhederne med at følge det lokale forbrug.

Som et første trin for at opnå dette, er det nødvendigt at konstruere en pålidelig realtidsmodel af det bornholmske distributionssystem ved anvendelse af en ”real-time digital simulator” (RTDS). Den resulterende model kan bruges til en dynamiske simulering af det bornholmske distributionsnet under ødrift for at evaluere frekvensreguleringens anvendelighed. Desuden er en generisk model af Bornholm distributionssystem konstrueret, som kan bruges som reference-model. Simuleringsresultater for begge modeller er sammenholdt og har givet et tilfredstillende resultat ifht ydelse og precision.

Det næste trin er at adoptere en simpel batterimodel som modelleret via RTDS'en for at undersøge BESS'ernes evne til at yde primære frekvensregulering under overgangen til ødrift. Effektiviteten af den foreslåede primære frekvenskontrol strategi er illustreret ved hjælp af to test scenarier (IEEE 9-bus og Bornholm). I begge tilfælde er frekvensreguleringens ydeevne stærkt forbedret uden at forringe ydelsen af den foreslåede kontrol.

Et tredje trin er udviklingen af en ny "fuzzy logic"-baseret sekundær frekvens kontrolstrategi mellem en BESS og kontrolerbare GD-enheder for yderligere at forbedre systemets styring af frekvens samt for at reducere udsving i udgangseffekten. Simuleringsresultaterne viser, at frekvensreguleringen er stærkt forbedret med "fuzzy logic" styring (FLC), når systemet overgår til ødrift.

Endelig beskrives en intelligent multi-agent baseret sekundær frekvens kontrolstrategi for ødrift af ADN. En komplet "software-in-the-loop" (SIL) simulering udføres og optimering af parametrene for den sekundære kontrol opnås ved en enkel, effektiv anvendelse af " particle swarm optimization" (PSO). Simuleringsresultaterne viser at den foreslåede multi-agent baserede sekundære frekvenskontrol strategi klarer sig godt i sammenligning med proportional integral (PI) kontrol designet.

Acknowledgement

First of all, I am thankful to my principal supervisor Prof. Jacob Østergaard for his invaluable guidance, dedication, support, enlightening instruction and encouragement during the course of my Ph.D work at Technical University of Denmark. I am also grateful for the opportunities that he provided for me to pursue Ph.D and work at Center for Electric Power and Energy (CEE) from the beginning. It would not have been possible to complete the dissertation without his continuous and generous support throughout the project. I would also like to express my sincere appreciation to my co-supervisor Assistant Prof. Qiuwei Wu for many fruitful and detailed discussions, and his insightful comments and suggestions. Financial supports from DTU, EnerginetDK and Energy Technology Development and Demonstration Program (EUDP) under project #55622 is gratefully acknowledged. The valuable comments and feedbacks from Energinet and EUDP staff are specially appreciated.

Equally, I must thank my previous colleague, Arshad Saleem at KTH, for his assistance and technical support in Java programming guidance to this work. In addition, I would like to extend my sincere thanks to Haoran Zhao for his guidance and support on the design of FLC and all of CEE scientific colleagues for the friendly, helpful and enlightening atmosphere, which makes the research work enjoyable.

I am also indebted to Associate Prof. Arne Hejde Nielsen and Dr. Ranjan Sharma at Siemens Wind Power for their assistance in assembling the power hardware-in-the-loop (PHIL) laboratory set-up and guidance on the testing procedures of the PHIL. I always enjoyed our discussions regarding PHIL testing. Also, special thanks to Peter, Sally for Danish translation, Louise for admin support and Philip for proof-reading the thesis.

During my external stay to RTI, Winnipeg, Canada, Dr. Ming and Dr. Yuefeung shared with me their knowledge and experiences of the research perspective of dynamic equivalencing and provided many useful references. Moreover, I had the pleasure of meeting many enthusiastic staff at RTI.

Finally, I cherish the friendships and the impressive time that accompanied my study and a daily life here. I thank my beloved family for their endless support, encouragement and enduring love.

Table of Content

Abbreviations

ABB : ASEA Brown Boveri
ADN : Active Distribution Network
AGC : Automatic Generation Control
AMI : Advance Meter Infrastructure
AVR : Automatic Voltage Regulator
BESS : Battery Energy Storage System
BRP : Balance Responsible Party
CBRP : Consumption Balance Responsible Party
CEE : Center for Electric Power and Energy
CHP : Combined Heat and Power
CVS : Controlled Voltage Source
DER : Distributed Energy Resource
DF : Directory Facilitator
DFIG : Doubly Fed Induction Generator
DG : Distributed Generation
DNP : Distributed Network Protocol
DSO : Distribution System Operator
EDISON : Electric Vehicle in a Distributed and Integrated market using Sustainable energy and Open Networks
EMS : Energy Management System
EMT : Electro Magnetic Transient
ENTSO-E : European Network of Transmission System Operator for Electricity
EPS : Electric Power System
ESS : Energy Storage System
EUDP : Energy Technology Development and Demonstration Project
FDNE : Frequency Domain Network Equivalent
FIPA : Foundation for Intelligent Physical Agents
FLC : Fuzzy Logic Control
GPC : Giga Processor Card
GTNET : Giga Transceiver Network Communication Card
GUI : Graphic User Interface
HIL : Hardware-in-the-Loop
HMI : Human Machine Interface
HVDC : High Voltage Direct Current
ICL : Intelligent Control Laboratory

ICT : Information & Communication Technology
IEA : International Energy Association
ISR : Islanding Security Region
JADE : Java Agent Development Framework
LAN : Local Area Network
LFC : Load Frequency Control
MAS : Multi Agent System
MMS : Main Management System
MPPT : Maximum Power Point Tracking
MVD : Multi Video Display
NERC : North American Electric Reliability Corporation
OLTC : On Load Tap Changer
OPC : OLE for Process Control
PBRP : Production Balance Responsible Party
PCC : Point of Common Coupling
PF : DigSILENT Power Factory
PHIL : Power Hardware-in-the-Loop
PI : Proportional Integral
PSO : Particle Swarm Optimization
PSS/E : Power System Simulator for Engineering
PV : Photovoltaic
RES : Renewable Energy Source
RISC : Reduced Instruction Set Computing
RMS : Root Mean Square
RSCAD : Real time Simulation Computer Aided Design
RTDS : Real Time Digital Simulator
RTU : Remote Terminal Unit
SCADA : Supervisory Control and Data Acquisition
SIL : Software-in-the-Loop
SOC : State of Charge
TSO : Transmission System Operator
UCTE : Union for the Coordination for Transmission of Electricity
UFLS : Under Frequency Load Shedding
WPP : Wind Power Plant
VSC : Voltage Source Converter
VSI : Voltage Source Inverter

List of Figures

List of Tables

1 Introduction

This chapter presents the background & motivation of the Ph.D project and the associated challenges that the current Danish power system is encountering, followed by a statement of problem and the main research objectives. In the last part, the thesis structure is presented and a list of publications is also included.

1.1 Background and Motivation

Climate change and new environmental concerns are tremendously influencing and reshaping the future power systems around the world. In the past years, this has certainly led to a remarkable and rapid increase in penetration of DG in ADNs [1] - [5]. Many studies contain analysis of the various technologies from leading experts and countries actively promoting DG [6] - [13]. Various benefits of these small to medium size onsite generation (i.e. close to load) has spurred a lot of renewed interests. The current signs show that there is no slowing down. This trend will have the potential to play a much larger role and will likely continue in the future. The described paradigm is also true for many countries. In this context, many countries have set their national policies and long term targets for the promotion of utilizing DG. One of the main drivers is the strong motivation by the government's continuing policy commitments to harness cleaner and greener power on a large scale deployment [14]. Some analysts have reported that DG unit market, specially based on RES, will experience strong growth over the next several years, with total system revenues increasing from $50.8 billion in 2009 to $154.7 billion by 2015. During this period, the annual RES capacity may increase from 5.9 GW in 2009 to 15.1 GW in 2015 [15]. However, the increase in popularity of DG is not only due to the environmental concerns (i.e. less effects), but also due to the various other benefits that DG can bring.

DG has a relative low capital cost. The smaller size of DG requires less installation time. Therefore, it can avoid transmission and distribution systems upgrade (i.e. deferral of system expenditures) by locating power where it is most needed. According to the International Energy Agency (IEA), on-site production could result in cost savings in transmission and distribution of 30% of the electricity costs [16]. DG can be used to supply some loads at peak periods when the electricity price is high. This may reduce the electricity costs for the customers. DG can reduce losses in the distribution system as well as in the transmission system [17]. The central generating companies can reduce load on their transmission equipment, provide local voltage support and increase economical benefits. Government may use DG to introduce competition in the electricity

supply market and thus create reduction in price [18]. Furthermore, DG may reduce the wholesale power price by supplying power to the grid, which leads to reduction of demand required. DG can yield a greater amount of flexibility, the security of power supply and improved performance [19]. All these benefits are making DG more attractive and economically viable. This will enable and require a transition from today's passive distribution networks to future ADNs which utilizes advanced operation and control strategies in order to improve power supply reliability, and realize the potential of DG to provide system support.

Moreover, with this significant DG penetration, islanding operation is an opportunity and might be a technically viable solution and/or it can be desirable to permit such an operation in order to improve power supply reliability and to maintain the security of power supply in future ADNs. Islanding operation can also be economically beneficial when properly addressed [20]. The current practice of disconnecting or shut down DG units after 'islanding' will no longer be a practical or reliable solution in the future. There are more benefits apart from improving system reliability. What islanding operation can bring to DG owners are the additional revenues from selling their energy. At the present time without the possibility of islanding operation, the additional revenue that a generator can receive from islanding operation will be small due to the fact that the DSOs are only allowed to keep a section of network separated from the main supply for a specified time. Operating the DG in islanding operation improves the overall reliability of power supply to customers. The DSO may gain additional revenue due to the improvement in the quality of power supply [21]. Also, the contribution of the DG to the reliability of power supply can reduce or delay the need to reinforce the network to comply with the statutory reliability standards, hence reducing the capital expenditure requirements. The main benefit that the islanding operation can provide to customers is the reduction in the frequency and particularly the duration of power interruption (i.e. decrease outage cost) caused by the disconnection of a section of the islanded system from the main supply.

Despite all these advantages, utilities and existing standards currently do not or at least reluctantly allow the islanding operation of distribution systems. Almost all utilities and DSOs require DG to shut down once a distribution system is islanded. IEEE 1547.4-2011 standard requires islanding to be detected and DG be disconnected at most within 2s [22]. Similarly, IEC 61727 also require islanding detection and DG disconnection at most within 2 s [23]. The Danish grid code requires that islanding operation of power plants up to 25 MW should be avoided [24]. DSOs still consider DG units as additional complexities in the network, and hence, the current operation of practices discourages the islanding operation for mainly safety and security reasons. For examples, safety rules say that all DG units should be disconnected in order to clear a fault during islanding operation. Line worker's safety can be threatened by DG units feeding an islanded system [25]. On the other hand, security aspect requires continuation of DG units operation as long as possible. However, the existing protection system may not be sufficient

enough to allow satisfactory operation. If this fault is not cleared fast enough, not only the loads but also some generating units might be lost. Most importantly, DG may not be able to maintain the voltage and frequency within permissible limits in distribution system when it is islanded [26]. Many technical issues (i.e state detection, voltage and frequency control, load control and protection, restoration strategy, etc) have to be considered and resolved before islanding operation can be realized. One of the major issues is maintaining frequency of islanded system within the power quality limit.

Several reports presenting various control methods on frequency regulation, automatic generation control (AGC) issues, and the use of intelligent control schemes that enable efficient control and management for islanding operation of ADNs have been published [27] - [31]. The approach is to implement a hierarchical control system capable of dealing with large numbers of DG units to cope with tasks related to coordinated frequency control. A hierarchical frequency control scheme for islanded microgrid operation is addressed in [28]. In [30], the Danish transmission system operator (TSO) has undertaken a project which utilizes the integrated DG units to support the islanding operation. It also provides the flexibility to the system operator to island the distribution systems with DG units capable of maintaining the power supply, in order to alleviate the system pressure caused by disturbances in the upstream grid. The islanding security region (ISR) concept to facilitate the islanding process by comparing the system state with the ISR has been reported in the literature [32]. Thus, the system operator can immediately assess if it is suitable to conduct islanding operation at one specific moment, so the security of power supply can be maintained and reliability can be improved. Hence, the customer satisfaction can be met. There have been different studies demonstrations and practice about islanding operation in the world. Among others, the microgrid concept has developed the strategies for islanding operation [33] - [36], and the Canadian utilities have experienced planned island operation in practice [37] - [38]. The capability of a real MV distribution system with medium scale DERs to sustain operation during and after pre-planned islanding manoeuvres is discussed [39]. In [40], discusses some of the key aspects for the design of islanding operation in a distribution network. An IEEE standard 1547.4 for islanding guide is also released [22]. Particularly, the DG units combined with BESS could have the potential to provide increased flexibility in islanded systems as they can react immediately to fluctuations in frequency through intelligent control scheme [41] - [47]. BESS is among the most efficient and compatible technologies because of its fast response time and large capacity such that the power can be uninterruptedly supplied to the load variations if disconnected from the main utility grid. BESS enables smoothing of fluctuations for wind and solar generation units. The system provides a mechanism to store intermittent energy generation, which provides consistent power to the grid. Quick-response characteristic alleviates rapid shifts in renewable energy generation and can therefore act as a frequency regulator. Recently, it is mainly used to improve system frequency performance with large renewable energy penetration. The complex context of the future distribution system motivates the re-

search and calls for defining the boundaries of the thesis scope. With adequate DG units available, how to utilize them for maintaining the security of the distribution system under emergencies has been of great interest for further exploration and study of the islanding operation. Hence, the Ph.D project is motivated towards developing effective frequency control strategies for the islanding operation of ADNs. The effective coordinated frequency control strategies are needed to ensure smooth transition to the islanding operation and reliable operation of the islanded system. The role of BESS as a provider of active power balancing reserve and its coordinated control with DG units have been analysed. Following is a **Table 1-1** showing the definitions of some key terms used throughout the thesis.

Table 1-1 : Definitions of some key terms used

Terms	Definition
Active Distribution Network (ADN)	Active distribution networks are capable of handling bi-directional power and information flows based on the latest automation, information and communication technologies, as well as on corresponding metering services. Distribution systems without any DG units are passive since the electrical power is supplied by the national grid system to the customers embedded in the distribution networks. It becomes active when DG units are added to the distribution system leading to bi-directional power flows in the networks.
Automatic Generation Control (AGC, also known as Load Frequency Control, LFC)	Automatic generation control (AGC) is a system for adjusting the power output of multiple generators at different power plants, in response to changes in the load. Since a power grid requires that generation and load closely balance, frequent adjustments to the output of generators are necessary. This function is also commonly referred to as load-frequency control (LFC)
Distributed Energy Resources (DERs)	DER comprises distributed generation, the storage of electrical and thermal energy and/or flexible loads. DER units are operated either independently of the grid or connected to the low or medium voltage distribution level of the main network. They are located close to the point of consumption, irrespective of the technology, but are smaller than 10 MWe of electrical power
Distributed Generation (DG)	DG is defined as an electrical generation unit connected to the distribution system, at or close to the poinit of consumption. It includes all types of generation technologies based on fossil fuels and RES.
Islanding Operation	Islanding operation is the generic term used to describe a scenario or a condition, where a section of a transmission or distribution network, which contains DGs, is separated from the main transmission or distribution network due to a fault upstream or any other disturbances. Subsequent to this separation, the DG continues (or is started) to power the loads trapped within the island.
Microgrids	Microgrids are just miniature versions of the larger utility grid, except for one defining feature: when necessary, they can disconnect from the main grid and can continue to operate in what is known as “islanding operation.” Because of this distinguishing feature, microgrids can offer a higher degree of reliability.
Renewable Energy Sources (RESs)	RES means renewable energy sources such as wind, solar, geothermal heat, wave, hydro, ocean energy, biomass, biogases and landfill gas, etc. They are generally not subject to depletion. They are virtually inexhaustible in duration but limited in the amount of energy that is available per unit of time.

In the following subsections, a brief introduction of the Danish power system is given to discuss; its typical characteristics, and future perspectives. Moreover, a statement of the problem is included and the main research objectives are briefly described.

1.2 Danish Power System and Future Perspectives

The Danish power system is electrically divided into two parts, Eastern and Western. Each of these regions belongs to different synchronous systems. The Western Danish system (DK1) belongs to the continental European system, Union for the Coordination of Electricity Transmission (also known as synchronous grid of Continental Europe, previously UCTE grid, now part of European Network of Transmission System Operators for Electricity, ENTSO-E) system, while the Eastern Danish system (DK2) belongs to the Nordic (previously Nordel grid) synchronous system. The Great Belt high voltage direct current (HVDC) link (Storebælt), an interconnection between these two areas was commissioned in July 2010 and started its commercial operation in August 2010. The 400 kV overhead lines with a power rating of 600 MW HVDC link has allowed access to reserves from other parts of the country, thereby increasing the security of power supply in Denmark and reducing operating costs for the whole Danish power supply. In the Eastern Danish (Zealand) system, the 132 kV transmission grids consist of ring connections, while the 400 kV grids are characterized by a radial structure. It is connected to Sweden via two 400 kV and two 132 kV ac lines (1700 MW import and 1300 MW export) and through a 400 kV HVDC connection to Germany, Kontek (transmission capacity of 600 MW). In the Western Danish (Jutland and Fyn) system, the 400 kV grids is a combination of ring connections and a radial structure. The 150 kV grids is a parallel grid which also plays a role in connection with the international transmission capacity. To the south, the Western Danish system is connected to the ENTSO-E system via two 400 kV (Kassø), two 220 kV (Kassø and Ensted) and one 150 kV (Ensted) ac lines to Germany (1500 MW import and 950 MW export, based on thermal, nuclear, and fast growing wind power generation). The total transmission capacity is determined by congestion in the surrounding grids and is normally 1500 MW in the southbound direction and approximately 950 MW in the northbound direction. To the north, it is also connected to the Nordic interconnected system via HVDC links to the Nordic neighbors, Skagerrak, Norway (via two 250 kV DC with a total transmission capacity of 540 MW and one 350 kV DC with transmission capacity of 500 MW, hydro-power dominated Norwegian system) and Sweden, KontiSkan (740 MW, hydro-power dominated Swedish system). These strong interconnections with its neighboring countries are one of the important factors that enable the stable and reliable operation of the Danish power system with a high penetration of wind power.

Figure 1-1 shows the map of the transmission system of Denmark. **Table 1-2** shows the main power system capacity figures of Denmark. The coal-fired power plants form the

primary electricity production units (central power plants) in the Eastern part, where the wind power installations contribute to 15 % of the total capacity. In the Western part, the larger power plants are either coal- or gas-based thermal units. More than 53% of the installed power capacities for electricity production units are from the land-based wind turbines and decentralized combined heat and power (CHP) units.
In this context, Bornholm is in the center of attention in most of Europe and some parts of the world due to the current characteristics of the Bornholm distribution system and on-going large demonstration of smartgrid projects related to Bornholm. Bornholm is a small Danish island on the outskirts of Eastern Denmark in the Baltic Sea, which is situated just south of Sweden as shown in **Figure 1-1**.

Figure 1-1 Map of Danish transmission system and Bornholm distribution system in red dotted box at the right corner (EnerginetDK Website)

Table 1-2: Key data for Eastern and Western Denmark

Eastern	(MW)	**Western**	(MW)
Central power plants	3800	Central power plants	3600
Local CHP units	650	Local CHP units	1800
Wind power	584	Wind power	2400
Offshore, Nysted	166	Offshore, Horns Rev	369
Peak load	2700	Peak load	3767
Base load	900	Base load	1400
		Norway interconnection	1040e
Sweden interconnection	1300e	(HVDC link, Skagerrak)	950i
(400 & 132 kV ac lines)	1700i	Sweden interconnection	680e
		(KontiSkan)	740i
Germany interconnection	600	Germany interconnection	950e
(HVDC link, Kontek)			1500i

Since, Bornholm already has a high share of electricity supplied by RESs, particularly wind power. Its system can be highly regarded as a future distribution system and can therefore be chosen as a test case for my Ph.D project. The Bornholm is a distribution system consisting of three voltage levels: 60 kV, 10 kV and 0.4 kV. The peak load in Bornholm is between 55 MW and 63 MW, while the minimum load is between 13 MW and 18 MW. The power generation in Bornholm contains 14 diesel units, 1 steam unit, 1 CHP unit, biomass and a large share of wind turbines exceeding 30% of total energy consumption with an additional 20 MW estimated to be installed in the near future. The wind turbines are situated all over the island and are mainly dominated by onshore wind turbines. This future scenario of increased capacity of wind power will certainly raise serious challenges to the system operation and control. Additional power balancing is required for dealing with the intermittent characteristics of the wind power. Moreover, the Bornholm distribution system (Halse S/S) is connected through a long submarine cable to the Swedish power system (Borrby S/S). The sea cable can be disconnected which gives the opportunity of 'islanding operation' to test in a restricted area with the presence of a very high amount of wind power. During this islanding operation, frequency control of the system becomes fairly difficult. TSO, DSO, utilities, academia and researchers will be faced with control issues and enabling high penetration of wind power into both existing and future distribution systems.

1.3 Problem Statement and Research Objectives

As there have already been great amount of DG units available in the distribution systems, the Danish utilities have been thinking of utilizing them to maintain the power supply to the customers, once a distribution system is islanded from the main utility grid under emergencies. The purpose of this study is to develop efficient frequency control scenarios to facilitate the transition and maintain the islanding operation and test the developed scenarios using the Bornholm distribution system.

Specifically, the main objectives of the work are as follows:

1. To develop effective frequency control strategies for the islanding operation of ADNs. The developed control strategies are comprised of a primary frequency control scenario with a BESS and DG units, and two secondary frequency control scenarios (i.e. fuzzy-logic & multi-agent based control) with a BESS and DG units.

2. To demonstrate and validate the effectiveness of the proposed control strategies through time-domain simulation studies conducted in the RTDS, DigSILENT Power Factory (PF), and MATLAB and JAVA software environments.

1.4 Scopes and Limitations

The scopes and limitations of this work are as follows:

1. Models have been developed in the RTDS and many of the standard models available in the RTDS library have been used.

2. Islanding detection technique and adaptive protection are not discussed.

3. Voltage control is not discussed.

4. Economics related to islanding operation is not considered. However, the control strategy of DG units can be modified to achieve economical operation of the islanded distribution system.

1.5 Outline of the Thesis and Contributions

The thesis is comprised of eight chapters.

Chapter 2, ***Frequency Control and Nordic Interconnected System***, provides an introduction on the general aspects of power system frequency control. Depending on the frequency deviation range, this could be divided into three different kinds of control: primary, secondary, and tertiary. These categories of different ranges of frequency deviation are briefly examined. In addition, emergency control and protection schemes, such as under-frequency load shedding (UFLS) strategies are reviewed and some references on optimal load shedding approaches are given. Moreover, the AGC basic concepts and its mechanism associated with a modern power system, the major functions as part of the energy management system (EMS), and characteristics are briefly described.

Chapter 3, ***Islanding Operation***, gives an overview on 'islanding operation' with the definitions used by different entities. The current utility practices in islanding operation in general are described, and is mainly focused on the definition used by IEEE Standard 1547.4-2011. Some of the new information regarding intentional islands will be highlighted. Danish experience of planned islanding operation is included.

Chapter 4, ***Modeling of Bornholm Distribution System***, gives a complete overview on the Bornholm distribution system. The simulation models, the typical data and the scenarios used are also introduced. A reliable real-time model of the Bornholm distribution system is constructed. The resulting model is capable of performing dynamic simulations of the islanded Bornholm distribution system to investigate the frequency regulation performance. In addition, a generic model of Bornholm distribution system is also constructed, which can be used as a benchmark model for smart grid testing purposes.

In both cases, the simulation results are compared and provided a desirable performance with very high degree of accuracy.

Chapter 5, ***Primary Frequency Control for Islanding Operation of ADNs using BESS***, introduces an effective frequency control strategy for the islanding operation of ADNs. The simplified battery model is adopted and has been modeled in the RTDS in order to investigate the role of the BESS as a primary frequency regulator during islanding operation. However, due to its capacity limitation (i.e. small-sized BESS), the power outputs of the dispatchable DG units should be coordinated to share the load following burden of the BESS and to keep the stored energy level on the BESS within the prespecified level. The effectiveness of proposed coordinated control strategy is illustrated by using two test cases (i.e. IEEE 9-bus and Bornholm). In both cases, the frequency regulation performance is highly improved without degrading the proposed control performance.

Chapter 6, ***Fuzzy-Logic based Secondary Frequency Control***. The concept of control strategy is similar to the previous chapter. However, the BESS will not only be involved in primary frequency control, but also in the secondary frequency control. In this case, a large-sized BESS is assumed. Therefore, the continuous charging and discharging operations are available in both grid-connected and islanding operation. The hierarchical control structure has two levels: central system and local controller. The new FLC strategy between BESS and dispatchable DG units in the high level of the MMS is proposed for further improving the system frequency performance. The effectiveness of proposed fuzzy-logic based secondary frequency control strategy is illustrated by using a test case (i.e. a typical microgrid). The simulation results show that the frequency regulation performance is highly improved with FLC when the system enters into islanding operation.

Chapter 7, ***Multi-agent based Secondary Frequency Control***. In this chapter, an agent based paradigm is utilized for the development of the control strategy. A multi-agent based secondary frequency control strategy for the islanding operation of ADNs is proposed. In addition, a stochastic algorithm approach, PSO technique is employed to search globally optimal parameters of the secondary controller in the AGC scheme. In particular, the load setting points of governors for DG units will be optimized. Hence, the obtained set points will be used instead of using arbitrary set points used in the previous Chapter 5. The modified IEEE 9-bus system, agent system, and especially its middleware based on the distributed network protocol (DNP) protocol have been used for bi-communication between the RTDS platform and the multi-agent framework. A real-time laboratory experimental setup is constructed in order to investigate the efficiency of the proposed control strategy. The application results show that the proposed multi-agent based secondary frequency control strategy provides a desirable performance, in comparison to PI control design.

Chapter 8, ***Conclusion and Future Work***, concludes the thesis with main findings and presents the future works on how the proposed concepts can be further developed.

The main technical contribution of this Ph.D project is the development of effective frequency control strategies for the islanding operation of ADNs. The models of thermal generator units used in the simulations are those actual plants. Also, the BESS is one of the alternative solutions for power balancing services which could substitute the reduced reserve power available from the central power plants in a future large wind-dominated Bornholm distribution system. The coordinated control strategy is formulated to incorporate the BESS in the presence of other dispatchable DG units in islanding operation. The simulation demonstrated the possible need of planning BESS, and showed that only the small amount of BESS capacity can improve the system frequency quality without degrading the proposed control performance. At the same time, the regulation power requirements from DG units are also greatly reduced with BESS participating in primary frequency control. This could benefit the system operation in deferring the need for capacity additions and costs. Moreover, fuzzy-logic based controller and the multi-agent based PSO controller are developed in the Matlab and JAVA framework environments. Simulation studies have been performed on the test cases to investigate the efficiency and the effectiveness of the proposed control strategies in the event of islanding operation. Coordination control strategy is rather simple, but the control effect is very good.

Furthermore, in addition to provide the proof-of-concept demonstration, the simulation and laboratory setup could also be used for other purposes such as testing different DER control strategies, power management strategy, hardware-in-the-loop (HIL) test of protection scheme, PHIL test of voltage source converter (VSC) HVDC for offshore wind power plants, and protection and control of the campus microgrid, etc. It also presents the possibility to extend such a small-scale demonstration into a large-scale demonstration.

1.6 List of Publications

During the Ph.D project, there are eight conference papers, one journal paper and one book chapter contribution in relation to thesis have been published or submitted, as listed below.

Conferences

[a1] Seung Tae, Cha, Haoran, Z., Qiuwei W., Jacob, Ø., T. Nielsen, Henrik M., "Evaluation of Energy Storage System to Support Danish Island Grid of Bornholm Power Grid," *in proceedings of the 10th IEEE International Power and Energy Conference (IPEC)*, 2012, Ho Chi Minh, Vietnam

[a2] Haoran, Z., Seung Tae, Cha, Qiuwei W., Ioannis M., Poul S., and Jacob, Ø., "Coordinated Control Strategy of Wind Power Plants and Battery Energy Storage System," *in proceedings of the KIEE International Conference on Wind Energy Grid-Adaptive Technologies (WeGAT)* , 2012, Jeju, Korea

[a3] Seung Tae, Cha, Haoran, Z., Qiuwei W., Arshad S., and Jacob, Ø., "Coordination Control Scheme of Battery Energy Storage System (BESS) and Distributed Generations (DGs) for Electric Distribution Grid Operation," *in proceedings of the 38th IEEE Industrial Electronics Society (IECON)*, 2012, Montreal, Canada

[a4] Seung Tae, Cha, Qiuwei W., and Jacob Ø., "A Generic Danish Distribution Grid Model for Smart Grid Technology Testing," *in the proceedings of the 3rd IEEE PES Innovative Smart Grid Technologies (ISGT)*, 2012, Berlin, Germany

[a5] Seung Tae, Cha, Arshad S., Qiuwei W., and Jacob Ø., "Agent based Particle Swarm Optimization for Load Frequency Control of Distribution Grid," *in the proceedings of the 47th IET International Universities' Power Engineering Conference (UPEC)*, 2012, London, UK

[a6] Seung Tae, Cha, I. K. Park, Qiuwei W., and Jacob Ø., "Real Time Hardware-in-the-Loop (HIL) Testing for Digital Controllers," *in the proceedings of the IEEE Asia-Pacific Power and Energy EngineeringPES Innovative Smart Grid Technologies (APPEEC)*, 2012, Shanghai, China

[a7] Seung Tae, Cha, Arshad S., Qiuwei W., and Jacob Ø., "Multi-Agent based Controller for Islanding Operation of Active Distribution Networks with Distributed Generation (DG)," *in the proceedings of the 4th IEEE International Conference on Electric Utility Deregulation, Restructuring and Power Technologies (DRPT)*, 2011, Weihai, China

[a8] Seung Tae, Cha, Jacob, Ø., Qiuwei W., and Francesco M., "A Real Time Simution Platform for Power System Operation," *in proceedings of the 8th IEEE International Power and Energy Conference (IPEC)*, 2010, Singapore

Journals

[j1] Seung Tae, Cha, Haoran Z., Qiuwei W., and Jacob Ø., "Application of Fuzzy Logic Control for Islanding Operation," *International Journal of Energies*, 2012 (in process)

Book Chapter

[b1] Seung Tae, Cha, Qiuwei W., Arshad S., Jacob Ø., and Yi D., "Modeling and Control of Sustainable Power Systems, Towards Smarter and Green Electric

Grids, Green Energy & Technology," ISBN 978-3-642-22903-9, Chapter 3, *Springer*, 2011

Publications [a1] - [a8], journal publications [j1] and book chapter [b1] are the direct contributions of the PhD project. Publications [a1] - [a3] develop a coordinated control scheme of BESS and DG units for distribution system operation. The BESS is designed to stabilize frequency as a primary regulation, while the DG units support the secondary frequency regulation. The proposed strategy can also be applied to large scale applications, which are explained in Chapter 5 and Chapter 6, respectively. Publication [a4] proposes a generic model of Bornholm distribution system, which can replicate the performance of the Bornholm distribution system under both steady state and dynamic conditions. This model and the corresponding result provide good agreement between the RTDS full model and the RTDS generic model, which are explained in Chapter 4. Publications [a2] and journal [j1] proposes a new application of FLC for the islanding operation of ADNs to help stabilize the frequency, which is explained in Chapter 6.

Other publications not listed were supported in part by the IEC 61400 TC 88 under wind turbine working group 27, electrical simulation models for wind power generation, Siemens Wind Power, International Network Program, and also by the electric vehicles in a distributed and integrated market using sustainable energy and open networks (EDISON) project. The Intelligent Control Laboratory (ICL) of PowerLabDK setup made a very well suited platform to carry out proof-of-concept tests using HIL and PHIL testing methods.

Book chapter [b1] examines a wide range of topics related to modeling and control for islanding operation of ADNs. A multi-agent based controller is proposed to utilize different resources in the distribution systems to stabilize the frequency in the event of islanding operation. Different agents are defined to represent different resources in the distribution systems. A test platform with the RTDS, an OLE for Process Control (OPC) protocol server and the multi-agent based intelligent controller is established to test and validate the proposed multi-agent based secondary frequency control strategy.

2 Frequency Control and Nordic Interconnected System

This chapter provides an introduction on the general aspects of power system frequency control. Depending on the frequency deviation range, this could be divided into three different kinds of control: primary, secondary, and tertiary. These categories of different ranges of frequency deviation are briefly examined. In addition, emergency control and protection schemes, such as UFLS strategies are reviewed and some references on optimal load shedding approaches are given. The characteristics of Nordic grid code and its power markets are highlighted as an example. Two different types of frequency controlled reserves, frequency controlled normal operating reserve and disturbance reserve is discussed. Moreover, this chapter presents the fundamentals of AGC, providing structure, definitions, and basic concepts associated with a modern power system. The AGC mechanism in power system, the major functions as part of the EMS, and characteristics are briefly described.

2.1 Frequency Control

The concept of frequency control is briefly discussed. The main cause of frequency deviations in power systems is the imbalance between generation and load. Frequency deviation is a direct result of this imbalance and provides a useful indication. During this period, the operating point of a power system changes. Hence, power systems may experience deviations in system frequency, which may yield undesirable effects and directly affects power system operation. Since the system frequency is proportional to the rotation speed of the generator, the problem of frequency control may be directly translated into a speed control of the turbine generator unit [14], [48] - [50]. Classically, three levels of the frequency deviation range are used to describe the control principle, as shown in **Figure 2-1**. The natural governor response known as the primary control (Δf_1), the secondary control (AGC or LFC, Δf_2), and emergency control (tertiary, Δf_3) may all be required to maintain system frequency. The following subsections summarize the characteristics of each level.

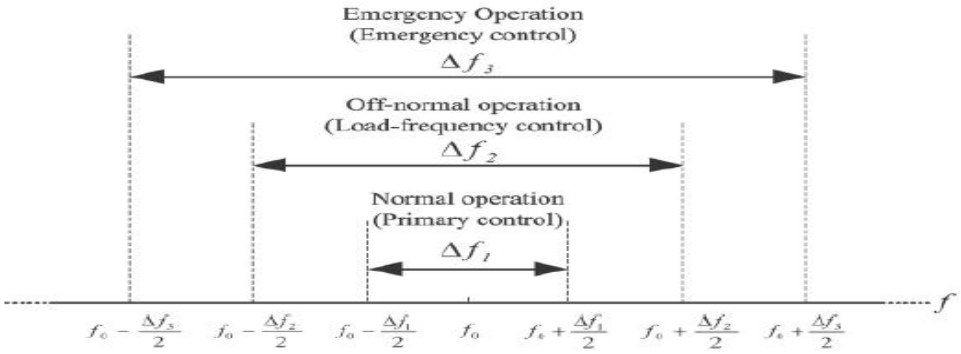

Figure 2-1 : Frequency deviations and associated operation control (H. Bevrani et al. 2011)

2.1.1 Primary Frequency Control

Depending on the type of generation, the real power delivered by a generator is controlled by the mechanical power output of a prime mover. In the case of a steam turbine, mechanical power is controlled by the opening or closing of valves regulating the input of steam into the turbine. Steam input to generators must be continuously regulated to match real power demand. Without this regulation, the machine speed will vary with consequence change in frequency. For satisfactory operation of a power system, the frequency should remain nearly constant [51]. Relatively close control of frequency ensures constancy of speed of generators. A schematic block diagram of a synchronous generator equipped with a primary frequency control loop is shown in **Figure 2-2**. Because, there are many different generators supplying power into the power system, some means must be provided to allocate change in demand to the generators. The speed governor senses the change in speed (frequency) via the primary control loop. In fact, primary control performs a local automatic control that delivers reserve power in opposition to any frequency change, while secondary control originating at a central control center allocates generation. The necessary mechanical forces to position the main valve against the high steam pressure is provided by the speed changer and provides a steady-state power output setting for the turbine [52]. The speed governor on each generating unit provides the primary speed control function, and all generating units contribute to the overall change in generation in the time frame of seconds, irrespective of the location of the load change, using their speed governing. However, as mentioned, the primary control action (automatic and using a local signal) is not usually sufficient to restore the system frequency, especially in a large interconnected power system, and the secondary or supplementary control is required to adjust the load reference set point through the speed changer [49], [53]. Adequate primary control depends on generation or load resources made available to the TSOs. The timing of the primary, secondary, and tertiary frequency control ranges is shown in **Figure 2-3**.

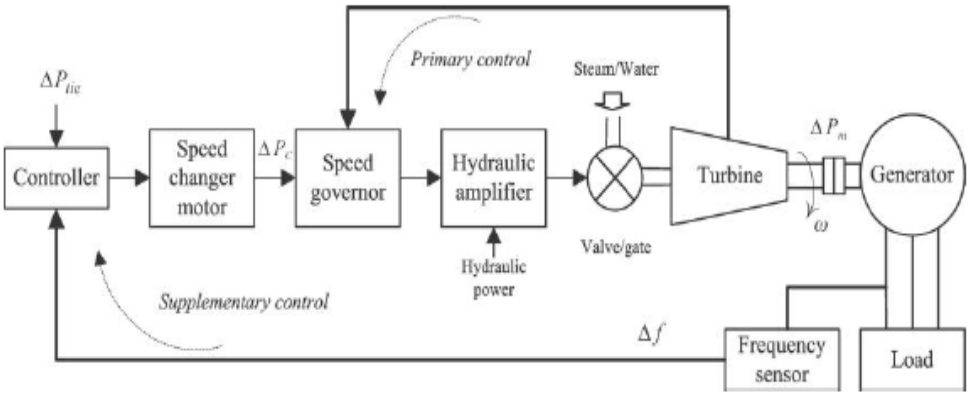

Figure 2-2 : Frequency control mechanism (H. Bevrani et al. 2011)

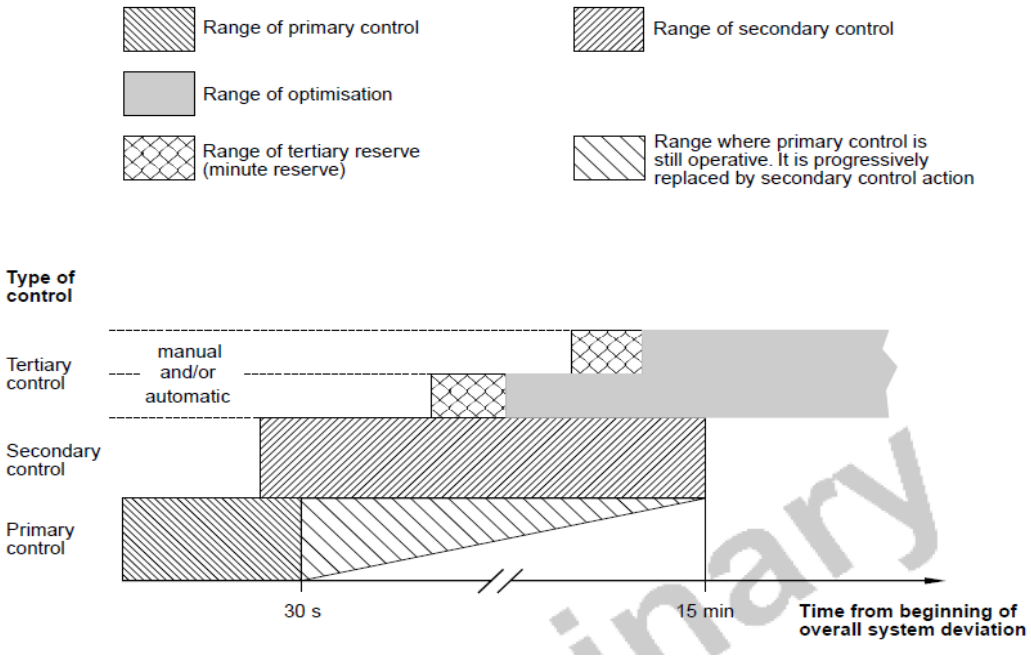

Figure 2-3 : Principle frequency deviation and activation of reserves (UCTE, Appendix LFC and Performance)

2.1.2 Secondary Frequency Control

In addition to primary frequency control, a large synchronous generator may be equipped with a secondary frequency control. A schematic block diagram of a synchronous generator equipped with both primary and secondary frequency control (supplementary) loops is also shown in **Figure 2-2**. The secondary loop gives feedback via the frequency deviation and adds it to the primary control loop through a dynamic controller. The resulting signal ΔP_c is used to regulate the system frequency. In real-world power systems, the dynamic controller is usually a simple integral or PI controller. Fol-

lowing a change in load, the feedback mechanism provides an appropriate signal for the turbine to make generation ΔP_m track the load and restore the system frequency. Secondary frequency control is a major function of AGC systems as they operate online to control system frequency and power generation. As noted, the AGC performance is highly dependent on how the participant generating units would respond to the control action signals. For example, the North American Electric Reliability Council (NERC) divides generator actions into two groups. The first group is associated with large frequency deviations where generators respond through governor action and then in response to AGC signals, and the second group is associated with a continuous regulation process in response to AGC signals only. During a sudden increase in area load, the area frequency experiences a transient drop. At the transient state, there are flows of power from other areas to supply the excess load in this area. Usually, certain generating units within each area are on regulation to meet this load change. At steady state, the generation is closely matched with the load, causing tie-line power and frequency deviations to drop to zero [54]. Likewise, in UCTE, secondary control makes use of a centralized and continuous AGC by modifying the active power set points/adjustments of generation sets/controllable load in the time frame of seconds up to typically 15 mins after a disturbance. Secondary control is based on secondary control reserves that are under automatic control using a signal sent by the TSO. Adequate secondary control depends on generation resources made available to the TSOs, independently from primary control reserves. Several frequency control criteria and standards are available to find how well each control area must balance its aggregate generation and load [55] - [56].

2.1.3 Tertiary Frequency Control

Tertiary control is any automatic or manual change in the working points of the generating units participating, in order to restore an adequate secondary control reserve (free up the secondary reserves) at the right time or to provide desired (in terms of economic considerations) allocation of this reserve within the set of generating units in the best possible way. Tertiary control may be achieved by means of changing the set operating points of generation sets participating in the secondary control (coordinated changes in dispatch to follow load), altering the power interchange program between interconnected systems (implement interchange transactions), and controlled load shedding. Tertiary control action is the slowest of frequency control action and is also known as minute reserve. This reserve must be used in such a way that it will contribute to the restoration of secondary control range when required. Tertiary control is typically operated in the responsibility of the TSO.

2.1.4 Emergency Frequency Control

The severe power system disturbances can result in cascading failures and isolation of power systems, causing formation of islands where the frequency exceeds the permissible limits. If such an islanded system, it will experience a frequency decline or rise. In many situations, the frequency decline may reach levels that could lead to tripping of other generating units. For example, where the frequency variation exceeds the permissible range, due to a significant loss of generation or consumed power, the system conditions are deemed impaired (emergency) conditions. In such circumstances supplementary actions are needed in order to re-establish the active power balance. These include system emergency load shedding in case of a major frequency drop or disconnection of generators in case of a large frequency rise. Emergency control, such as load shedding, shall be established in emergency conditions to minimize the risk of further uncontrolled separation, loss of generation, or system break-down. A restoration of normal frequency operation as soon as possible is essential. Load shedding is an emergency control action to ensure system stability by curtailing system load and is employed to reduce the connected load to a level that can be safely supplied by available generation. Load shedding will only be used if the frequency (or voltage) falls below a specified frequency (voltage) threshold. Typically, the load shedding protects against excessive frequency (or voltage) decline by attempting to balance real (reactive) power supply and demand in the system. The load shedding curtails the amount of load in the power system until the available generation can supply the remaining loads. If the power system is unable to supply its active (reactive) load demands, the under-frequency & under-voltage condition will be intense. The number of load shedding steps, the amount of load that should be shed in each step, the delay between the stages, and the location of shed load are the important objects that should be determined in a load shedding algorithm. A typical load shedding scheme is usually composed of several stages as shown in **Figure 2-4**.

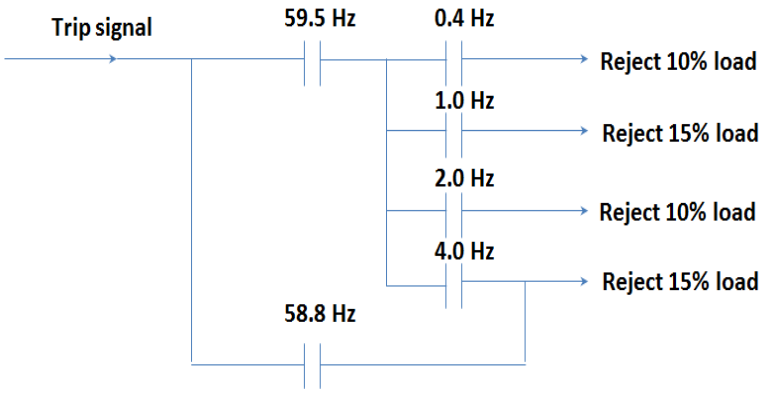

Figure 2-4 : Tripping logic for under frequency load shedding (P. Kundur et al. 1994)

Each stage is characterized by frequency threshold, amount of load, and delay before tripping. The objective of an effective load shedding scheme is to curtail a minimum amount of load (no more than required), and thereby provide a quick, smooth, and safe transition of the system from an emergency situation to a normal equilibrium state. Hence, the initial step of load shedding is critical making sure that the frequency does not reach a certain level where it might be difficult to recover. Therefore, the problem of optimal load shedding has been extensively investigated. A fast acting load shedding is proposed for implementation in control center [57]. Load shedding scheme based on SCADA for islanded system is presented [58]. General approach is to use the strategy based upon on-line measurement of the loads and load frequency characteristics [39]. Load with smaller frequency dependency are shed first, and with larger frequency dependency are shed later. In reality, the real-time information of loads is not always available and implementing online load measurement is very expensive for small distribution systems. Furthermore, system's load frequency dependency is often very hard to determine especially with constantly changing load. There is an adaptive load shedding scheme, which changes the relay settings according to the frequency decay curve as well as frequency information and integration of df/dt to find the amount of load to be shed [59] - [60]. Particularly, the load shedding problem for the islanded system must be treated differently due to its characteristics. Islanded systems often have small generating units and hence small inertia. Thus, the frequency tends to decay much faster. An UFLS scheme combined with DG units based on frequency information, rate of change of frequency, customers' willingness to pay and loads' histories feature might be a good optimal load shedding strategy. The discussed frequency control comprising primary, secondary and tertiary control ensures the frequency control under normal operating conditions of a power system.

2.2 Nordic Interconnected System

2.2.1 Nordic Grid Code

The Nordic interconnected system covers the countries of Finland, Sweden, Norway and the eastern part of Denmark (DK2). The operation of the system is ruled by the Nordic grid code. The Swedish TSO and the Norwegian TSO have the task of maintaining the frequency and time deviation within prespecified limits. The permissible variation in the frequency during the normal state is between 49.9 and 50.1 Hz. The time deviation should be kept with the range of +/- 30 s. When the time deviation is, in absolute value, more than 15 s, further action is planned by the Swedish and Norwegian TSOs. The frequency regulation has a higher priority than the time deviation and the costs of frequency regulation. There are two different types of frequency controlled reserves. First, the 'frequency controlled normal operating reserve' is used in the frequency range from 49.9 to 50.1 Hz. It is used for maintaining the system frequency at a

reasonable level during normal operation (i.e. to compensate for minor deviations in the expected production or consumption). With a sudden drop in frequency, this reserve (also known as load following reserve) should be available within 2 to 3 mins at a frequency deviation of 0.1 Hz. The total amount of frequency controlled normal operating reserve in the Nordic interconnected system is 600 MW which should all be deployed when the frequency level reaches 49.9 or 50.1 Hz. The Danish TSO is obliged to provide +/- 23 MW regulations for this purpose, out of a total requirement for the Nordic interconnected system of +/- 600 MW. Second, the 'frequency controlled disturbance reserve' is available for the frequency range from 49.5 to 49.9 Hz. It must compensate for a sudden loss of production (i.e. 1200 MW of production), and it is therefore only an upward regulation (emergency block islanding on selected power stations is used for downward regulation). It must be delivered linearly with a frequency drop between 0.1 Hz and 0.5 Hz. Half of the total required reserve should be available in 5 s, and the remainder in 30 s. Automatic frequency dependent load shedding may be considered a disturbance reserve. The Danish TSO must supply 168 MW of the frequency controlled disturbance reserve to the Nordic interconnected system, which in total requires 1160 MW. Momentary area control errors are calculated for each subsystem (in practice for each country). However, the area control error is not used as a regulation criterion.

2.2.2 Nordic Power Markets

The Nordic interconnected system is a large deregulated market to a certain extent. Each player in the system has well defined and different roles. First, the most important players in relation to the market are the balance responsible parties (BRPs). There are separate BRPs for consumption (CBRPs), and production (PBRPs). The BRPs are not responsible for the system balance, but are financially responsible for their clients' consumption or production of electricity. Every individual consumer or producer must have a BRP, who trades the electricity for them and handles the financial obligations related with the electricity markets (in principal everyone can act as their own BRP, but it requires a certain size, due to lower limits in the bids, collateral obligations, administration overhead, etc.). Second, they are the TSOs and DSOs. These are regulated, natural monopolies that operate and usually own the physical transmission and distribution lines. In addition, TSOs have the overall system responsibility, which includes maintaining the system wide continuous balance between production and consumption. The DSO's role in relation to the market is metering, and forwarding of the readings for end user settlements. Moreover, both TSOs and DSOs purchase the energy lost in their respective grids in the market. The market consists of several forward markets with different time scales and is illustrated in **Figure 2-5**.

1. Financial bilateral contracts, traded months or year ahead.

2. The day-ahead power exchange Elspot. This is the main coordinating Nordic power market. It is a uniform price double auction with implicit auctioning of transmission capacity. The market established an equilibrium price (possibly offset in predefined price zones) for each hour in the following day of operation.

3. The intra-day market Elbas. This is a pay-as-bid bilateral market place, where power contracts can be traded up to one hour before the beginning of the hour of operation. Congestion is handled by a first-come and first-served policy. Elbas is introduced to let market players with forecast errors, typically wind power, adjusts their schedules as the hour of supply approaches, with less financial penalty than they would have otherwise suffered. However, Elbas does not attract sufficient market players to be considered liquid.

4. The regulating power market is a uniform price auction with the TSO as a single buyer that accepts bids continuously during each hour, to maintain the system's energy balance. Bids must be submitted no later than 45 mins before the start of each hour of operation. All bids are sorted by price, and the best bids are accepted, that is the ones with the lowest price for up regulation (i.e. TSO is buying energy, i.e. more production or less consumption), and the highest price for down regulation (i.e. TSO is selling energy). For each hour, marginal up and down regulation prices are determined and applied accordingly to all accepted bids, however, in Elspot, congestion may lead to different prices in each price zone.

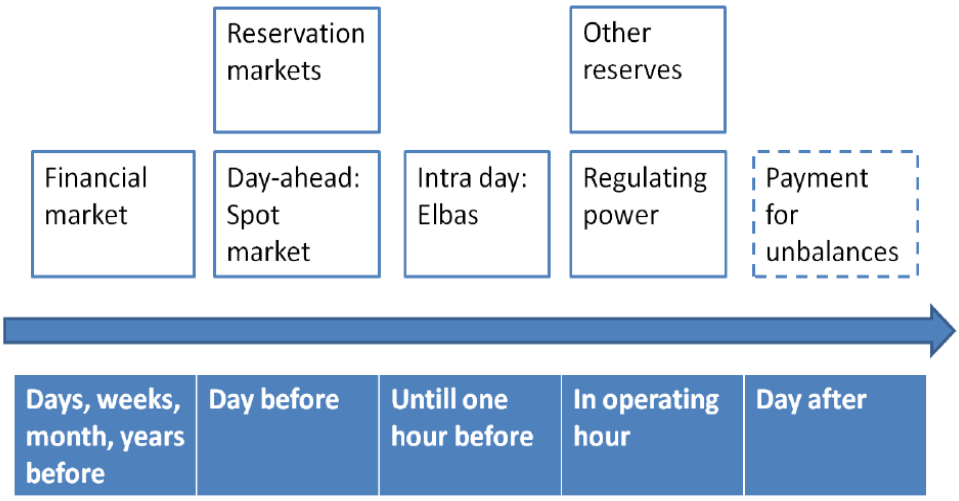

Figure 2-5 : Major components of Nordic Power Market (EDISON Deliverable 2.3, 2010)

2.3 AGC in a Modern Power System

AGC is an essential requirement and one of the most important components in the daily operation of a modern power system. This function is the primary concern of the control center, and is largely provided by an AGC system implemented as part of the EMS as shown in **Figure 2-6**. The AGC, security control, SCADA, and load management are the major units in the application layer of a modern EMS. The AGC provides an effective mechanism for adjusting the power output of multiple generators at different power plants, in real-time response to changes in the loads or disturbances, to keep the system frequency at nominal value and maintain tie-line power flows at the scheduled value. Since a power system requires that generation and load are balanced simultaneously, frequent adjustments to the output of different generators are necessary. The balance can be easily judged by measuring the system frequency. If the system frequency is increasing, more power is being generated than used, and all the machines in the system are accelerating and vice versa. The governors of generators sense the changes in the system frequency and adjust electrical power output. This governor control is the primary frequency control for maintaining balance between generation and load. The secondary frequency control to set the generator load reference is used to ensure that the steady-state frequency returns to 50 Hz or 60 Hz – the nominal system frequency. The governor control is local at the generator site and fast. On the other hand, the secondary control is carried out over the wide area or the whole system. This secondary control is done by the central controller or system operator and is slower compared to that of the primary frequency control. It is implemented as a feedback loop in which the generator outputs and tie-line flows are measured and brought back to the control center. Then, the governor control set points are calculated and sent out again to the generators from the control center. This control is also known as AGC or LFC. The primary control is continuous whereas the secondary control is discrete usually using 2 - 4 second sampling [48]. The AGC system realizes the instantaneous generation changes by sending the active power set-point signals to the under control selected generating units (i.e. load reference set-points of selected generating units). The AGC performance is highly dependent on how those generating units respond to the commands. Many generating units in the system would be designated the regulating units and would be automatically adjusted to control the balance between generation and load to maintain system frequency at the desired value. The remaining units in the system would be controlled with speed droop to proportion their share of the load according to their ratings. With the AGC system, many units in the system can participate in regulation, reducing wear on a single unit's controls and improving overall system efficiency, stability, and economy. The generating unit response characteristics are dependent on many factors, such as type of unit, fuel, control strategy, and operating point. The AGC process is performed in a control center remote from the generating plants (i.e. all units on regulation), while the power production is controlled by turbine-governors at the different generation site. The

AGC communicates with SCADA, the load management unit, and the security control center in the EMS [49].

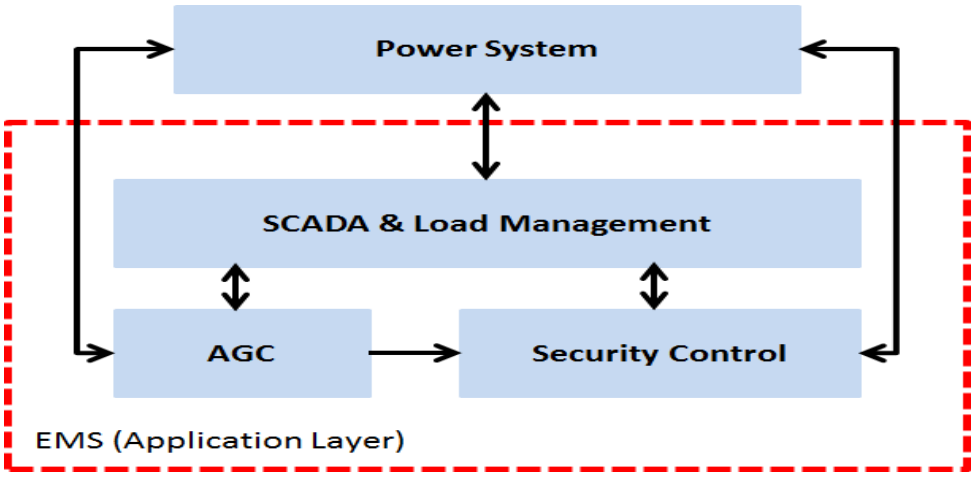

Figure 2-6 : Application layer of a modern EMS (H. Bevrani et al. 2011)

For example, the TSO (REE, Spain) has its own control center for its renewable generation, which applies different mechanisms to different renewable energies control centers. All renewable facilities higher than 10 MW should be assigned a control center. **Figure 2-7** shows the TSO in the high level, the renewable energy control center called CECRE in the middle layer and renewable energy producer in the bottom layer. In a modern SCADA system, the monitoring, processing, and control functions are distributed among various servers and computers that communicate in the control center using a real-time local area network (LAN) and a simplified SCADA center is also shown in following **Figure 2-8**.

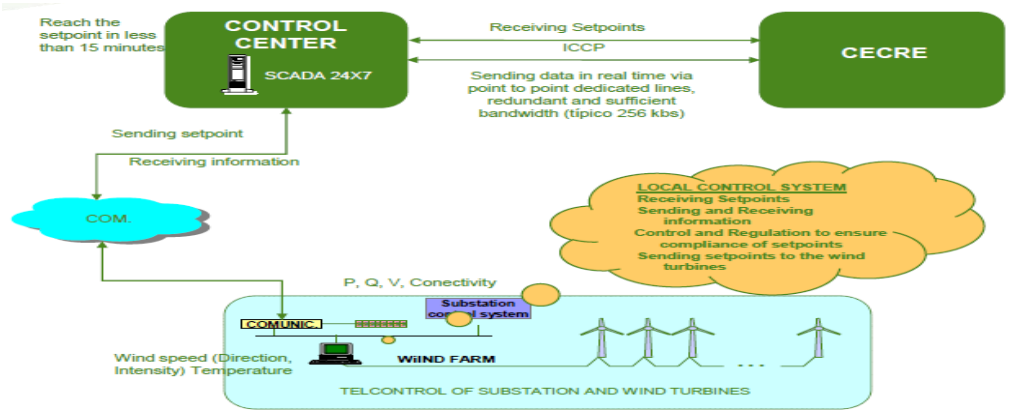

Figure 2-7 : Renewable energy control center, CECRE, REE in Spain (Gustavo M. et al. 2010)

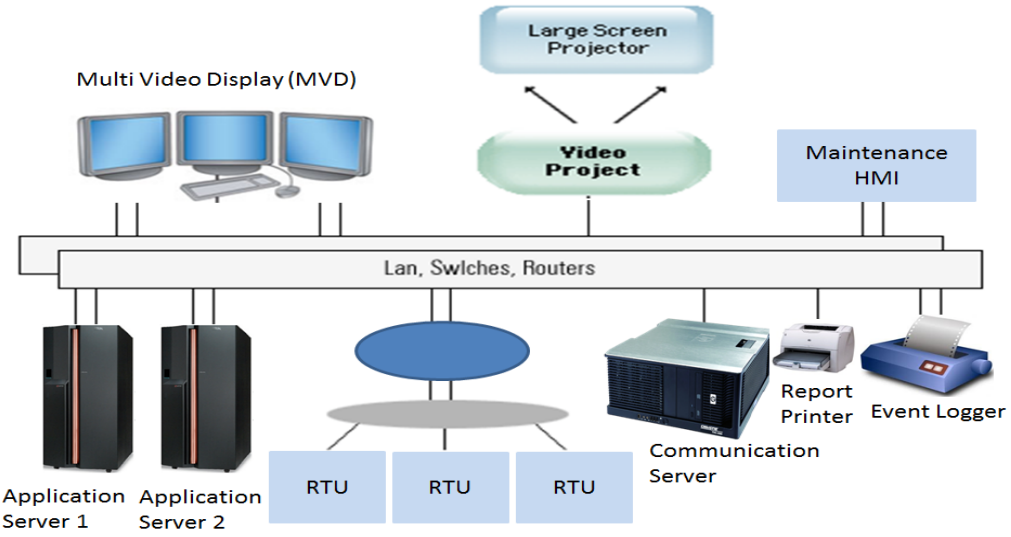

Figure 2-8 : A simplified structure for a typical SCADA

As shown in **Figure 2-8**, the human-machine interface (HMI) with remote access, application servers, a supervisory computer system, and communication servers are the major elements of the SCADA system. The HMI consists of a multi-video-display (MVD) interface and a large display or map board/mimic board to display an overview of the power system. Below is a real view of PowerLabDK SCADA system interacts with 21 lab cell boards on campus microgrid as shown in **Figure 2-9**.

Figure 2-9 : A full scale SCADA system, ICL

2.4 Summary

For satisfactory operation of a power system, the frequency should remain nearly constant. Relatively close control of frequency is vital. So far this chapter has concentrated on the concept of power system frequency control, providing an introduction on the general aspects of frequency control. Depending on the frequency deviation range, this could be divided into three different kinds of control. Namely, these categories are the primary, secondary, and tertiary frequency control. The primary frequency control involves automatic actions to arrest deviations in system frequency whenever imbalances arise between generation and load. The primary frequency control actions are fast and include governor response. The secondary frequency control involves centrally coordinated actions to return frequency to its scheduled value. The secondary frequency control actions are slower. They are deployed both during normal operations and after primary frequency control resources have arrested frequency following major disturbances. The secondary frequency control actions include generation (or load) that responds to AGC signals or to operator dispatch commands. The tertiary frequency control involves centrally coordinated actions to dispatch generation (or load) to move to a new operating point while maintaining balanced operation. The tertiary frequency control actions are the slowest. They include coordinated changes in dispatch to follow load, implement interchange transactions or coordinated changes in generating unit loading to redistribute reserves. In addition, emergency control and protection schemes, such as UFLS strategies are briefly reviewed. Some references on optimal load shedding such as load shedding scheme based on SCADA for islanded system and based upon on-line measurement are given. The characteristics of Nordic grid code and its power markets are highlighted as an example. Particularly, in DK2, there are two different kinds of frequency controlled reserves. First, the frequency controlled normal operating reserve must be activated automatically within a ± 0.1 Hz deviation and shall be regulated within 2-3 mins. The joint requirement for the synchronous system is 600 MW. This service can be exchanged to a certain degree. Each subsystem shall have at least 2/3 of the frequency controlled normal operation reserve within its own system in the event of splitting up and island operation. Second, the frequency controlled disturbance reserve must be activated automatically at 49.9 Hz and fully activated at 49.5 Hz. At least 50 % shall be regulated within 5 s and 100 % within 30 s. Joint requirements for the synchronous system is approx. 1,160 MW, depending on the relevant dimensioning fault. Moreover, this chapter presents the fundamentals of AGC, providing structure, definitions, and basic concepts associated with a modern power system. The AGC mechanism in power system, the major functions as part of the EMS, and characteristics are briefly described.

3 Islanding Operation

This chapter gives an overview on the generic term ‘islanding operation’ with the definitions used by different entities. The formation of a microgrid due to islanding is briefly described. The current utility practices in islanding operation in general are described, and is mainly focused on the definition used by IEEE Standard 1547.4-2011. Some of the new information regarding intentional islands will be highlighted. Danish experience of planned islanding operation is briefly discussed.

3.1 Introduction

As an effective solution for the application and utilization of DG units, the concept of microgrid has attracted more and more attentions due to its control flexibility to the main utility grid [35]. A microgrid is a relatively novel concept, consisting of small power systems owning the capability of performing islanding operation from main utility grid and is shown as a dotted line in **Figure 3-1**.

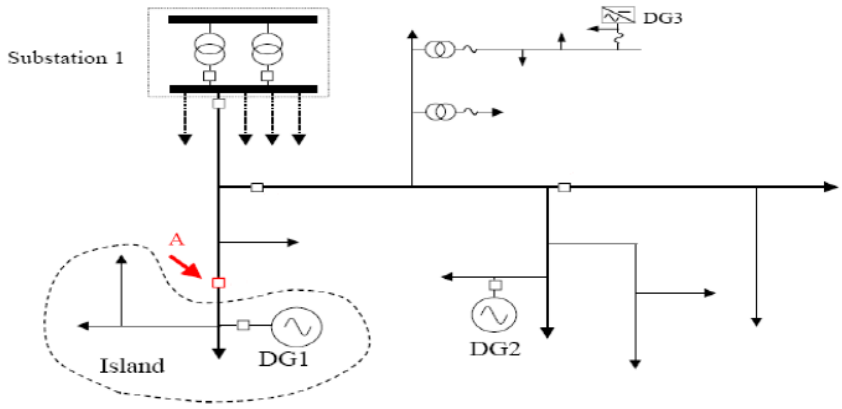

Figure 3-1 : An example illustrating islanding process and formation of a microgrid with DG units (Prabhu et al. 2006)

This miniature version of the grid in dotted line is known as a microgrid. This microgrid is capable of operating either grid-connected or islanding operation. Particularly, DG units based on RESs such as wind and solar can be effectively integrated into a microgrid to supply rapid load growth demand. This is one of the major advantages of forming microgrids in distribution systems.

As illustrated in **Figure 3-1**, presents the islanding process and formation of a microgrid due to islanding, for example, when re-closer opens and DG1 feeds into the resultant islanded system. Large DG units are typically connected to the primary feeders (i.e. DG1 and DG 2). Most of them are synchronous or induction generators at present. Small DG units (i.e. from 1kW up to a few MW) such as inverter based photovoltaic (PV) are connected to the low voltage secondary feeders (i.e. DG3). Many customers could be supplied from decentralized sources. In the context of **Figure 3-1**, the islanding phenomenon that results in the formation of a microgrid can be due to either planned or unplanned switching incidents. In the case of a planned microgrid formation, appropriate sharing of the microgrid load amongst the DG units and the main utility grid may be scheduled prior to islanding. Thus, the islanding process results in minimal transients and the microgrid continues operation, albeit as an autonomous system. Planned islanding and subsequent microgrid operation is discussed in [62]. In the context of [62], a planned islanding of the 11-kV system can happen by scheduled opening of the circuit breakers at both ends of the 60-kV line, e.g., for line maintenance.
However, an unplanned islanding and its microgrid formation are due to either a fault and its subsequent switching incidents or some other unexpected switching process. Prior to islanding, the operating conditions of microgrid could be widely varied, e.g. the DG units can share load in various manners and the entire microgrid portion of the network may be delivering to or importing power from the main utility grid. Furthermore, the disturbance can be initiated by any type of fault and line tripping may be followed up with single or even multiple reclose actions. Thus, the severity of the transients experienced by the microgrid, subsequent to an unplanned islanding process, is highly dependent on i) the pre-islanding operating conditions, ii) the type and location of the fault that initiates the islanding process, iii) the islanding detection time interval, iv) the post-fault switching actions that are envisioned for the system and v) the type of DG units within the microgrid.

3.2 Definitions of Islanding Operation

Islanding operation is the generic term used to describe a scenario or a condition, where a section of a transmission or distribution system, which contains DG units, is separated from the main transmission or distribution system. Subsequent to this separation, the DG continues (or is started) to power the loads trapped within the islanded system. There are several different definitions of ‘islanding operation’ defined, used and are being developed by different entities. Following is a **Table 3-1** summarizing the definitions used by different entities.

Table 3-1 : Islanding definitions used by different entities

Entity	Definition	
Energinet DK, Denmark	**Isolated islanding operation :** Operating condition that occur *a* power station unit supplies an isolated grid area either alone or as a significant unit. **Islanding operation :** Mode of operation comprising house-load operation and isolated operation	Regulation for grid connection Task Force 3.2.3, Version 5.1, Oct 1, 2008 Regulation for grid connection Task Force 3.2.4, Version 4.1, Oct 1, 2008
European Network of Transmission System Operators for Electricity (ENTSO-E)	**Islanding operation :** Island operation is the unusual operation mode, where all interconnections / TIE-LINES of a CONTROL AREA / BLOCK are disconnected (e.g. after a disturbance the CONTROL AREA is not connected to the rest of the SYNCHRO-NOUS AREA any more) **Island :** An ISLAND represents a portion of a power system or of several power systems that is electrically separated from the main INTERCONNECTED SYS-TEM (separation resulting from the disconnection/failure of transmission system elements).	UCTE Operation Handbook-Policy 1 : LFC and Performance, Mar 19, 2009 UCTE Operation Handbook-Glossary, Ver 2.2, June 24, 2004
BC Hydro, Canada	**Power generator islanding :** Islanding is defined as the condition when a portion of the BC Hydro system is energized by one or more PG facilities and that portion of the system is separated electrically from the rest of the BC Hydro system. PG islanding may be inadvertent or intentional. **Generation islanding :** Islanding is a condition where the power system splits into isolated load and generation following operation of a transmission CB, substation bus or feeder CB, distribution line recloser or line fuses.	Distribution Power Generator Islanding Guidelines, 2006 35 kV and below interconnection re-quirements for power generators, May, 2010

3.3 IEEE 1547.4™- 2011 Standard

IEEE Std 1547.4 is part of the IEEE 1547™ series of standards. IEEE Std 1547.4 was specifically developed to address the lack of information included in IEEE Std 1547-2003 regarding intentional islands by IEEE Standards Coordinating Committee 21 on fuel cells, PVs, DG, and energy storage. The IEEE 1547.4 (i.e. latest release version, July 20, 2011) provides an introduction and overview and addresses engineering concerns related to DER islanded systems. This document also provides alternative approaches and good practices for the design, operation, and integration of DER islanded systems with electric power systems (EPS). This includes the ability to separate from and reconnect to part of the area EPS while providing power to the islanded local EPSs [22]. Some of the new information regarding intentional islands will be extracted and highlighted.

3.3.1 DER Island System Configurations

There are a variety of operating configurations for intentional islands that incorporate DER. **Figure 3-2** shows examples of seven planned island configurations in the area EPS mentioned in the IEEE standard. There may be additional DER island system circuit topologies other than the ones pictured. The planned DER island systems in the figure include: (1) local EPS island (facility island, black dotted circle), (2) secondary island, (gray square box), (3) lateral island (red dotted rectangular box), (4) circuit island (blue dotted box), (5) substation bus island (red dotted box), (6) substation island (green dotted box), and an (7) adjacent circuit island (green box + black dotted arc). These terms describe the majority of DER island systems covered in this guide.

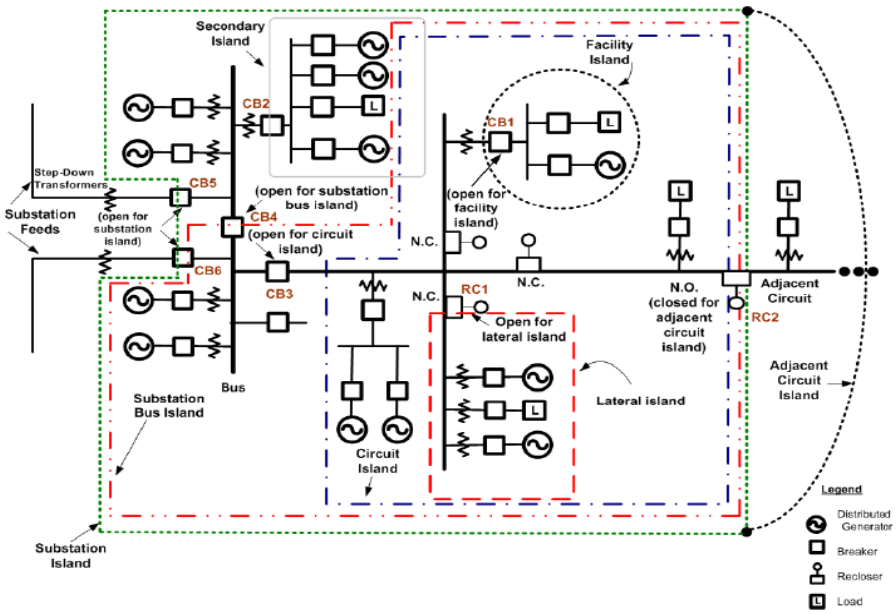

Figure 3-2 : Examples of DER island systems

- **Local EPS Island:** It is formed from generation and load normally served within a customer facility and is also called a *facility island.* This DER island system has only one point of common coupling (PCC, CB1) with the area EPS. The local EPS island can be operated to serve the load of the facility when there is a loss of the area EPS.

- **Secondary Island:** It is one or more DER and multiple customers connected to the secondary side of one distribution transformer. There may be multiple secondary islands on a single distribution lateral. For example, community energy storage units can be deployed in secondary islands. In these systems, an area EPS-owned storage device is connected on the secondary side of the distribution transformer with multiple customers connected to the secondary.

- **Lateral Island:** It is formed from load normally served from a lateral on a distribution circuit. The generation can be operated to serve the load of the island when the lateral switching device (e.g., the breaker, recloser, or sectionalizer) opens (RC1).

- **Circuit Island:** It is formed from load normally served from a single distribution circuit. For loss of the substation feed, transformer, or bus, DER can be operated to serve the load of the circuit by opening (CB3).

- **Substation Bus Island:** It is formed from load normally served from a single bus within a substation, though multiple buses may be used to serve loads from the substation. The DER on a specific bus can be operated if there is a loss of a substation feed or substation transformer. This operation entails opening the transformer secondary (low-voltage side) breaker (CB6) on the lost feed or transformer and operating the section breaker (CB4) either opened or closed.

- **Substation Island:** It is formed from load normally served from a single substation. This island may be used when the distribution substation is out of service or when one transformer is out of service and the remaining transformer is not capable of supplying the entire substation load. This island can be used to alleviate a thermal (overload) or voltage problem on the substation feeds or an overload problem on the step-down transformers. Running the DER on both buses reduces the loading on these feeds and transformers and may improve voltage levels. The substation transformer secondary (lower-voltage side) breakers (CB5 and CB6) are open to create the DER island system.

- **Adjacent Circuit Island:** Load from an adjacent circuit can be served from the islanded portion of the system. This provides service in the event of the loss of

the adjacent circuit feed and the loss of the main substation feeds. The DER on the substation bus, and on the circuit, could be run, including the facility DER by opening CB5 and CB6 and closing RC2.

3.3.2 Operating Modes of Islanded System

This section explains the four operating modes of the islanded system. Under most cases, this guide should be followed for strategies to maintain desirable operation of the system under normal parallel and island modes of operation. Some type of monitoring (voltage, frequency, etc.) and control equipment would be needed to control islanding operation and to implement the transition from normal mode to island mode and return. Depending on the degree of monitoring and control features needed, this controller may need to be very sophisticated.

3.3.2.1 Normal Parallel Mode

During normal parallel operation with the area EPS, all of the DER on the planned island system shall operate in accordance with IEEE Std 1547.4 unless agreed upon by the area EPS operator. The monitor and control equipment required for islanding operation needs to be in operation during normal parallel mode. It is necessary to make this information available to the island control scheme such that a transition can be planned in advance. This should include information about the protective device status, generation levels, load levels, and system voltages and frequency.

3.3.2.2 Transition-to-Island Mode

A transition-to-island mode can be a result of scheduled or unscheduled events. Scheduled transitions are intentional events for which the time and duration of the planned island are agreed upon by all parties involved. Unscheduled transitions are inadvertent events that are typically initiated by loss of area EPS or equipment failure, and the DER island system may be automatically sectionalized from the area EPS by protective relays (B1). Knowledge of the operating conditions of the system prior to islanding and control of those operating conditions will facilitate smooth transfer to an intentional island, particularly in response to abnormal events and when the area EPS is included in the island. **Figure 3-3** shows that, in the case of intentional island operation, the “tie” breaker (B1) will open for the fault shown.

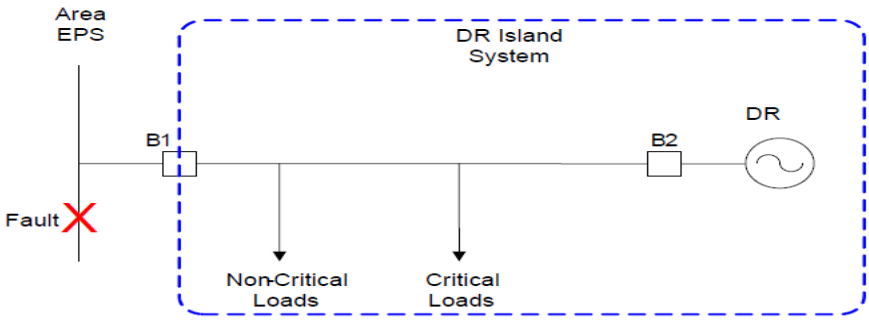

Figure 3-3 : DER island system connected to the area EPS

3.3.2.3 Island Mode

The island system needs to be designed to provide the real and reactive power requirements of the loads within the island and serve the range of load operating conditions. The DER island system should be able to actively regulate voltage and frequency within the agreed upon ranges. Also, there should be an adequate reserve margin that is a function of the load factor, the magnitude of the load, the load shape, reliability requirements of the load, and the availability of DER. To balance the load and generation within the islanded system, various techniques (e.g., load-following, load management, and load shedding) can be used. In island mode, there is a need to provide dynamic response from the DER that may have not been necessary in normal parallel operation. The DER sources should have adequate real and reactive power capability and response characteristics. During the island mode condition, transient stability should be maintained for load steps, DER unit outage, and island faults. Protective device coordination should be maintained in both area EPS connected and islanding operation to effectively meet the needs of the island.

3.3.2.4 Reconnection Mode

For reconnection of the island system to the EPS, monitoring should indicate that the proper conditions exist for synchronizing the island with the EPS. After a disturbance, no reconnection shall take place until the area EPS voltage is within Range B of ANSI/NEMA C84.1-2006, Table 1, the frequency range is between 59.3 Hz to 60.5 Hz, and phase rotation is correct. The voltage, frequency, and phase angle between the two systems should be within acceptable limits (i.e., as specified in IEEE Std 1547-2003, Table 5) in order to initiate a reconnection. The island interconnection device may delay reconnection for up to five minutes after the area EPS steady-state voltage and frequency are restored to the ranges identified above. Grid restoration is identified when system voltages and frequencies have returned to, and been maintained in, a normal range for a

reasonable period of time, e.g., 5 mins. This reconnection must be carried out through proper synchronization of the islanded system to the utility at PCC. Limits have been proposed for acceptable voltage magnitude error, frequency error and phase-angle error between the islanded system and the main utility grid. For distribution system with DG units in 1.5 MW to 10 MW range, reconnection is acceptable if voltage error is below 3%, frequency error below 0.1 Hz, and phase-angle error below 10 degree [22]. Adhering to these limits ensures reconnection of the distribution system may be achieved with minimal transients in the overall system.

3.4 Danish Experience - Bornholm Islanding Operation

The Bornholm distribution system is able to intentionally go from grid-connected operation to an islanding operation. The regional DSO, Østkraft conducted a planned islanding operation test for the period between September 11th and September 14th in the year of 2007. The whole operation was conducted in three major stages. First, the Bornholm distribution system was operated under the grid-connected operation, where it was synchronized to the Nordic interconnected system and participated in Nord Pool, i.e., the Nordic power market. The demand was supplied mainly by the Swedish interconnection cable, onshore wind turbines, and Rønne unit 6. Prior to a planned islanding operation, several required operations have been conducted by the local DSO in sequence. During islanding operation, the shedding of wind power is necessary to avoid unwanted power oscillations, which lead to uncontrolled oscillations in the power plant control (i.e. Unit 6 was unable to follow up with the fluctuations of wind power if too much was integrated). Second, the normally out-of-service Unit 5 was gradually started to produce power in order to replace the power supplied by the sea cable (i.e. a matched power preplanned, etc.). Once the sea cable was disconnected, the Bornholm distribution system was asynchronous to Nordic interconnected system and became a separated 60 kV medium voltage microgrid [63]. As a last procedure, three Vestas wind turbines with a total of 6 MW capacities were forced to start, and continued producing power. At this stage, Rønne unit 5 and unit 6 supplied the most demand while the three wind turbines only supplied less than 4% of the total demand, which was much lower than the level under grid-connected operation. The Bornholm distribution system was then synchronized and returned to grid-connected operation by reconnecting the sea cable. Subsequently, the power from unit 5 was gradually decreased to zero, and the power through the sea cable was increased to the normal level within an hour after reconnection. Extensive measurement has been performed during islanding operation to enable investigation of the islanding transition and the impact of the wind power during islanding [64] - [65]. The purpose was to obtain experience and learn difficulties about islanding operation is when to transfer the system with many DG units into the islanding operation, where the system can still meet the system stability criteria with DG units in operation. Major

findings are listed and summarized in **Table 3-2**. This particular work is part of the More Microgrid project funded by the EU 6th framework programme.

Table 3-2 : Experience, challenges and suggestions (Yu Chen et al. 2010)

Experience	It was feasible to conduct planned islanding operation with the generation mix: wind turbines, steam and CHP plant Back up steam plant (unit 5) was needed to be started before islanding. Data measurement favored the simulation and analysis work.
Challenges	Poor system frequency quality was observed. More oscillation and fluctuating frequency events under islanding operation. Wind turbines were shut down during transitions, and only three wind turbines were connected under islanding operation (i.e. low penetration) Small power transfer through sea cable was required before islanding, which was not flexible and made it almost impossible to perform islanding operation during emergency. Non high quality data measurement led to time consuming effort on data processing.
Suggestions	Criteria for acceptable system parameters during islanding operation should be studied and designed accordingly. Due to less power reserve during islanding operation, traditionally passive loads should be made active to contribute to the reserve and system support. A coordination control scheme is needed. It would be beneficial if the degree or region of security for islanding operation can be acquired for system operator, which increases the flexibility for islanding operation. An intelligent real-time measuring and communication system is a necessity.

3.5 Summary

Many utilities and existing standards currently do not or at least reluctantly allow the islanding operation of distribution systems. Almost all utilities and DSOs require DG to shut down once a distribution system is islanded. Both IEEE 1547.4-2011 and IEC 61727 standard require islanding to be detected and DG be disconnected at most within 2 s. Islanding operation is simply avoided due to the concerns of equipment failure and safety issues for maintenance man and power quality reasons. Because, islanding operation keeps a region of the utility, still being energized by DG, this is hazardous for line operators who could suppose it is disconnected. Moreover, a long duration of the island could produce conflict in case the automatic reclosing of the utility protection devices. This is the case when the reconnection is done before the island has been extinguished. An island could get desynchronized during the stand alone period of operation, forcing the protections to fail again and being potentially dangerous for the electronic equipment due to the apparition of short-circuits at the moment of reconnection. DSOs still consider DG units as additional complexities in the network, and hence, the current operation of practices discourages the islanding operation for mainly safety and security reasons. However, as the amount of DG increases, it is appropriate to review this policy, especially as there are many potential benefits to customers, DSOs and DG owners. For examples, in some cases, allowing of islanding of DG connected to radial sub transmission system could improve the system reliability and decrease outage cost during power outage or schedule maintenance. The fault repairing time for rural cable network can be time consuming, if the restoration time equals to or even less, then islanding operation may become more beneficial. Moreover, it can also bring to DG owners is the additional revenues from selling their energy and the improvement in the quality of power supply. Nevertheless, the success of islanding operation depends on many complex factors. It is very important to examine how islanding operation can be accommodated and if so, under what conditions. This also consists of technical issues such as state detection, control of voltage and frequency, load control and protection. It is also appropriate to define and find potential sites, best locations for DG connections, communications, good working relations, etc. Obviously, communication is costly if the working sites are far from the communication spots. In this regard, the IEEE 1547.4-2011 standard is helpful since it is intended to provide an excellent introductory overview and address engineering concerns of islanding operation. Also, the Danish utilities have experienced planned islanding operation in practice. The Bornholm distribution system has experienced higher and more frequent voltage and frequency excursions from their nominal values during islanding operation. Prior to a planned islanding operation, several required preparations and operations have been conducted. Maintaining the same settings and operation strategies as in grid-connected operation may lead to failure. A new effective solution to stabilize the frequency has to be offered under this islanding operation. Hence, islanding operation could eventually be of great importance in order to guarantee the continuity of power supply under emergencies.

4 Modeling of Bornholm Distribution System

The Danish island of Bornholm is chosen as a smart grid test site (i.e. a representative of future energy systems) for a number of practical reasons. Firstly, the Bornholm is a typical energy system as the mainland Denmark with high penetration of wind power and CHP units. Secondly, the Bornholm is a test site for testing new types of technologies such as PV, electric vehicle, fuel cell, biogas, and future power regulation services. Lastly, the Bornholm distribution system is capable of undergoing a planned islanding operation as reported in [63], [64] - [65]. In view of this, this chapter aims to address the question "how to develop a detail model of Bornholm distribution system as well as a generic model of Bornholm distribution system which benefit all parties" by presenting both benchmark cases to enable investigation of the transition to islanding operation scheme with an energy storage system (ESS). A complete overview of Bornholm distribution system (i.e. a basic topology and layout) is introduced in Section 4.1 and Section 4.2, respectively. In Section 4.3, the available capacity of power generation and the Swedish interconnection are presented. In Section 4.4, the basic information of the RTDS is briefly introduced. In Section 4.5, the tasks involved in the modeling and implementation of Bornholm distribution system using the RTDS is described and a detailed model of the Bornholm distribution system, capable of simulating both steady-state and dynamic simulation is constructed using recommended guidelines. The simulation models, the typical data used and the scenarios are also introduced. In Section 4.6, several simulations on the detailed model of Bornholm distribution system are presented to show that the simulated results agree with PF simulation. In Section 4.7 presents a generic model of Bornholm distribution system, which can be used as a Danish benchmark model for smart grid testing purposes. The simulation results are given and compared.

4.1 Bornholm Distribution System at a Glance

The Danish island of Bornholm is located to the south of Sweden in the Baltic Sea and has a population of more than 42,000. The Bornholm distribution system has a peak demand for electricity of approximately 55 MW - 63 MW and a base load of 13 MW - 18 MW [66] - [69]. The electricity demand is mostly covered by the 68.6 MVA capacity ac submarine cables to Sweden. This can surely provide all the power needs of the island. The Bornholm distribution system, however, has its own generating capacity such as thermal power plants, diesel generators, the coal-fired CHP in Rønne, biomass and a

large share of wind turbines exceeding 30% of total energy consumption. The wind turbines are situated all over the island. **Figure 4-1** shows a map of Bornholm with MV grid, major generation plants, wind turbines and CHP unit locations and the key data. The Bornholm distribution system is a part of the Nordic synchronous area interconnected to the 132 kV Swedish power systems through a long 60 kV ac submarine cable and is fully integrated in the Nordic power market as a part of the Eastern Denmark price area (DK2). The DSO (owned by the Bornholm municipality), Østkraft in Bornholm supplies electricity to more than 27,895 customers. The Bornholm distribution system comprises of a meshed 60 kV ring structure as well as underlying lower voltage network of radial 10 kV and 0.4 kV buses.

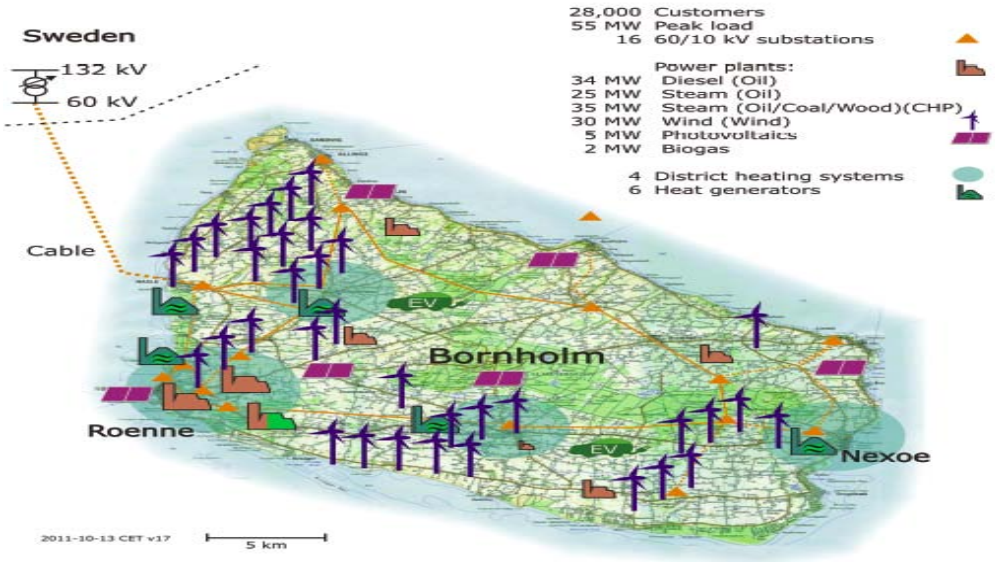

Figure 4-1 : Medium voltage (MV) grid, major generation plants, and wind and CHP locations in Bornholm (J. Østergaard et al. 2009)

Table 4-1: Key electricity data for the Bornholm distribution system, 2011

Property	Unit
Number of customers	28,000
Number of customers (100,000 kwh/year)	300
Total energy consumed	268 GWh
Peak Load	55 MW
Wind power plants	30 MW
Biomass	2 MW
60 kV grid	131 km
Number of 60/10 kV S/S	16
Number of 10/0.4 kV S/S	1006

4.2 Basic Network Topology

4.2.1 132 kV/60 kV Substation in Sweden

E-ON is a power company in the southern part of Sweden. The company owns the equipment in the TOMELILLA and BORRBY substations. From 132 kV TOMLILLA substation, there is an overhead line connected to 132 kV BORRBY substation. The 60kV side of the transformer (BOR132-BOR60) in the BORRBY substation, Sweden is connected to the 60kV HALSE substation, Bornholm, Denmark by the mixture of overhead lines and ac submarine cables (total length of 49.8 km).

4.2.2 Swedish Interconnection

The power consumption of Bornholm is primarily supplied through the 60 kV ac submarine cables between Sweden and Bornholm, Denmark. The cable has a rated transmission capacity of 68.6 MVA. The Swedish interconnection BORRBY to HALSE consists of both overhead lines and land cables totalling up to four parts. The overhead line transmission is from 132 kV/60 kV BORRBY substation to the coastal line (4.2 km). The land cable connects from coast to the actual shoreline (0.7 km). From this point, it is connected by the submarine cable (43.5 km). The submarine cable ends at the shoreline near HALSE. Then, the land cable connects to the transformer station in HALSE (1.4 km). The Danish TSO, Energinet.dk owns the equipment between the BORRBY substation in Sweden and the HALSE substation in Bornholm, Denmark. A summary of the data concerning the interconnection is presented in **Table 4-2**.

Table 4-2 : Connection between BORRBY and HASLE

Type	**Dimension** (mm^2)	**Length** (km)
Overhead line	127 Cu	4.2
Cable (land)	400 Cu	0.7
Cable (submarine)	240 Cu	43.5
Cable (land)	400 Cu	1.4
		49.8

The Swedish TSO, E-ON requires the transmission of reactive power through the sea cable to be as close to zero as possible. Through the interconnection, it is possible to supply the active power required in most operational situations, but occasionally the peak load exceeds the maximum transmission capacity, and local generation is necessary.

4.2.3 60 kV/10 kV Distribution System

The 60 kV meshed distribution system consists of the generators, distribution transformers, wind turbines, shunts and aggregated loads in the 10 kV systems. The distribution system is a 60 kV MV network connected to the 132 kV BORRBY substation in Sweden. There are 16 substations at the 60 kV voltage levels, 23 on load tap changer (OLTC) power transformers (60kV/10kV) with a total capacity of 219 MVA, and 22 cables / 26 overhead lines in the region. The 60 kV system and transformer stations are shown in **Figure 4-1**. The ratings of main backbone network components are given in **Appendix A**. Seven out of sixteen substations are equipped with two parallel 60 kV/10 kV transformers supplying the distribution system. In order to keep the short circuit current below its threshold limits, only one of two transformers is operating under normal conditions. The other nine substations have only one 60 kV/10 kV transformer. All 60 kV/10 kV transformers are Y-connected on the high voltage side with a neutral, and D-connected on the low voltage side. The regulation of a distribution line voltage has adopted automatic OLTC operation, automatically altering the winding ratio to increase or decrease voltage on the low voltage side in order to maintain a constant voltage level. Each OLTC has 15 steps in total with a voltage change per tap of 2% of nominal voltage. The tap changer is symmetric, so step 8 corresponds to the neutral tap position.
The switch shunt capacitors have been installed at 60 kV/10 kV substations (10 substations), which are rated at 2 Mvar at a nominal voltage of 12 kV. These capacitors were previously used to compensate for the voltage drop of the system during heavy load periods, but they are rarely used. The local DSO, Østkraft manages approximately 1007 10 kV/0.4 kV substations, and 91 10 kV feeders. The substation comprises of six 10 kV outgoing feeders (i.e. average number of feeders per substation) in which one 10 kV is connected to the loads and the other feeders connected as lumped loads to another 10 kV feeder. As of 2009, the total length of overhead lines is 184 km and the total length of cables is 730 km. The 60 kV/10 kV networks and substations are monitored and controlled by SCADA systems. These systems feature distribution facility improvements and control automation to enhance power supply reliability. Measurement systems are presented in **Table 4-3**.

Table 4-3 : Measurement systems in Bornholm

System	Supplier	Time Resolution	Data Type
SCADA system network manager	ASEA Brown Boveri (ABB)	10 s 1 min 1 hour	Current, voltage, power factor, tap position, frequency, active power, reactive power

4.3 Power Generation

There are different types of generation units in the Bornholm distribution system. The power generations include 14 diesel (oil-fired) units with a total capacity of 39 MW, 1 steam (oil-fired) power plant with 25 MW capacity (Unit 5), 1 combined heat and power plant (coal- and oil-fired, biomass such as wood chips, CHP) with 37 MW capacity (Unit 6), 35 fixed speed onshore wind turbines with a total capacity of 30 MW, and one 2MW biomass plant (Unit 7). The largest generation site is the power plants in Rønne (the capital of Bornholm) region, which contains 14 diesel units, oil-fired unit 5, and coal-fired CHP unit 6. The power plant also covers the need for central heating to the customers in the Rønne region. The Bornholm distribution system has very high penetration of a variety of low-carbon RESs, including wind power (30 MW), PV (1 MW under roll-out), biomass power plant (2 MW), and electric vehicle (under roll-out). All these fore mentioned generation units add up to a total installed capacity of 133.5 MW. In the following section a detailed description of the Rønne power plants (Unit 5 and Unit 6) are presented. A summary table of generating units are listed in **Appendix B**.

4.3.1 Rønne Unit 5

Rønne unit 5 thermal power plant (oil-fired), which is located on the southwest tip of the Bornholm Island, operates 1 x 25 MW thermal power generation units. The commission of unit 5 was completed in 1974. The generator, manufactured by Brown Boveri, is rated at 29.4 MVA, 10.5 kV nominal voltages, 3000 rpm and 0.85 pf. The boiler is from Vølund Energy Systems. The excitation system, also manufactured by Brown Boveri, consists of a power transformer based static exciter directly fed from the generator terminals, and a controller. The excitation controller features a variety of regulating, limiting and stabilizing functions implemented. The steam turbine is a condensing reheat turbine, rated at 25 MW under rated steam conditions and 3000 rpm. The steam turbine is installed with a governor, all manufactured by Brown Boveri. Most of the data were taken from the manufacturer's documentation and from Østkraft.

4.3.2 Rønne Unit 6

Rønne unit 6 CHP production unit (coal- and oil-fired, biomass such as wood chips), which is located on the southwest tip of the Bornholm island, operates 1 x 37 MW thermal generating unit. The commission of generating unit 6 was completed in 1995. The synchronous turbo generator (2 poles) with wound rotor, manufactured by ABB, is rated apparent power at 46.8 MVA, 10.5 kV nominal voltages, 3000 rpm and 0.85 pf. The boiler is also from Vølund Energy Systems and has a power capacity of 140 tons/hour. The excitation system, also manufactured by ABB, consists of a power transformer based static exciter directly fed from the generator terminals, and a digital controller. The excitation digital controller features a variety of regulating, limiting and

stabilizing functions implemented. The steam turbine (G40, high pressure/LT22, low pressure) is a condensing reheat turbine, rated at 37 MW and 3000 rpm. The steam turbine is installed with a digital governor; all manufactured by ABB. Unit 6 is equipped with a power factor controller. These controller features are primarily used in islanding operation mode, as the frequency and voltage stability normally is maintained by the interconnection to the Swedish power system. Most of the data were taken from the manufacturer's documentation and from Østkraft.

4.3.3 Diesel Units Rønne

Apart from the large CHP, thermal unit and wind, the Bornholm has other generating units like diesel plants. Rønne power plant has a total of 14 diesel generators. Ten of them were installed in August 2007. These newly installed diesel units are identical, and have a total apparent power of 10.5 MVA manufactured by Mitsubishi. These units are equipped with automatic voltage regulators (AVR) and could be typically used for peak load or emergency modes. The older types are Leroy Somer AC generators with four salient poles.

4.3.4 Wind Power

The Bornholm distribution system is characterized by a significant penetration of wind power. Some are outdated, small & fixed speed wind turbines. As of 2006, Østkraft installed 6 new wind turbines, three of which are the Vestas V80-2MW type wind turbines, and other three units are the Vestas V60-1.75MW type wind turbines. These new turbines equipped with doubly-fed induction generators (DFIG) with advanced frequency control and voltage control. The remaining wind turbines are primarily land-based older, smaller wind turbines under private ownership. Many of these turbines have a rated power in the range of several kWs up to 1300 kW, the highest power is 1300 kW (Nordex, Knudsker/Åker) and the smallest wind turbine being is 11 kW (Gaia-møllen, Østermarie). The total amount of grid-connected wind power approached 30 MW corresponding to more than 33% of the energy consumption. At present, most on-land sites in Bornholm with good wind conditions are already occupied by existing distributed wind turbines. An increase of on-land wind power will be achieved by the Danish replacement scheme, e.g., replacement of smaller, older wind turbines with newer, more powerful MW class units (as part of 'repowering' plan) [70]. The share of wind power in the Bornholm power generation mix will continue to increase. A summary of installed wind turbine types are also listed in **Appendix B**.

4.4 RTDS Simulation Platform

The RTDS simulator is a fully digital electromagnetic transient power system simulator, designed specifically to simulate the power systems and to conduct closed-loop testing of physical equipment. As mentioned, a real-time model of the Bornholm distribution system will be implemented by the RTDS. The brief description is provided.

4.4.1 RTDS Algorithm

The algorithm represents power systems on the basis of nodal analysis techniques. The inverse conductance matrix is multiplied by a column vector of current injections in order to calculate the instantaneous voltages at various nodes within the system. In general, the conductance matrix is a square, rather sparse matrix whose entries depend on the circuit components connected to the nodes. The ability to separate the conductance matrix into block diagonal pieces enables the simultaneous solution of the node voltages associated with each block. This so-called *subsystem* solution method is an important consideration in the parallel processing implemented in the RTDS. Each subsystem is simultaneously solved by different portions of the specialized hardware. The concept of mathematically isolated subsystems proved to be an important consideration during the development of an interface to the analog simulator.

4.4.2 Software and Hardware

The RTDS is a powerful simulation tool that accomplishes the task of real-time simulation via parallel computation as shown in **Figure 4-2**. Exploiting the delay in travelling waves on transmission lines and using trapezoidal integration, the system is capable of performing time-domain simulation at real-time speed using time-steps less than 50μs. Such small time-steps enable the RTDS to accurately and reliably simulate power system phenomena in the range of 0 to 2 kHz. A power system to be simulated is constructed using a dedicated software suite called real time simulation computer aided design (RSCAD). This software provides an easy to use graphic user interface (GUI) as well as large libraries containing numerous power system component and control models. The RSCAD suite is separated into different modules, the most important of which are Draft and Runtime. A system model is first built and compiled using Draft before the compiled file is used by Runtime to execute the simulation in real-time. The Runtime module enables the users to interact with the simulation in real-time by modifying various parameters during the simulation.

- Year of Installation : Dec 3, 2010
- 1st Phase Configuration : Three mid-size cubicles, total of 5 Racks
- Maximum Node Capability
  - 5 Racks x 22 nodes = 110 nodes
  - 4 GPC/rack
- Flexible and Expandable I/O cards
  - 3 GTAI (12CH, 16-bit Analogue Input Card)
  - 3 GTAO (12CH, 16-bit Analogue Output Card)
  - 3 GTDI (64CH, Digital Input Card)
  - 3 GTDO (64CH, Digital Output Card)
  - 3 GTFPI (Interface to digital & high voltage interface panels)
  - 1 GTNET (Ethernet Interface System, supports GSE, SV, DNP3 protocols)
- Portable I/O Cubicle for HIL & PHIL Testing

Figure 4-2 : RTDS specification and performance

4.5 Modeling Procedure

In order to conduct power system analysis, a sufficiently accurate model is required. The tasks involved in the modelling of Bornholm distribution system with the RTDS that need to be performed, are listed as follows. The work is divided into several different steps. For validating purposes, previous PF load flow results were used and compared.

Objective:

Develop the Bornholm distribution system in the RTDS simulation environment

Step 1

Prepare the Bornholm distribution system data and information for

- Data conversion
- Subsystem allocation

Step 2

Develop model blocks for 60 kV/10 kV substation buses, distribution lines including ac submarine cable, 132 kV/60 kV/10 kV transformers, RL loads, and major generation sites (Rønne Unit 5 and 6) including their associated controls.

Step 3

Start implementing each generation site one by one. Perform simulation and verify that the RTDS and the PF simulation models are consistent.

Step 4

Development of Frequency Domain Network Equivalent (FDNE) for major generation sites (i.e. refers to generic model of Bornholm distribution system in Section 4.7)
I.e. Substation names such as VAE, AAK, BOD, HAS, OLS, POU, SNO

Step 5

Perform simulation on various FDNE configurations and verify that the original RTDS simulation model is consistent with an equivalent.

Step 6

Develop a full 3-rack simulation case for Bornholm distribution system and verify that the degree of accuracy be acceptable.

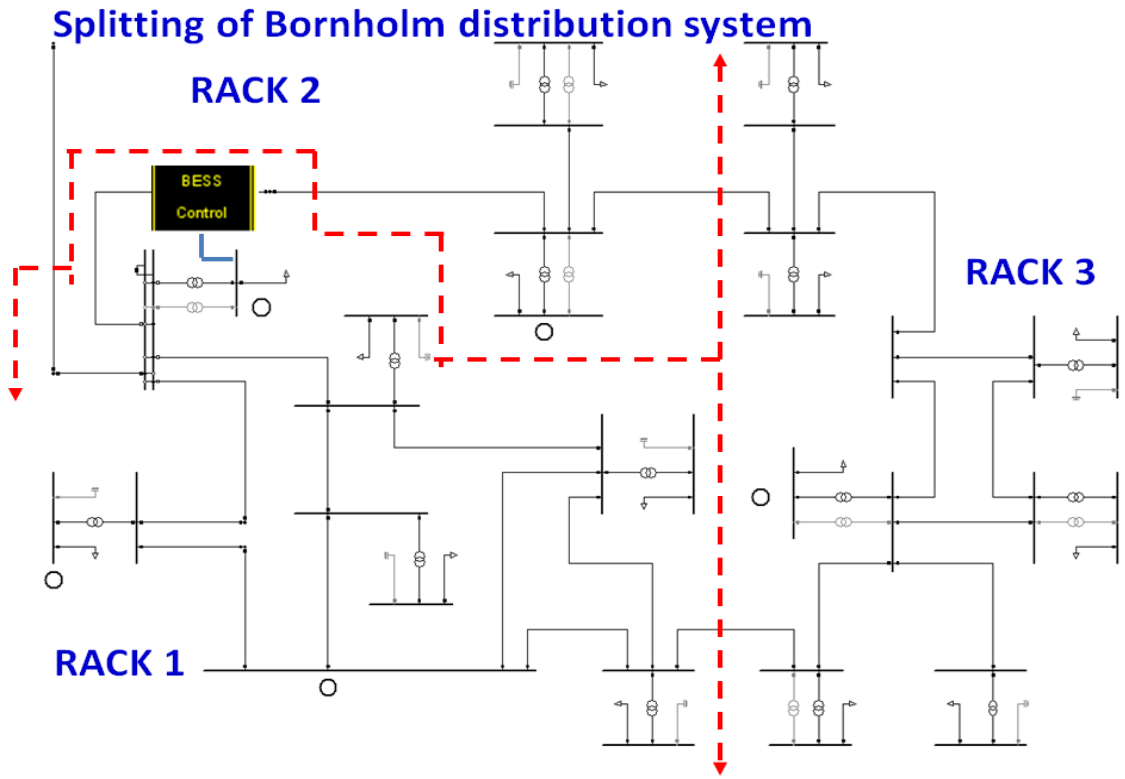

Figure 4-3 : A single line diagram of Bornholm distribution system showing the sub-system rack assignment

As mentioned, the Bornholm distribution system has been chosen for demonstrating various features of the RTDS in conjunction with the Ph.D. project (i.e. a small closely coupled distribution system modelling, islanding capability, integration of ESS, AGC design, coordinated control strategy of BESS and DG units, fuzzy-logic and agent-based control, etc.). The description of real time model of Bornholm is well documented with a number of technical papers referencing the distribution system [71] - [75].

4.5.1 Data Conversion

System parameters of all of the components (e.g. generator data, line data, etc.) are provided in PF format 'parameters' file. Initial conditions and system layout is provided in PF 'load flow data' file. Prior to the Ph.D project, it would have been required for the user to layout the system and enter all the parameters using the RSCAD/Draft. In order to automate the task of converting the data contained in the PF data files to a format, which can be used as input by the RTDS, a data conversion software package was used for seamless conversion. The feature available on PF takes the PF parameters as input and generates the power system simulator for engineering (PSS/E) files, which can be directly used by the built-in RSCAD conversion module. In order to permit conversion of the generator controls defined in the PSS/E parameters file to a form in which they can be automatically created in the RTDS software, new RTDS controls function blocks were created to represent the various exciters and governor/turbine models which are available in PSS/E and PF. The new function blocks are supersets of existing low level function blocks available as part of the RTDS controls compiler library. The new control function blocks can be initialized with parameters taken from the PSS/E parameters file. The data conversion process is further complicated by the fact that the RTDS requires that the power system circuit is split into subsystems according to specific rules so that parallel processing techniques can be used to achieve continuous real-time operation. This particular feature made the start-up of the large scale simulations virtually seamless. The following subsection outlines the subsystem allocation (i.e. splitting the entire system into sub-systems) procedure used in the preparation of the Bornholm base case and its implementation using recommended guidelines.

4.5.2 Subsystem Allocation

This subsection explains processor allocation guidelines for both large time-step and small time-step implementation. Because small time-step implementation consumes more processors than large time-step implementation, the guidelines are different for each situation. In general, a reduced instruction set computing (RISC) processor can assign a maximum of 10 units and the processor utilization for passive components (i.e. shunt reactors) are solved by the network solution and do not require additional processors. **Figure 4-3** is a single line diagram of the Bornholm distribution system implemented in RSCAD and shows the subsystem rack assignment. It seems quite feasible to model these systems on the RTDS. The recommended approach in this case is to model the 60 kV systems with the lines, cables, transformers, loads, source, etc. using the standard large time-step components using one network solution. Since each giga processor card (GPC) card has two RISC processors and each network solution requires one GPC processor. Therefore, the large time-step network solution can have a maximum of 66 single-phase nodes and 56 single-phase switches. In other words, the large time-step network solution only allows 22 three-phase buses to be included in the circuit which is

almost enough for the 60kV Bornholm distribution system. For example, **Figure 4-3** has 18 three-phase buses. The following formula is used to find the required number of processors for large time-step network solution is:

Number of required processors for nodes: 54 (1Ø) / 18 = 3 processors

The 10kV substations could be split off to separate subsystems using the subsystem splitting transformers as the interface points. The 10 kV subsystems could be modelled as large time-step networks at the respective substation. If the subsystem splitting transformers will be used to separate out the 10kV substations, it will require 10% (≈1 unit) of one RISC processor per one step-down transformer. Since there are 19 transformers,

Number of required processor for transformers: 19 x 0.1 = 1.9 processors

Likewise, the single circuit lines, there are a total number of 26 distribution line models connected to a system equivalent. Each one requires 2 units (20% of one RISC processor). The following formula is used to find the required number of processors,

Number of required processor for single circuit lines: 26 x 0.2 = 5.2 processors

Then, repeat the process for the remaining components, the following **Table 4-4** can be obtained.

Table 4-4 : Processor allocation for Bornholm implementation

Component	Quantity	# of GPC (RISC)	Comments
Nodes (3Ø)	54	3 RISC	3 Network Solutions
Subsystem Splitting TR	19	1.9 RISC	60/10 kV Transformers
Single Circuit Lines (3Ø)	26	5.2 RISC	Travelling wave, Bergeron model with embedded breakers
DFIG Wind Generator	6	12 RISC	Power electronic converters modeled in detail
Generator / TR (3Ø)	1	0.2 RISC	Integrated generator transformer model
Source (3Ø)	1	0.1 RISC	Swedish Network Equivalent
Controls		3 RISC	
Total No. Processors		25.4 RISC	
Total No. Cards		26/2 = 13	Requiring a minimum of 13 GPC = 3 racks

Furthermore, if the 10 kV distribution systems are modelled as small time-step sub networks to accommodate VSC based converters associated with the wind generators, the hardware requirement could be 5 racks depending on the configuration of the wind gen-

erators and the level of detail implemented. The system would require approximately 16 small time-step sub networks that would be connected to one another via travelling wave transmission lines. However, the 10 kV distribution systems are modelled as aggregated lump load. It should be noted that the real system also comprises a large number of 0.4 kV lines which have not been modelled.

4.5.3 Implementation

In order to have confidence, a significant portion of the Bornholm distribution system would have to be modelled. Certainly the major 60kV/10kV distribution lines, ac cable model between Sweden and Bornholm, Denmark and major generation sites including Unit 5 and Unit 6 with their associated controls and loads had to be represented so that system transient stability, inter-area oscillations and generator swings caused by system disturbances could be observed. By using the RTDS simulator capable of modelling a large portion of the power system, many different operating conditions and fault scenarios could be studied once the dynamic data is entered. It must be kept in mind that the available data have been treated cautiously, represent the best possible approach and based on the existing PF data availability. The scope of the work is to model and validate the above mentioned components in the RTDS simulation environment. This section contains the development of RTDS model blocks for large time step implementation. **Figure 4-4** shows a portion of the 60/10kV Bornholm distribution system with HAS 10kV wind generators implemented in the RTDS.

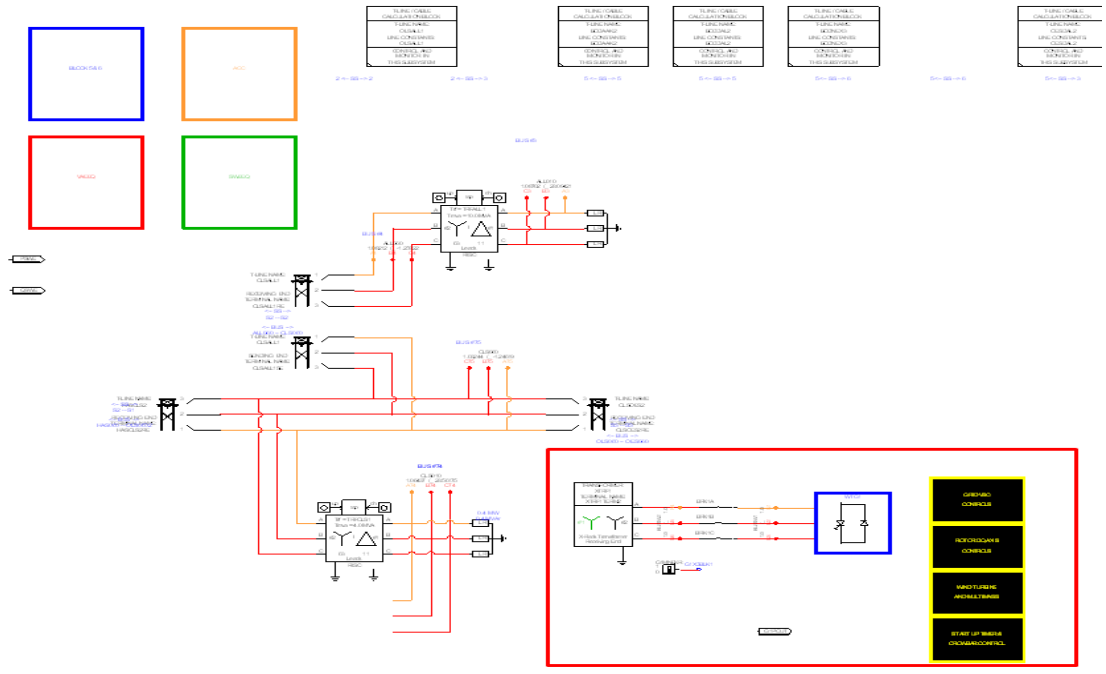

Figure 4-4 : A portion of the Bornholm power system implemented in RSCAD (i.e. a red box contains DFIG wind turbine)

The main strategy to implement the Bornholm distribution system is to use only one or two rack for the main MV backbone of the network and to use both cross-rack transmission lines and the cross-rack transformers wherever possible to split the network into different racks. In view of this, it seems feasible to model Bornholm distribution system on the RTDS using both cross-rack transmission lines and the cross-rack transformers approach. However, the following recommendation should also be noted and considered regarding the Bornholm case;

1. The distribution lines in the network are all very short (i.e. the distribution lines are too short to utilize the travelling wave algorithm). There is no chance to divide the power system into several racks if the normal approach is taken.

2. Plan out the allocation of the Bornholm distribution system considering that there are really no long lines to split between racks and what portion of a system will be mapped to different racks.

3. Using a single line diagram, identify which lines are long enough to split the system and sketch out the allocation as shown in **Figure 4-3**.

4. After carefully selecting the distribution lines that separate the subsystem, the following modifications are performed (i.e. traveling wave model).

- Combine T-line 34 and T-line 35 so the line is about 11.4 km. Then, the line Length is increased to 15km.
- The cable T-line 55 is used. This cable is about 43.5 km in length and the Shunt admittance B is increased to a more reasonable value.
- The T-line 46(13.05 km) and T-line 51(10.995 km) are combined.

5. With these modifications, only three overhead lines and one cable line are used as cross-rack transmission lines. As explained above, the modifications might bring some error. But the consequences are not very significant. Here, all the lines are extremely short so it is the best approach taken to implement the system.

6. Included in the **Appendix C** of the report, a very simple example of using the subsystem splitting transformer is provided. A small shunt capacitance is added to the transformer so it can be modelled with a travelling wave model and split between racks.

The Bornholm distribution system was modelled entirely using large time-step techniques to accommodate mainly 60kV grid and radial 10kV grid. As a result, the total number of subsystems on the RTDS was five taking into account wind generators to be added in the subsystem 4 through subsystem 5. The recommended approach in this case is to model the 60kV network with the Bergeron T-lines, cables, two winding transformers, RL loads, source, etc. These models have been mainly constructed in subsystem 1 through subsystem 3, respectively as shown in **Figure 4-4**. For example, **Figure 4-4** of the red box shows the connection of cross-rack transformer component to the 10kV bus named HAS010 (Bus #68) in three phase line diagram mode. The 10kV substations have been added to the main MV grids. Consequently, the 10kV bus is connected to ZIP load in the subsystem 1-3. This is because that the particular subsystem still has some availability of node processors remaining. Load buses are usually assigned as PQ buses. Since the RTDS is not a load-flow platform, it is very important to get dynamic data on different types of generation units such as Rønne (Unit 5, Unit 6), diesel units, biomass units and wind turbines. Inclusion of these as synchronous generator models and their associated controls in simulation cases permits the user to study the interactions of the generator mechanical dynamics and control loops with the power system. The effect of generator dynamics and control action may have critically important implications towards the stability of the power system. If detail parameters for the particular machine of interest are not available, approximate parameters may be obtained from example data contained in references [53], [76]. The generator type and MVA rating can be used to choose the generator data to approximate the unit of interest if necessary. The available data are taken from the previous CEE projects for the Unit 5 and Unit 6 accordingly. The resulting model comprises a meshed 60 kV system with the cable connection to Sweden at the 132 kV level, 60 kV/10 kV substations with distribution transformers, shunts, loads and generation units. For distribution line models which have travel times which are shorter than one time-step, π-equivalent will have to be used. At a 50 μs time-step the minimum length line that can be simulated using the travelling wave model is approximately 15 km. Any line shorter than this length will have to be modelled using π-equivalent. Single π-equivalent models for short lines yield acceptable simulation accuracy. Second, it is also important to investigate the concept of secondary frequency control for islanding operation of the Bornholm distribution system as mentioned earlier, and therefore it is necessary to implement the AGC scheme as depicted in **Figure 4-5**.

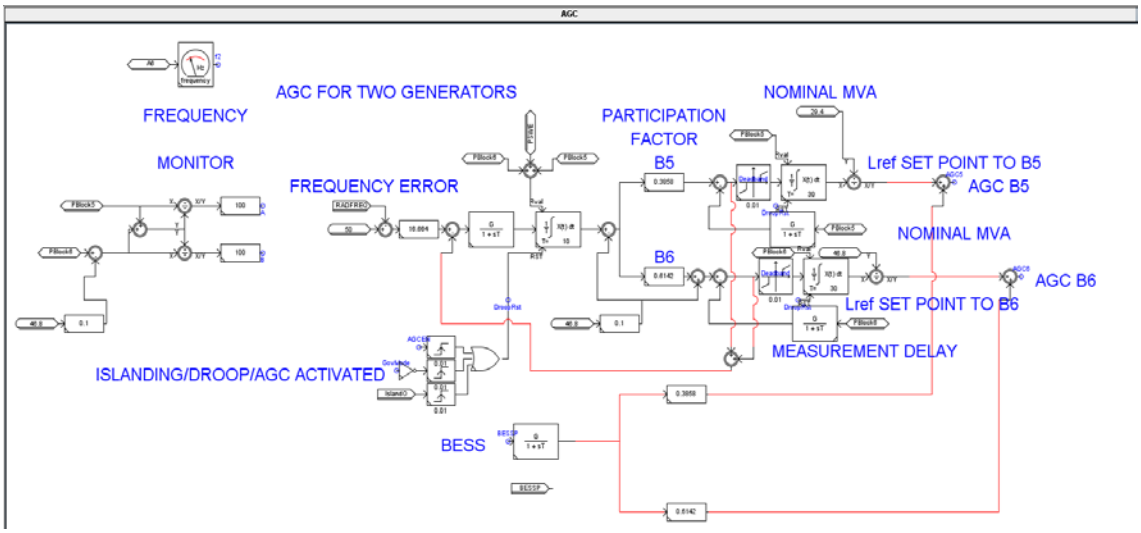

Figure 4-5 : AGC scheme for unit 5 (B5) and unit 6 (B6)

The work is to develop effective control strategies for islanding operation of ADN or a small island, Bornholm distribution system. Particularly, this control strategy consists of a primary control action of the BESS and a secondary control action of the MMS. During the islanding operation, the frequency and voltage are regulated by the fast-acting primary control of the BESS. The secondary control of the MMS detects the change of the power output of the BESS and tries to return the power output of the BESS to reference value by assigning the difference to the dispatchable DG units. The dispatchable DG units should be coordinated to share the load following burden of the BESS. The Bornholm distribution system will be used to carry out case studies to verify the proposed primary frequency control performance. General assembly of the Bornholm distribution system and its associated controls are documented in the reference [71]. The technique of bringing the Bornholm distribution system model to a steady-state operating condition is briefly described in the following subsection.

4.5.4 Initialization

Manual initializing a simulation case can be very complicated and time consuming, especially for large power systems. If the initialization is not done correctly, the simulation will take longer to reach a stable operating point or may even become unstable. The basic idea of the load flow and initialization module is illustrated in **Figure 4-6**. The results of the load flow performed by the PSS/E software are used as the initial conditions for both the PSS/E transient simulation and the RTDS simulation. The RTDS uses the following output from the PSS/E load flow to initialize the generator models.

- Generator bus voltage and angle
- Generator initial real and reactive power

When the RTDS simulation is started, all bus voltages are initially zero and the generators are set to operate in locked mode. Locked mode operation for the generators causes each generator to spin at exactly synchronous speed at the initial rotor angle. The mechanical torque signal coming from the governor/turbine model is ignored during locked mode operation. While the generators are locked, the exciters are functional and bring up the system bus voltages according to their set points which are preset based on information from the load flow data. Once all of the system bus voltages have reached steady-state, the generators may be taken out of locked mode and switched to free mode. In free mode, the generator speed is determined by the system conditions and mechanical torque produce by the governor/turbine models. If the initial conditions provided by the load flow do not accurately represent the system parameters and conditions simulated on the RTDS, the generator will exhibit a swing when it is changed from locked to free mode. Once all generators in the system model have been changed from their locked to free operating mode, the RTDS simulation is running in steady-state with the same bus voltages and power flows described by the initial conditions. At this time the predefined disturbance can be applied to the system model and the reaction of the system to the disturbance can be observed.

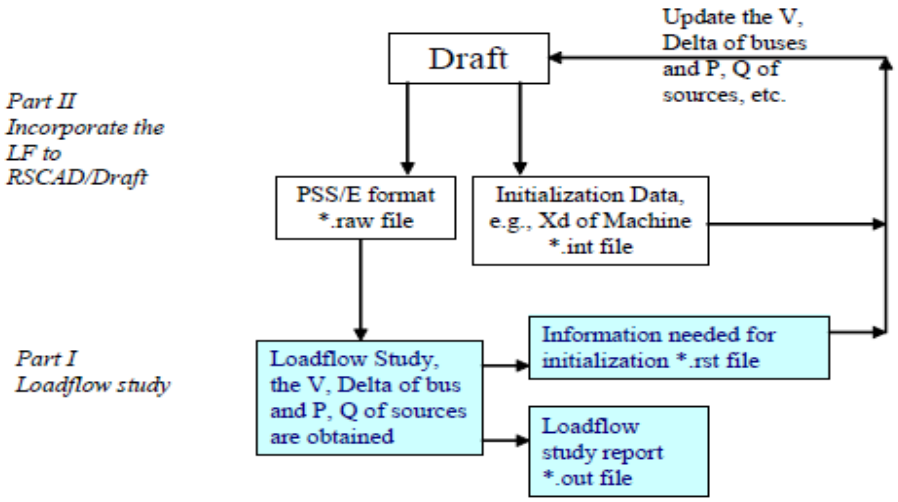

Figure 4-6 : Flowchart of the RTDS load flow and initialization concept

4.6 Comparison of RTDS and PF Simulation

PF includes both load flow and transients stability algorithm while the RTDS implements the electromagnetic transient algorithm. Transient stability software simulates both the electrical and mechanical aspects of the power system. The electrical portion of the power system is represented using root mean square (RMS) quantities which are recomputed every few ms (i.e. 8 ms). Typically, the system load flow is solved and is used as the initial condition for a transient simulation defined by some disturbance. Generator rotor angles are monitored to determine the system's ability to recover from the particular disturbance. The electromagnetic transients algorithm implemented in the RTDS represents the electrical aspects of the power system using instantaneous quantities. Typically, the state of the power system is computed every 50 µs (i.e. corresponds to approximately every 1 electrical degree at 50 Hz). The electromagnetic transient simulation not only computes the 50 Hz characteristics of the system, but also the harmonic response. The RTDS results will include the consequences of higher harmonics which may be produced by the simulated disturbance. With a time-step of 50 µs harmonics of some kHz may be represented accurately. Simulation of identical power system models by PF and the RTDS should yield comparable results at or near 50 Hz which has been observed in the following Section 4.7.

4.7 Simulation Results

4.7.1 Steady-State Simulation

All simulation results described in this chapter have been successfully completed. Please refer to the reference [71] for more details on the description of simulation.

Table 4-5 : Steady-state voltage comparison between RTDS and PF

	RSCAD(kV)	PF (kV)	Difference (%)		RSCAD(kV)	PF (kV)	Difference (%)
AAK010	10,8872	10,87812	0,083470306	**OLS010**	10,6437	10,64337	0,003100522
AAK060	65,097	65,09102	0,009187135	**OLS060**	64,947	64,95413	0,010976977
ALL010	10,8702	10,86244	0,07143883	**POU010**	10,5146	10,50521	0,08938422
ALL060	64,9278	64,93489	0,010918629	**POU060**	65,073	65,0587	0,02198015
BOD010	10,4923	10,48645	0,055786277	**RNO010**	10,6947	10,68252	0,114018041
BOD060	65,0808	65,07135	0,01452252	**RNO060**	65,2146	65,21463	4,60019E-05
BOR060	63,8472	63,82999	0,026962248	**RSY010**	10,6613	10,6557	0,052554032
BOR130	129,6	129,6	0	**RSY060**	65,2512	65,24819	0,004613155
CAB0601	64,9332	64,94732	0,021740697	**SNO010**	10,717	10,7139	0,028934375
CAB0602	64,2138	64,20595	0,012226281	**SNO060**	65,2248	65,22358	0,001870489
CAB0603	64,1976	64,18935	0,012852599	**SNO0602**	65,0772	65,08377	0,010094683
DAL060	65,0754	65,06809	0,011234385	**SVA010**	10,6246	10,61944	0,048590133
GUD010	10,5801	10,5783	0,017015967	**SVA060**	65,07	65,06189	0,012465054
GUD060	64,9998	64,99956	0,000369233	**VAE010**	11,62686	11,59867	0,243045108
HAS010	10,4637	10,44844	0,146050511	**VAE060**	65,2854	65,28206	0,00511626
HASF60A	64,9452	64,96013	0,022983328	**VAE0602**	65,247	65,24474	0,003463881
NEX010	10,6103	10,60643	0,036487301	**VES010**	10,6767	10,66818	0,079863669
NEX060	65,0688	65,06032	0,013034058	**VES060**	65,2512	65,24903	0,00332572
OES010	10,6671	10,65684	0,096276194	**VIA010**	10,6765	10,66379	0,119188394
OES060	65,0076	65,00728	0,000492253	**VIA060**	65,2524	65,24984	0,003923381

4.7.2 Dynamic Simulation

For the dynamic simulation cases, several fault scenarios (i.e. three phase line to ground, single phase to ground and b, c phase to ground temporary, unclear faults on transmission, transformer & buses faults, etc.) are applied to the Bornholm distribution system and the simulated Bornholm distribution system, is actually able to operate and remain stable under different fault conditions as shown in **Figure 4-7**. A three phase fault of 6-cycle duration on bus 98 is simulated. Inside a solid red box, a view of 3 phase voltage changes of around 5 s is shown. It can be seen that bus voltage returns back to the initial value after fault has been cleared.

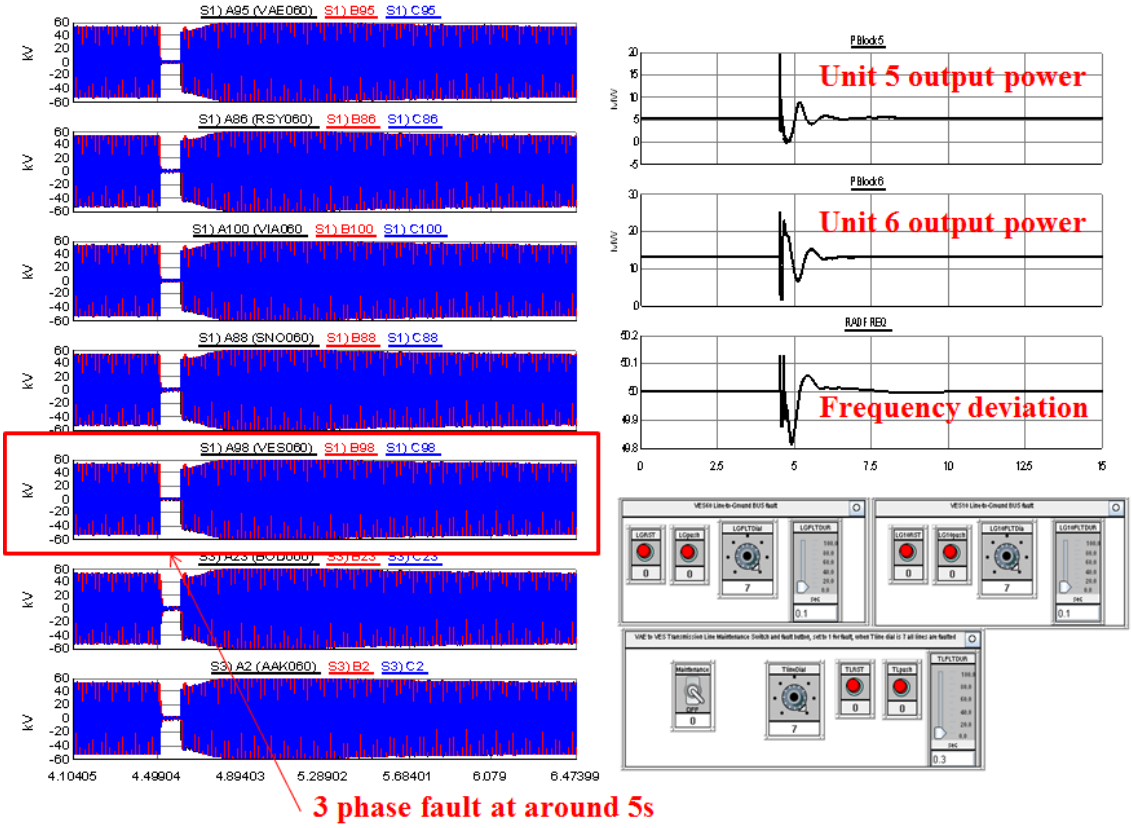

Figure 4-7 : Monitoring of bus voltage after 3 phase fault at VES 60 kV bus and nearby buses (duration fault = 6 cycle, a view around 5s)

4.7.3 Simulation of Islanding Operation

4.7.3.1 VES 60 kV 3 Phase Line to Ground Fault

Two simulation runs are compared with and without AGC during islanding operation. A three phase fault of 0.1 second duration on bus VES 60kV is simulated. The simulation results of the active power output of unit 5 and unit 6, and the system frequency are shown in **Figure 4-8**.

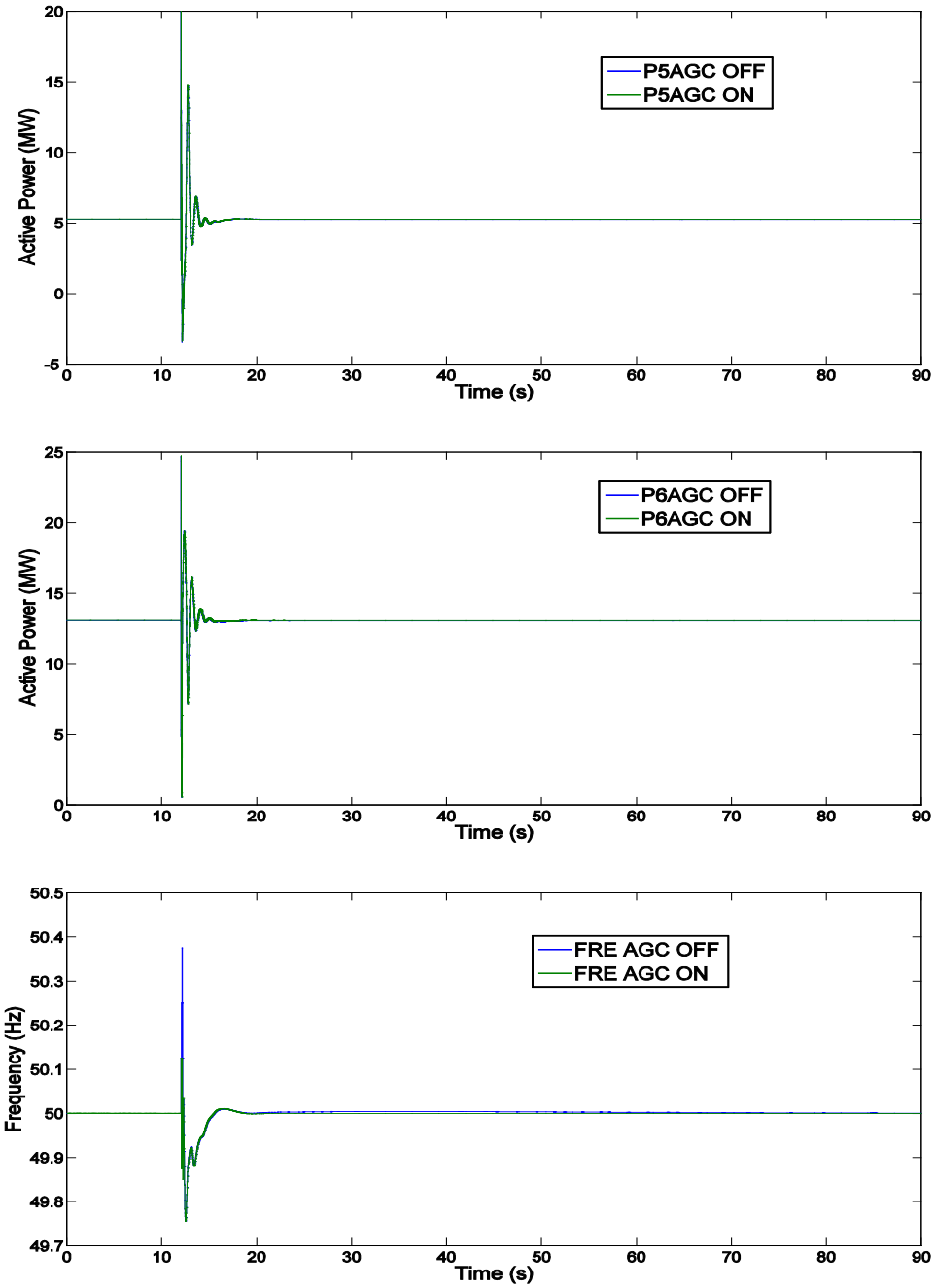

Figure 4-8 : Droop mode, islanding operation, fault duration = 0.1s (P_5,P_6 f , *top to bottom*)

4.7.3.2 20 MW Load Increase

A sudden load demand change is presented with and without AGC during islanding operation. The load at HAS010 bus is varied from 3 MW to 20MW, while the simulation is running. It can be seen from **Figure 4-9** that both the active power of generator unit 5 and 6 (AGC participating units) increase from 5.25 MW to 11.66 MW, and 13 MW to 23.35 MW, respectively to control the overall island frequency by sharing or rescheduling between two units based on their participation factors. The implemented AGC ensures that the frequency remains within threshold limits of the system as evident from the frequency variation on the bottom graph. In this case, the frequency returns to the nominal value with AGC enable (blue curve), whereas the frequency does not return to the nominal value without AGC (green curve).

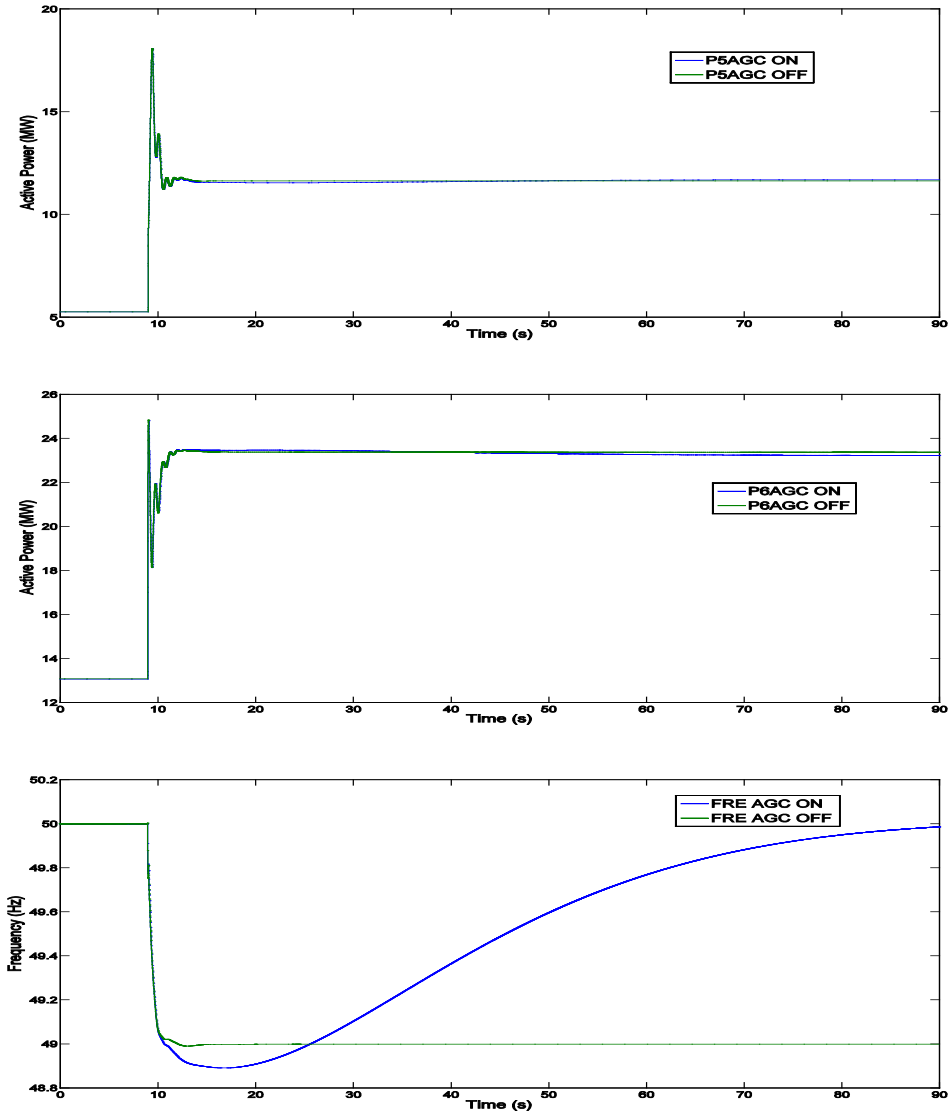

Figure 4-9 : Droop mode, islanding operation, 20 MW load increase (P_5, P_6, f, *top to bottom*)

4.7.3.3 Bornholm imports more power from Sweden

This particular situation is when Bornholm is importing most of power from Sweden. The Swedish interconnection is disconnected and the Bornholm distribution system is under islanding operation. The simulation results of the active power output of unit 5 and unit 6, and the system frequency are shown in **Figure 4-10**.

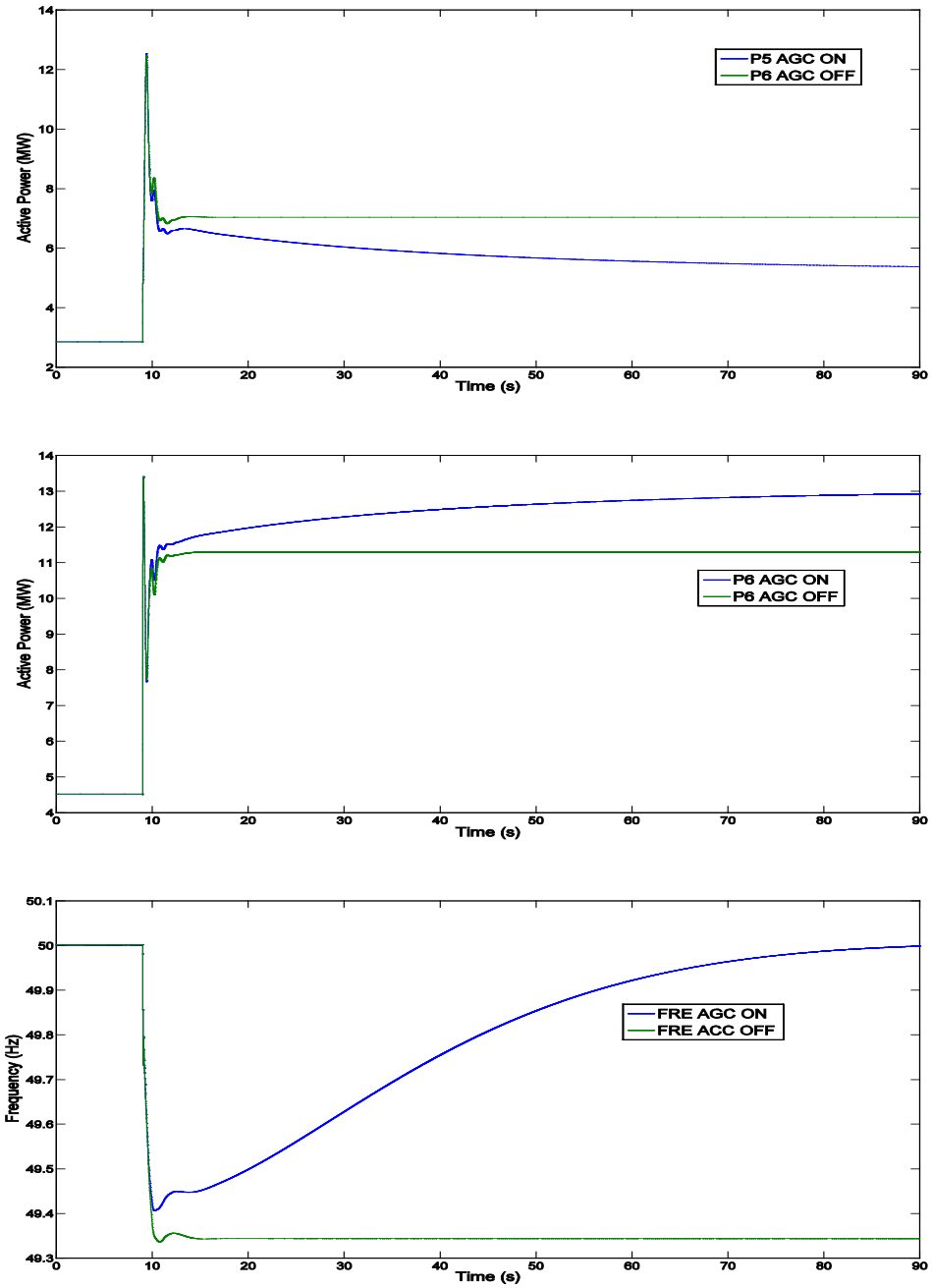

Figure 4-10 : Droop mode, islanding operation

4.7.3.4 Bornholm exports more power to Sweden

This particular situation is an opposite case to the previous case. Hence, Bornholm exports more power to Sweden immediately prior to the islanding event, both generator units' responses deviated beyond the acceptable limits as expected. The simulation results of the active power output of unit 5 and unit 6, and the system frequency are shown in **Figure 4-11**.

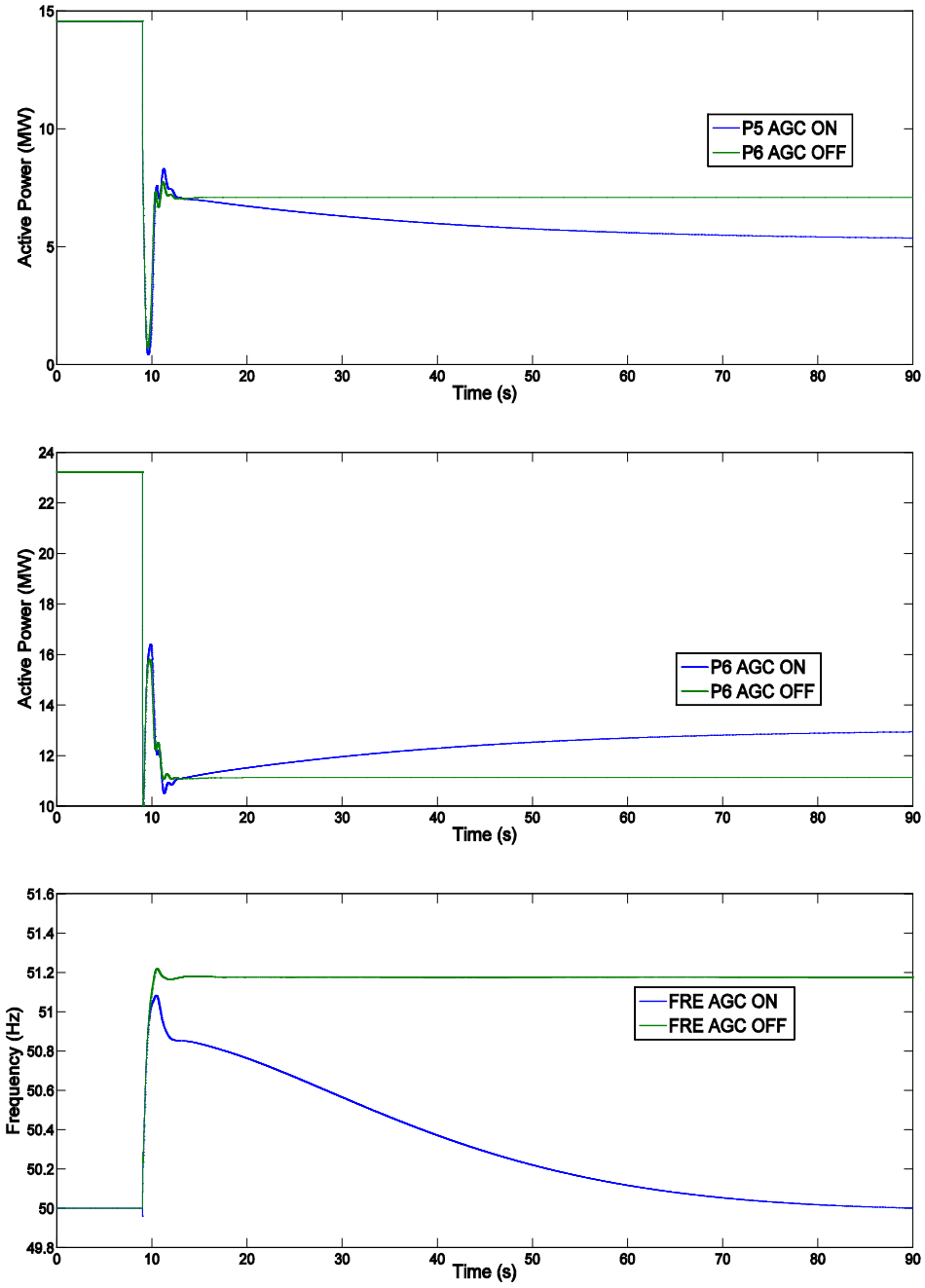

Figure 4-11 : Droop mode, islanding operation

4.7.3.5 Different Participation Factors

This particular simulation case is to verify that the AGC provides a desirable performance based on participation factors in order to adjust the production levels and consequently correct the frequency offset. It can be seen from **Figure 4-12** that the active power of generator unit 6 increases from 4.5 MW to 15.5 MW, while the unit 5 decreases from initial value 2.5 MW to 1.4 MW to control the overall island frequency by rescheduling between two units based on their participation factors. It is clear that the most of burden is imposed on the unit 6. The larger the participation factor the more power contribution it makes.

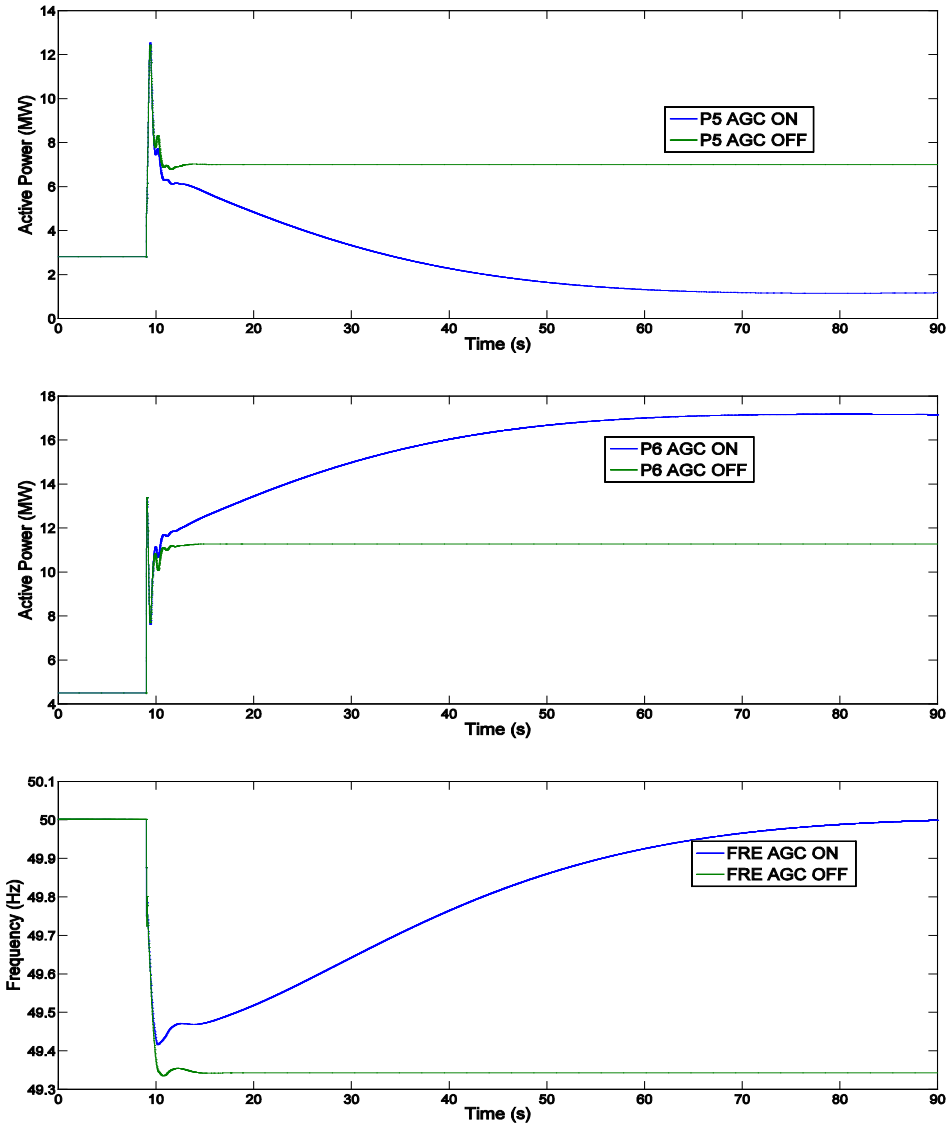

Figure 4-12 : Droop mode, islanding operation, different participation factors P_5=0.1, P_6=0.9)

4.8 Generic Model of Bornholm Distribution System

An equivalent generic model is of great interest that does not contain the confidential information meanwhile conserves the original system characteristics or retains most properties of the original system. It is also becoming increasingly important to be able to build equivalent systems or generalized systems, which could provide similar dynamic responses as the actual power system, however avoids the detailed information on the original power system components such as generators, transformers, and lines [77] - [78]. Thus, a strong stimulus exists for the development of equivalent or generalized model of the Bornholm distribution system in order to optimize the resources necessary to analyse in detail the dynamic behaviour of the Bornholm distribution system.

4.8.1 Proposed Equivalent

The algorithm used in this work is based on the author's previous research in [79], and is an extension of the earlier research of [77] improving dynamic reduction of power systems using relation factors combining with FDNE feature available in the RTDS. The proposed equivalent procedure is illustrated in **Figure 4-13**. In the earlier work [79], a dynamic equivalent approach using the relation factors and errors between generators has been developed in order to identify the groups. Also, the participation factors are used to aggregate the generators in the same group. Once the coherency identification procedure creates a reduced network in which coherent groups of generators are each replaced by a single representative generator in the first step. In the second step, the network is then modified and the parameter randomization takes place in which Mat lab's NORMRND function is used to generate random numbers from the normal distribution with mean parameter μ and standard deviation parameter σ. The μ is set as the original value of the distribution lines, cables, and transformers' leakage reactance's, and σ varies in the different cases. As the last step, FDNE is adopted with the above two steps to accurately capture the high frequency behaviour. Together, these three steps create an equivalent system that is valid for the Electromagnetic Transient (EMT) simulation. The advances of the FDNE algorithm are adopted from the previous research work [80] - [81]. The detailed procedure is available in literature [79] - [85], and hence is briefly discussed.

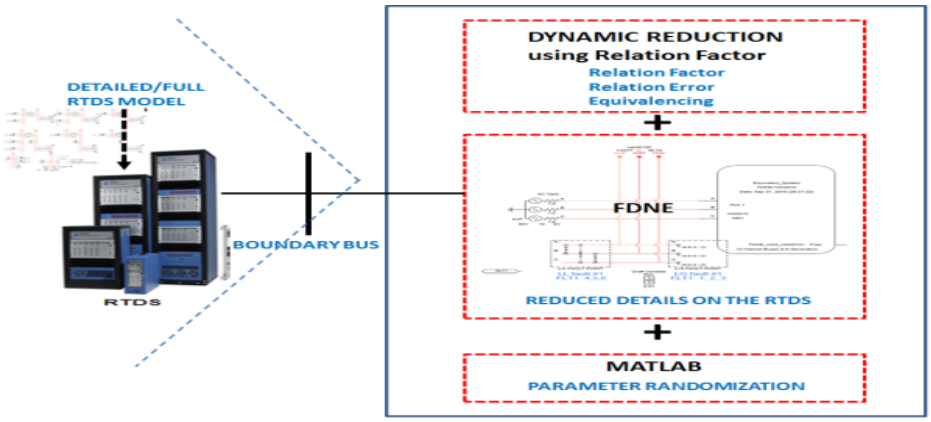

Figure 4-13 : Proposed equivalent procedure

4.8.1.1 Dynamic Reduction

A reliable coherency measure is the rotor angle and machine speed deviation. The coherency procedure is applied to the generator buses in order to reduce their numbers and is typically made up of three steps. In [79], the coherent group is directly identified from the state matrix according to the relation factors, which represent the relative coupling degree between the generators. The first step is the identification of groups with coherent generators, which have similar characteristics for certain disturbance. The second step is the aggregation of equivalent generators among discriminated groups. All generators and associated controllers in the coherent group are weighted by participation numbers, and aggregated to construct a dynamic equivalent. The third step is the network reduction considering the power flows and bus voltages of the original system. This coherency based network reduction procedure gives a reduced model of the network representing its electromechanical behavior. The external systems (is referred to as equivalents) or reduced systems, shown in **Figure 4-15**, consist of some buses such as boundary buses, retained buses and deleted buses when the network reduction is performed.

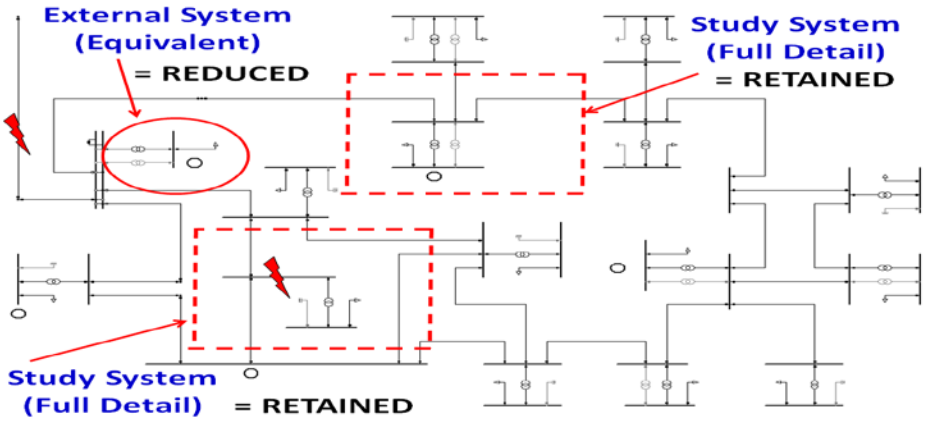

Figure 4-14 : Reduced system and retained systems

4.8.1.2 Parameter Randomization

This part of the work develops the generic model of the network. It includes two steps. In the first step, a generic topology of the network is proposed to represent the common topology patterns of the real network [77]. In parallel, the transmission/distribution lines, cables, and transformers are categorized based on their types, material properties, parameters (e.g. length, leakage reactance), etc., and the generic parameter sets are developed from each category and used in the equivalent RTDS model for further process which later combines with above FDNE process into form a simpler equivalent. The line parameters of the proposed generic distribution systems are identified, averaged and randomized based on the complete data of the 60 kV and 10 kV lines using Matlab's NORMRND function. This is a useful technique for obtaining the randomized numbers. It generates random numbers from the normal distribution with mean parameter μ, and standard deviation parameter σ. The following **Figure 4-15** is a simple explanation of this technique.

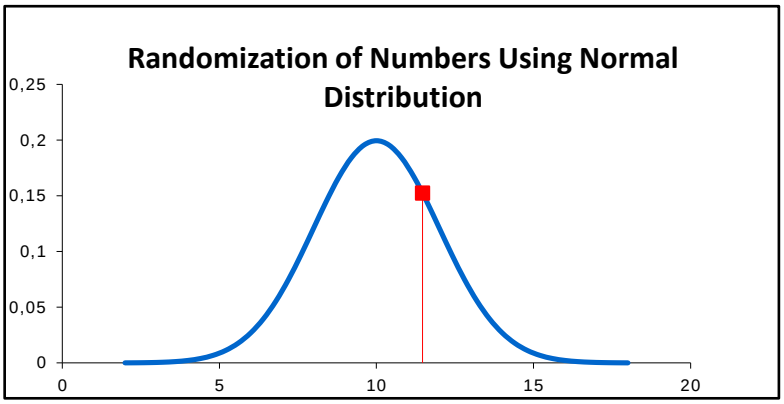

Figure 4-15 : Result of randomization for type C, 60kV distribution line

This resulted in 38 groups in which 14 of the typical categories are used in the proposed generic model, which is summarized in **Table 4-6**.

Table 4-6 : Categories of distribution line types, sizes and properties

Category	Material Properties
Type A	*Cab_3x1x150 PEX Al+25Cu.TypLne*
Type B	*Ohl_3x1x130 StAl+50Fe.TypLne*
Type C	*Ohl_3x1x130 StAl+50Fe.TypLne*
Type D	*Cab_3x1x095 PEX Al+25Cu*
Type E	*Cab_1x3x240 PEX Al+35Cu*
Type F	*Cab_1x3x095 APBF Cu*
Type G	*Cab_3x1x300 PEX Al+35Cu*
Cable A	*Island to sea cable bus*
Cable B	*Sea cable*
Cable C	*Inland bus to sea cable bus*
Type H	*AL095*
Type I	*AL050*
Type J	*CU050*
Type K	*CU035*

4.8.1.3 Frequency Domain Network Equivalent

The concept of FDNE is making a model which can be simulated in the time domain and at higher frequencies has essentially the same frequency response as the reduced network and hence has the same essential time domain response. The FDNE is a two part equivalent that provides a way of simulating larger power systems with reduced details on the RTDS. Therefore, the equivalent uses far less hardware resources (i.e. less computational processing power) compared with simulating the original system with full details and allows users to simulate a much larger overall power system using currently available hardware with minimum loss of accuracy [83]. The general idea of such equivalent is illustrated in **Figure 4-16**.

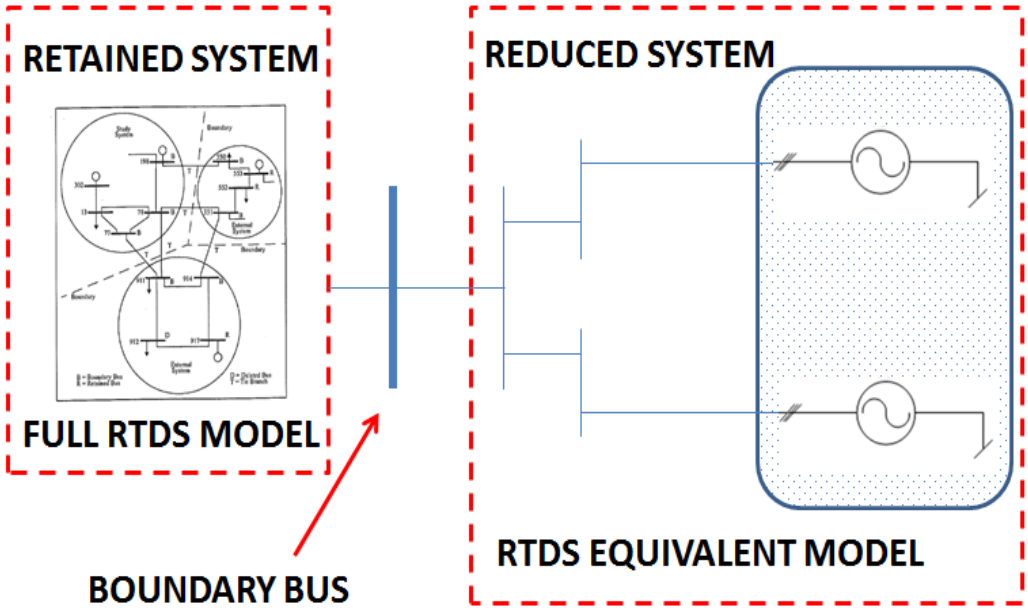

Figure 4-16 : General concept of FDNE

The Bornholm equivalent generic model has been implemented and the final test system used in the simulation is depicted in **Figure 4-17**. The real system is firstly modeled entirely on the RTDS and named as 'RTDS Full Model Original' in the simulation results. As they are represented in full detail, their results can be regarded as benchmark for validating the proposed 'RTDS Equivalent'.

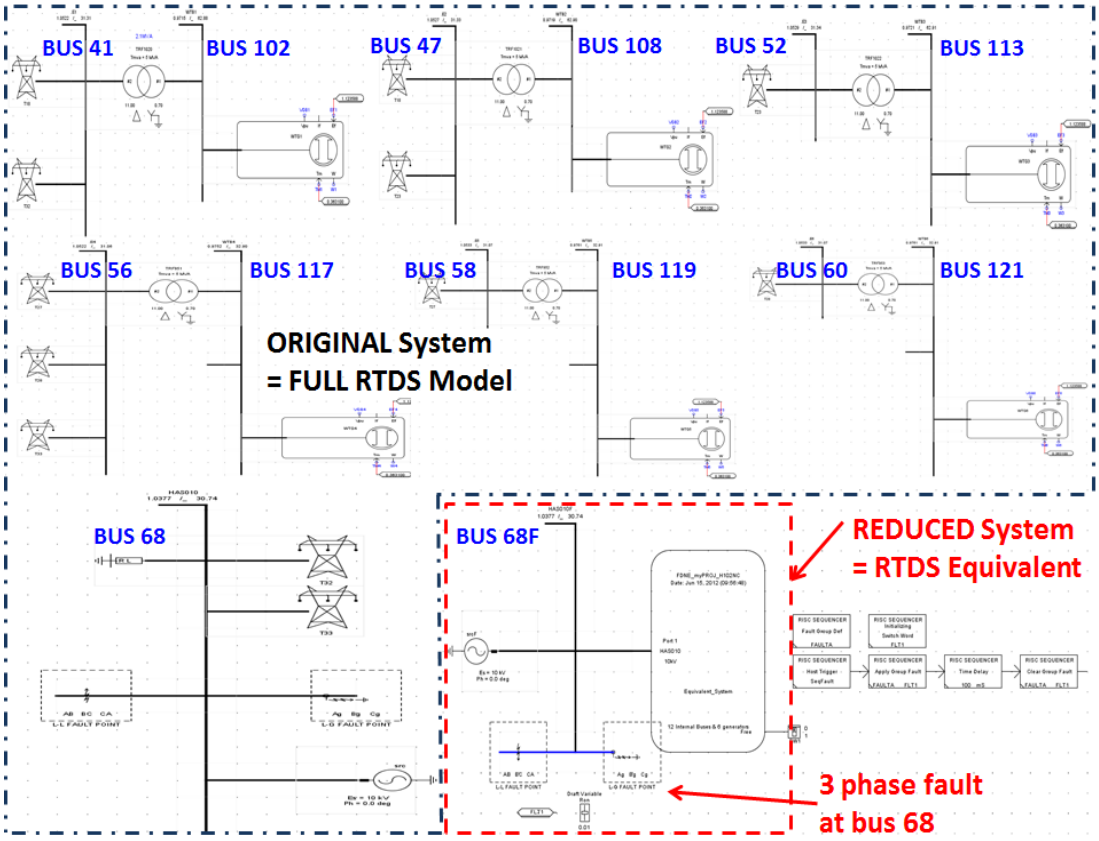

Figure 4-17 : A portion of RTDS equivalent generic model of Bornholm distribution system

4.9 Simulation Results

Several simulations were performed in order to validate the proposed equivalent approach. A three phase fault of 6-cycle duration on bus 68 is simulated. The simulation results of the RTDS Full Model Original and RTDS Equivalent model are shown in **Figure 4-18**. It can be seen from the **Figure 4-18** (a) – (b) that the active and reactive power of generator #1. The first one is shown with legend RTDS Full Model Original (blue curves) and the second one is the proposed RTDS Equivalent model (green curves), respectively. **Figure 4-18** (c) shows the transient behaviour of the relative generator speed after the disturbance.

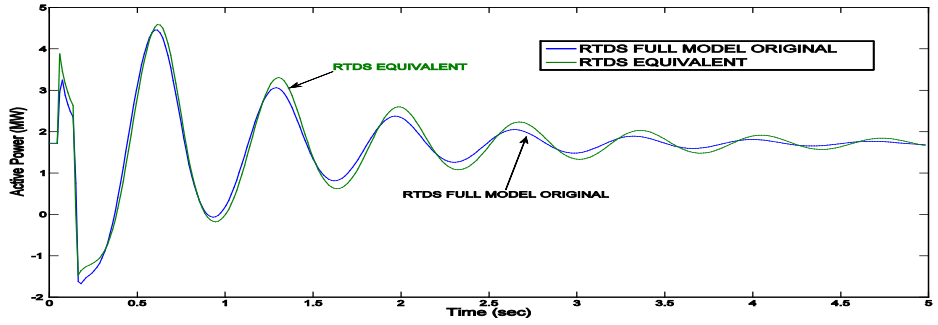

(a)

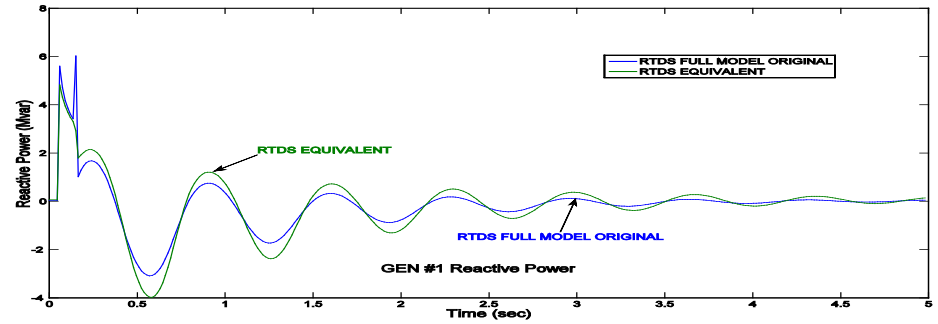

(b)

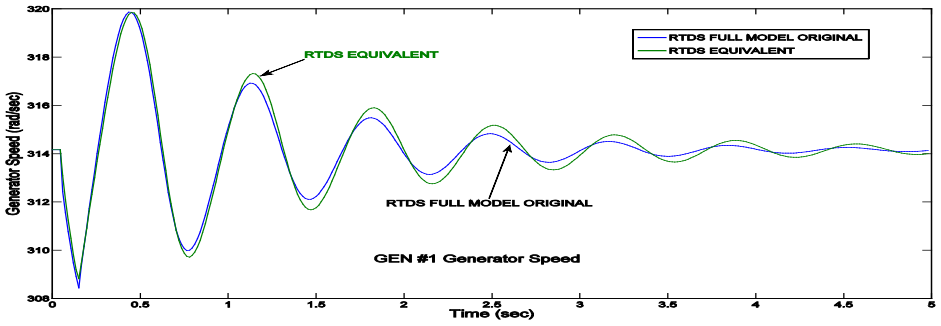

(c)

Figure 4-18 : Comparison of RTDS Full model and RTDS Equivalent is subjected to a three phase fault of 6 cycle duration on bus 68 (a) generator #1 P_{out}, (b) generator #1 Q_{out}, (c) generator #1 rotational speed

Figure 4-19 shows the three phase voltage of the bus 68 of the retained and reduced system. Two curves are shown. The first one is shown with legend RTDS Full Model Original (blue curves) and the second one is the proposed RTDS Equivalent model (green curves), respectively. The two curves are nearly identical and appear as one, strongly indicating that the proposed method provides an accurate equivalent of the external system.

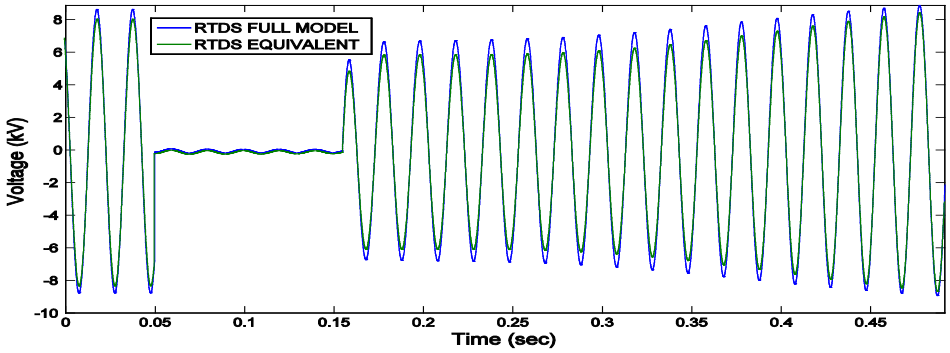

(a)

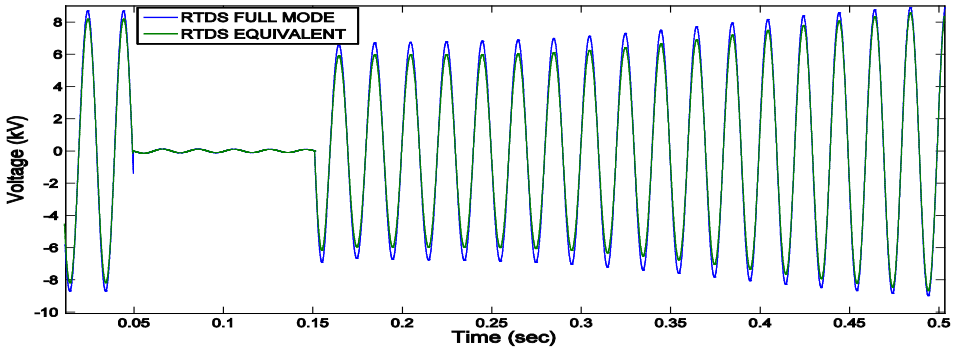

(b)

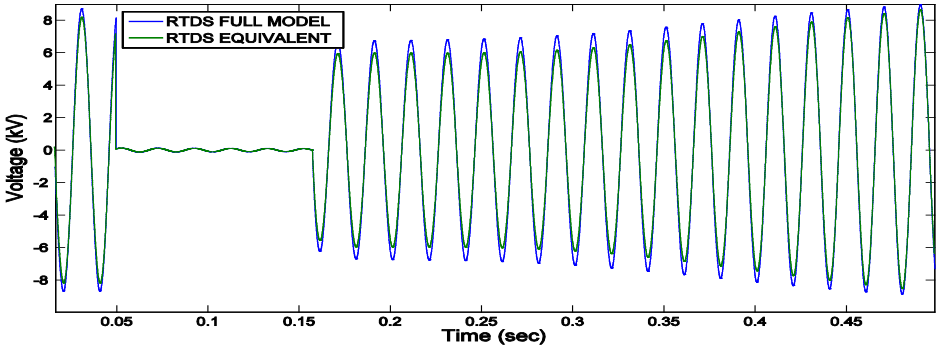

(c)

Figure 4-19 : Comparison of RTDS Full Original model and RTDS Equivalent is subjected to a three phase fault of 6 cycle duration on bus 68 (a) A phase voltage, (b) B phase voltage, (c) C phase voltage

The result of the RTDS equivalent model is very close to the benchmark of RTDS Full Model Original. As the captured plots agree very closely, the RTDS equivalent of the external system can reproduce the dynamic response of the full external system.

As an additional comparison, a sudden load change is presented during islanding operation. The load is varied from 3 MW to 4 MW, while the simulation is running, in order to simulate an increase in load demand. The main results obtained are as shown in **Figure 4-20**. It can be seen from the **Figure 4-20** (a)-(b) that both of the active power of generator unit 5 and 6 increase from 5.25 MW to 5.6 MW, and 13 MW to 13.6 MW to control the overall island frequency by sharing or rescheduling between two units based on their participation factors. **Figure 4-20** (c) show the frequency deviation caused by the load change.

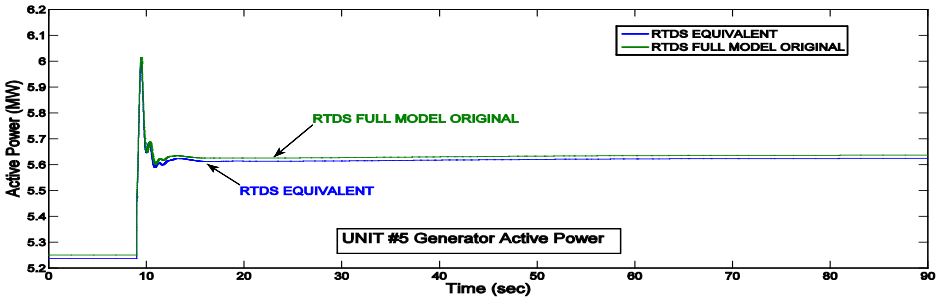

(a)

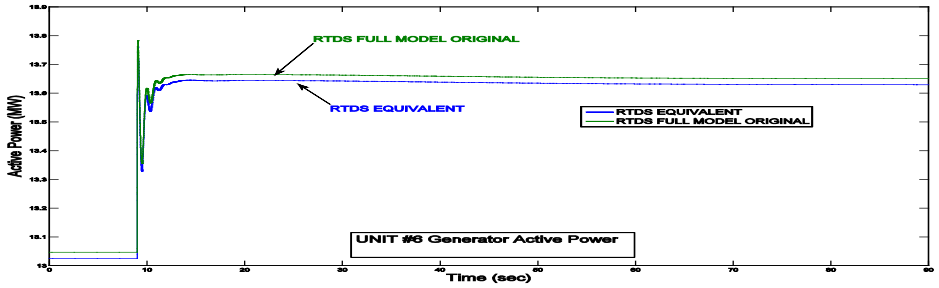

(b)

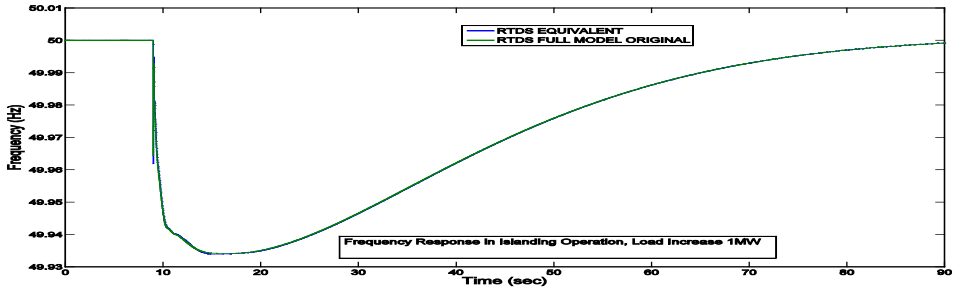

(c)

Figure 4-20 : Comparison of RTDS Full model and RTDS Equivalent is subjected to 1MW load increase at 60 kV during islanding operation mode (a) generator #5 P_{out}, (b) generator #6 P_{out}, (c) system frequency, P_5=0.3858, P_6=0.6142)

4.10 Summary and Discussion

This chapter gives a complete overview of Bornholm distribution system. Based on these information, a reliable real-time model of the Bornholm distribution system, capable of simulating both steady-state and dynamic simulation is constructed for a wide range of operating conditions. The simulation models, the typical data, and the scenarios used are also introduced. The AGC model is described and the role of AGC model in connection with the Bornholm distribution system to manage the islanded system is emphasized. The outcome of simulation results have shown that the contribution to AGC is effective for a successful islanding manoeuvre performed under different power levels.
In addition, an equivalent generic model of Bornholm distribution system is also implemented, which can be used as a benchmark model for other smart grid testing purposes. It should be noted that the equivalent must be able to properly represent the high frequency electromagnetic as well as the low frequency electromechanical transient behaviors. The algorithm used in this work is based on the earlier research of improving dynamic reduction of power systems using relation factors combining with FDNE feature available in the RTDS. The dynamic reduction technique uses a coherency based reduction of the electromechanical model of the power system to be equivalence. The low frequency behaviour is being modelled by dynamic reduction technique. A FDNE is placed in parallel with this model to accurately capture the high frequency behaviour. An improved equivalent approach is presented, which reduces a large power network into a small manageable equivalent model with reduced hardware costs. Also, the generic parameter sets are developed for further process which later combines with above two processes into form a simpler equivalent. The system parameters are identified, averaged and randomized based on the complete data of the Bornholm distribution system using Matlab's NORMRND function. By using a modified procedure, an equivalent generic model of the Bornholm has been implemented. Its scale is reduced within the hardware capacity (i.e. greatly reduce the computational effort and allows the RTDS to handle very large system with much less hardware) for the RTDS. The application results exhibit a desirable performance and good agreement between the RTDS Full model original and the RTDS equivalent. Two resultant curves match to a very high degree of accuracy, which demonstrates the confidence that the proposed equivalent approach has been performed properly. It can be concluded that the equivalent system retains the dynamic response of the original system accurately. The algorithm is capable of creating equivalents of real distribution system, thereby in the future, bringing entire Danish systems containing thousands of buses into the realm of real time digital simulation.

5 Primary Frequency Control for Islanding Operation of ADNs using BESS

This chapter presents an effective frequency control strategy for islanding operation of ADNs. The use of BESS in providing primary frequency control is emphasized. New challenges and key issues concerning ADNs are briefly discussed in Section 5.1. The descriptions of test cases (IEEE 9-bus and Bornholm) are addressed in Section 5.2. Also, the simplified model of BESS and an aggregated wind turbine model are described. In Section 5.3 discusses the overall coordinated frequency control strategy between a small-sized BESS and DG participating units in the AGC scheme to improve the frequency regulation performance. In the proposed strategy, the charging and discharging operation is performed on the BESS to balance the total power generation with the total power demand. However, a small-sized BESS is assumed; therefore, the continuous charging and discharging operations are not available on the BESS because the stored energy level hits its capacity limit. To avoid this undesirable effect and to perform the continuous frequency regulation on the BESS, the power outputs of the dispatchable DG units can be coordinated to share the load following burden of the BESS and to keep the stored energy level on the BESS within the prespecified level. The power generation from the DG units increases whenever the stored energy level on the BESS decreases. On the other hand, the power generation from the DG units decreases whenever the stored energy level on the BESS increases. In Section 5.4, the simulation results are presented to show the improved frequency control performance. The results reveal that the secondary control reduces the reserve requirement of the BESS by sharing the load between the selected DG units. Finally, the summary is included in Section 5.5.

5.1 Introduction

The future scenario of increased capacity of renewable generation penetrations in the distribution systems will raise significant challenges to the reliability of the system operation and control. And, this trend is anticipated to continue in the future. Any additional increase of wind power capacities could deteriorate system stability. This is in contrast to the general experience and to the goal of many countries to reach higher levels of wind power generation in future. New features addressing the intermittent nature of these resources should be added into system control and planning, so that systems can be operated safely. New regulation solutions have to be implemented in such a future scenario. Possible solutions to this problem are increased capacity of the cross-

border transmission lines, demand side response, distribution automation, enhancement of maintenance, increased flexibility of DG units, and energy storages [39], [61], [88] - [89]. Particularly, the BESS is among the most efficient and compatible technologies for an improved system operation and control with large renewable-based electricity generation. The operation of BESS is complementary to the stochastic behaviour of the renewable energy. The BESS can charge whenever there is an excess of electricity in the connected system and discharge when required by the grid. This solution is one of the emerging concepts and is the focus of this work as energy storages may become cost effective in future. Recently, the concept of integrating small-size generation units into low voltage distribution networks as an alternative generating source is also gaining popularity, which resulted in large scale deployment of DG units or high penetration of multiple DG units in distribution systems. This has certainly brought the concept of the sustainable energy system called micro-grid, where small generating sources located close to load centres are dispersed in the distribution systems. Moreover, in islanding operation, with relatively few DG units, the frequency and voltage control is not straightforward. The frequency of the microgrid or islanded system may change rapidly due to its low inertia presented. Frequency change is a direct result of the imbalance between the load and the power supplied by system connected generators. Therefore, AGC is one of the important issues in islanded system operation. However, it is a challenge to utilize the DGs within distribution systems both efficiently and economically to assist the islanding operation of the distribution systems. A well designed and operated distribution system should cope with changes in the load and system disturbances. It should provide an acceptable high level of power quality in islanding operation while maintaining both frequency and voltage within tolerable limits. The main challenge of islanding operation is the coordination of several DG units in order to control the system frequency and voltage and is the development of effective frequency control strategies to improve the probability of success of such an islanding operation, taking into account various initial operating conditions. Many efforts have been dedicated to design novel control strategies for microgrid operation, especially in islanding operation to correctly manage a microgrid during its transition from a grid-connected to an islanding operation, as well as during its autonomous operation [43], [87]. In [87], a frequency stabilizing system using flywheels has been proposed to the islanded system and revealed a great performance for mitigating frequency deviation. The cooperative control scheme of micro sources and an ESS during islanding operation is presented in [43]. Also, several projects in Denmark have been investigated by Energinet.dk, TSO [64], [71], [86]. During these particular projects [71], [74], a newly developed real-time model for Bornholm distribution system is proposed and thoroughly analysed.

5.2 Description of Test Cases

5.2.1 Modified IEEE 9-Bus System Example

The modified IEEE 9-bus test system is used to illustrate the islanding operation of a distribution system, and to validate the proposed primary frequency control strategy. A single line diagram of the modified IEEE 9-bus system in RSCAD is depicted in **Figure 5-1**. The modified IEEE 9-bus system comprises a 60kV, 50 Hz grid which feeds an 11 kV network through a 60/11kV transformer. It consists of three dispatchable DG units are AGC controlled (regulating units), eight transmission lines, one transformer and four loads. Three DG units with nominal power of 4.85 MVA are connected to bus 1, 3 and bus 4, respectively, and 2.5 MW power supplied by external grid before islanding operation. The loads, totaling 9 MW, are distributed along the bus 5,6,7,8 and are modeled as constant impedance loads. Parameters of the distribution system model were from [71] - [72] and the parameters used for the generator and associated controls are also given in **Appendix D**. The test case also consists of a wind power plant (WPP) modeled jointly as a 2 MW generation unit plus the BESS. The WPP and BESS are connected to the grid at the PCC to be utilized when the system transit into islanding operation mode. Both load and wind speed can also be modified in order to simulate a drop or increase in load demand & wind power production, respectively.

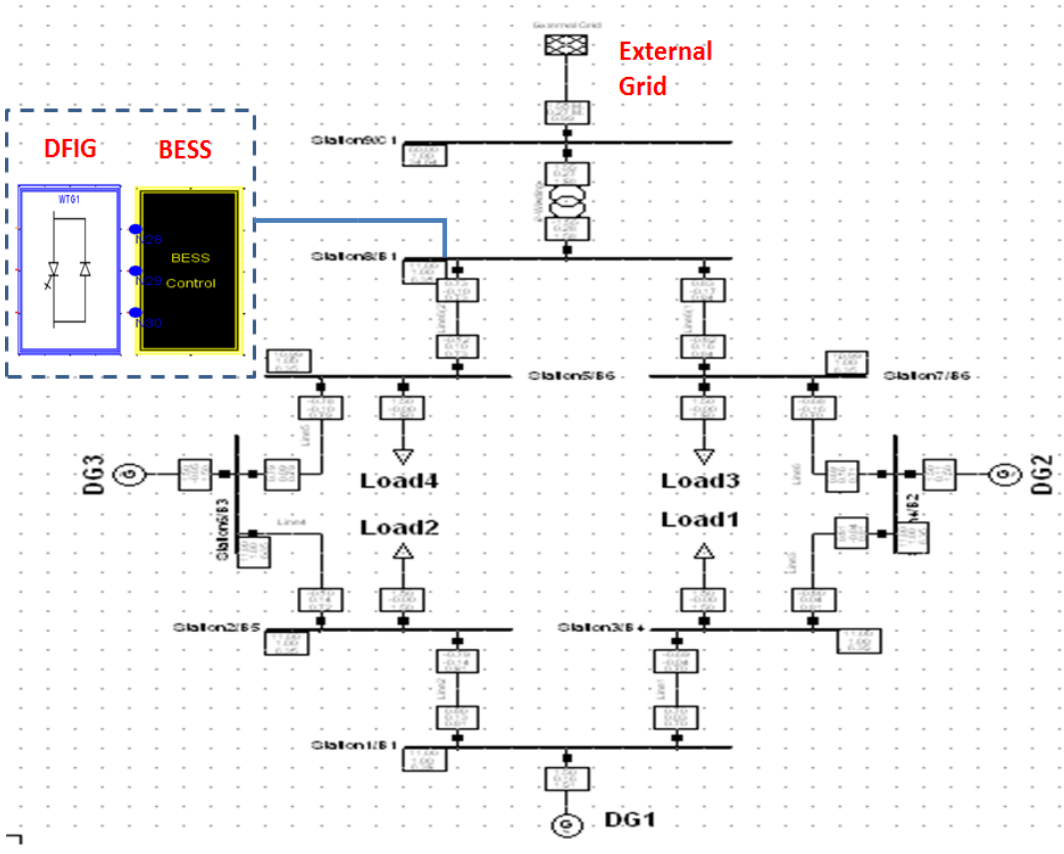

Figure 5-1 : Modified IEEE 9-bus system

5.2.1.1 Basic Structure of Doubly-Fed Induction Generator

The variable speed wind turbine model used in the study system is based on the work of [14] and is depicted in **Figure 5-2**. The principles and mathematical models of DFIG are well documented in literature and hence are only briefly outlined. An interface transformer, a high-pass filter and two VSCs, as well as the DFIG (controls & wind turbine) are included. The DFIG has become the choice of many utilities for harvesting wind energy due to its ability to provide reactive power support to the power system during low voltage conditions. The DFIG can also extract the optimum wind energy over a wide range of wind speeds, a feature not possible with fixed speed induction generators. The actual DFIG parameters used are typical of a 2 MW, 690 V machine. The high pass filter is rated at 10 percent of the interface transformer MVA and tuned to remove the switching voltage and current components generated by the VSCs (21 x 60 Hz). The grid side VSC operates to control voltage on the capacitor connected between it and the rotor side VSC, while the rotor side VSC controls voltages applied to the rotor to maintain reactive power flow into the DFIG and to control torque. The grid side VSC can also regulate reactive power flow into the system. The wind turbine allows the selection of either of two commonly used power coefficient curves along with user entered parameters. Both wind speed and rotor speed are inputs into the model and mechanical torque is the output. Rotor speed is determined by the DFIG based on inertia and on the difference between mechanical and electrical torques. An optimum torque reference is included to produce maximum power at any rotor speed. Also, a simple pitch control is used to protect the rotor from over speed in the event of strong wind.

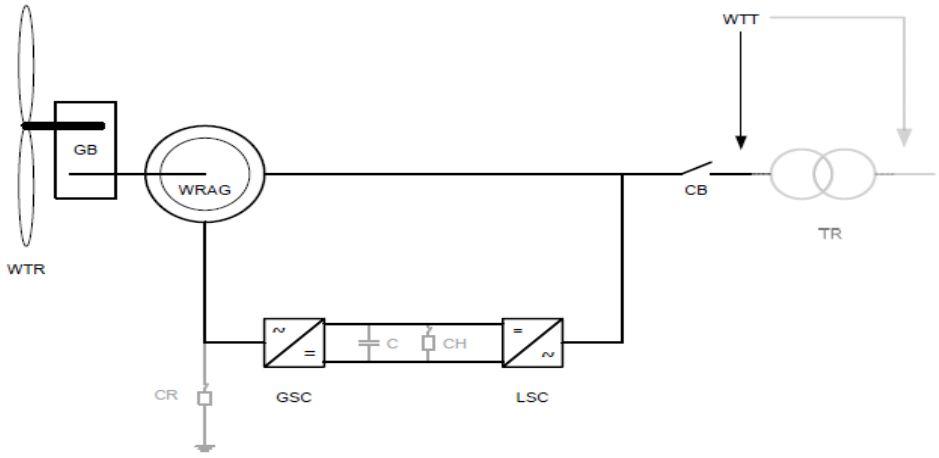

Figure 5-2 : Basic structure of DFIG wind power generation

5.2.1.2 Battery Energy Storage System

The BESS enables smoothing of fluctuations for wind and solar generation units. The system provides a mechanism to store intermittent energy generation, which provides consistent power to the grid. Quick-response characteristic alleviates rapid shifts in re-

newable energy generation and can therefore act as a frequency regulator. In this study, the simplified battery model is adopted with constant internal resistance and a controlled voltage source (CVS), and is depicted in **Figure 5-3**. The BESS aims to regulate the two current components: id (current in d-axis) and iq (current in q-axis). These components equate to the real and reactive power accordingly. Normally, there are three different control modes: (a) Active and reactive power is regulated according to the set point; (b) Droop control; (c) Frequency/Voltage (F/V) control. In this chapter, different control schemes switch based on the operations. For the grid-connected operation, mode (a) is applied. The set point is decided by the MMS and reactive power is always set to be zero, which means no reactive power injection. In islanding operation, BESS should contribute to stabilize the frequency and voltage. Therefore, mode (c) is utilized.

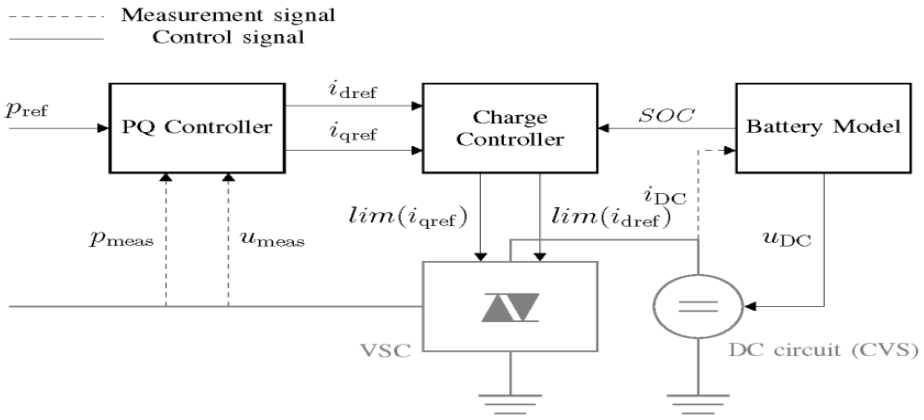

Figure 5-3 : Simplified model of BESS

5.2.2 Bornholm Power System Example

The Bornholm distribution system with a BESS is used as a second test case. A detailed description and the parameters can be found in [71], [74] - [75]. The basic Bornholm model has been slightly modified. The modification is to include the BESS from [45], [88]. Instead of an existing manual frequency control in Bornholm, an AGC with the BESS regulation is simulated and analyzed.

5.3 Coordinated Frequency Control Strategy

5.3.1 Primary Frequency Control

The main concept of control strategy is the coordination control between a BESS and dispatchable DG units as shown in **Figure 5-4**. With the control strategy, the following objectives are achieved.

1) Grid-connected operation

The objective of BESS is maintaining the system frequency and voltage within the prespecified limits. In grid-connected operation, the task is mainly carried out by the external grid. Therefore, the BESS is not active.

2) Islanding operation

The power generated by RES varies faster than traditional power generation. If there is no BESS, the power balance between the generated power and the existing loads does not always match due to the renewable energy fluctuations. As a result, the frequency and the voltage of the distribution system will fluctuate. This must be synchronized or it can lead to system instability. Once the islanding situation is detected, BESS is activated. Clearly, the BESS can provide fast response by proper power balancing as other DG units have a relatively slow response time. Thus, the frequency and the voltage of the islanded system can be regulated at the nominal values. However, due to its capacity limitation (small-sized), the power outputs of the dispatchable DG units should be coordinated to share the load following burden of the BESS and to keep the stored energy level on the BESS within the prespecified level. According to the proposed coordinated control strategy as shown in **Figure 5-4**, the MMS detects the change in the power output of the BESS and assigns the total power difference to the DG units. This secondary control can reduce the consumption of the stored energy of BESS without degrading the control performance.

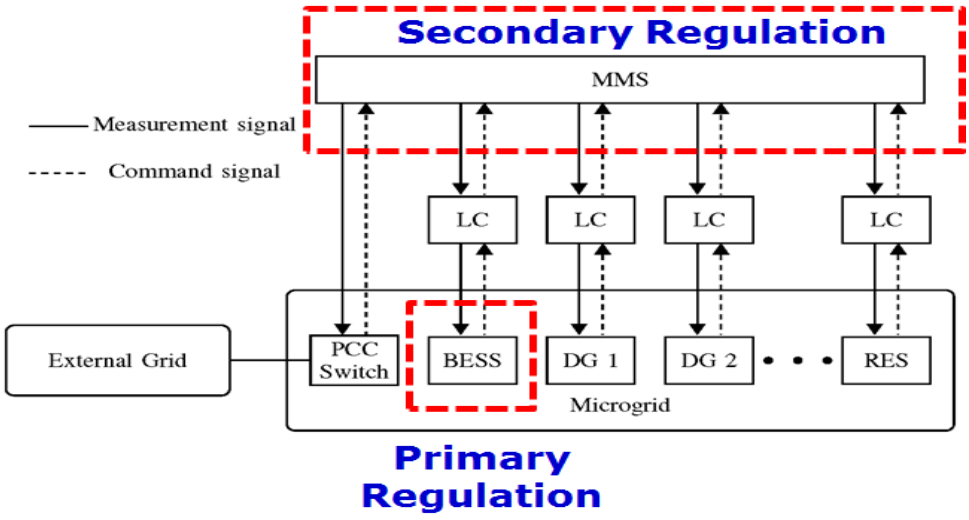

Figure 5-4 : The hierarchical control structure

In islanding operation, the quality of the frequency and voltage in the islanded system are the key issues of concern and these mainly depend on the control performance of the BESS.

5.3.2 Secondary Frequency Control

The secondary frequency control can be built in a number of ways, either locally or in a centralized and automatic way. The MMS control structure used in this work is based on the author's previous research [72].

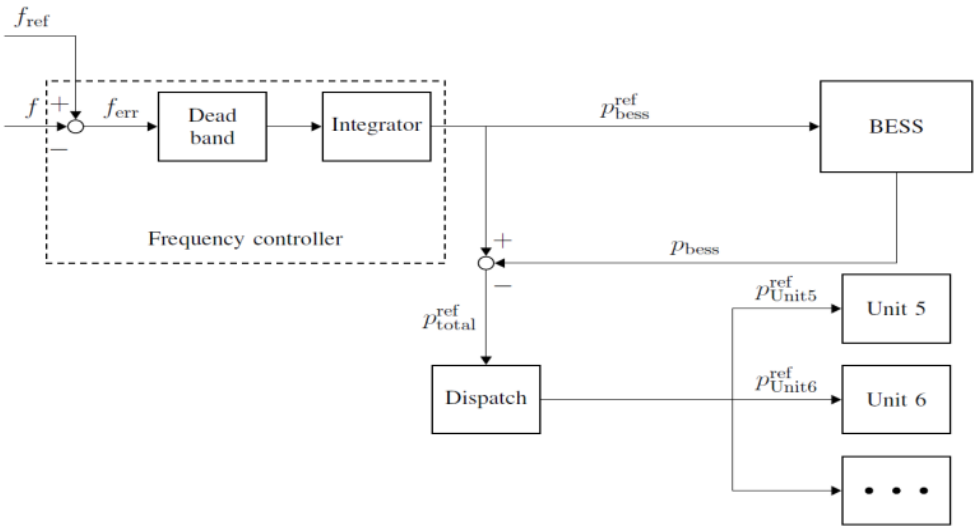

Figure 5-5 : Concept and structure of secondary control of MMS

The secondary frequency control is performed as shown in **Figure 5-5**. If the system is operating in grid-connected operation, the BESS is disabled. However, if the system becomes islanded, BESS is activated and then the secondary control of the MMS detects the change of the power output of the BESS and tries to return the power output of the BESS to reference value by dispatching the power output set points of dispatchable DG units (i.e. governor load reference set points) in order to adjust the production levels and consequently correct the frequency offset as shown in **Figure 5-6**. The main objectives of the secondary control are to keep the system frequency at or close to 50 Hz and to maintain each DG unit's generation at the most economic value.

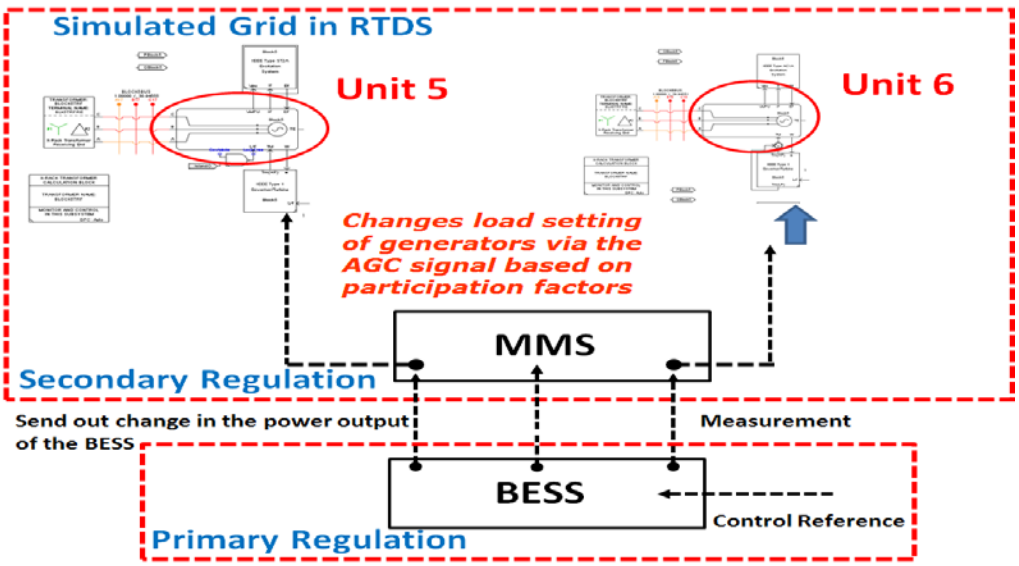

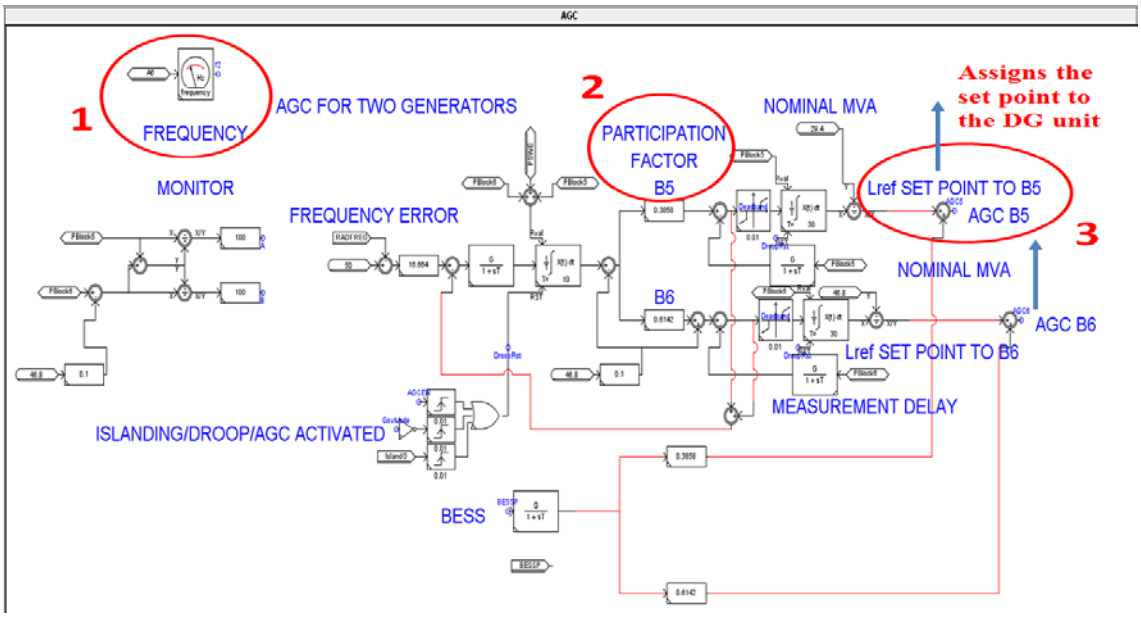

Figure 5-6 : Block diagram of secondary control of MMS

For our simulation case, the power generation for two DG units can be calculated as following:

Generation Unit 5:

$$P_{G5} = \left(P_{SYS} - P_{base,G6}\right) \cdot pf_{G5} \qquad (1)$$

Generation Unit 6:

$$P_{G6} = \left(P_{SYS} - P_{base,G6}\right) \cdot pf_{G6} + P_{base,G6} \quad (2)$$

Where, P_{sys} and $P_{base,G6}$ are the total system power and the base load of the unit 6 (rated MVA) respectively, pf_{G5} and pf_{G6} are the participation factors, respectively.

The load reference of each DG unit must then be set in order to reach nominal frequency:

$$L_{ref,G5} = \frac{(P_{SYS} - P_{base\,G6}) \cdot Pf_{G5}}{S_{rated},G5} \quad (3)$$

$$L_{ref,G6} = \frac{(P_{SYS} - P_{base\,G6}) \cdot Pf_{G6} + P_{base\,G6}}{S_{rated},G6} \quad (4)$$

Where, $S_{rated,G5}$ and, $S_{rated,G6}$ are the rated MVA of the machines.

The secondary frequency control of MMS, as shown in **Figure 5-6**, measures the system frequency and changes load reference settings of DG units via the AGC signal. The MMS calculates the average power that has to be distributed among the DG units connected to the frequency controller. The resultant control signal specifies the active power set points (i.e. changes required to restore the frequency) to the selected DG units for power production adjustment based on participation factors, p_{f5}, p_{f6}, where the sum of the participating factors are equal to unity.

5.4 Simulation Results

5.4.1 Test Case 1 (IEEE 9-Bus System)

To investigate the performance of the proposed coordinated control strategy, two simulation cases were performed. The voltage and frequency response is conducted with/without an option of the secondary control of MMS after switching to islanding operation as the first case. As a second case, the wind speed variation is considered. The initial condition for each case is that the load is balanced with the production at exactly 50 Hz. This system initially has about 9 MW load. The centralized MMS control is continuously monitoring the voltage and frequency to respond to any disturbance. A 3-phase fault disconnecting from the utility grid is applied at ($P_{scr} = 1pu,\ \delta_0 = 0, initial\ power\ flow\ of\ 2.5\ MW$) at t = 10 s.

5.4.1.1 Simulation Case I

The scenario is characterized by a total load of 9 MW and three DG units add up to a total power of 4.5 MW, one wind farm with 2MW, and external grid supplying 2.5 MW. The simulation sequence is described as follows;

- Step 1. Loss of 2.5 MW power from the external grid
- Step 2. Created an imbalance in the islanded system
- Step 3. Observe voltage & frequency drop
- Step 4. BESS activated as a primary control
- Step 5. With/without the secondary control of MMS
- Step 6. Voltage & frequency recover

In **Figure 5-7**, the voltage response with the secondary control of MMS is shown with legend BESS ON + MMS ON (green curve) and the voltage response without the secondary control of MMS is also shown with legend BESS ON + MMS OFF (blue curve), respectively. The operation control strategy is to use BESS as primary regulation and all three dispatchable DG units for providing secondary regulation.

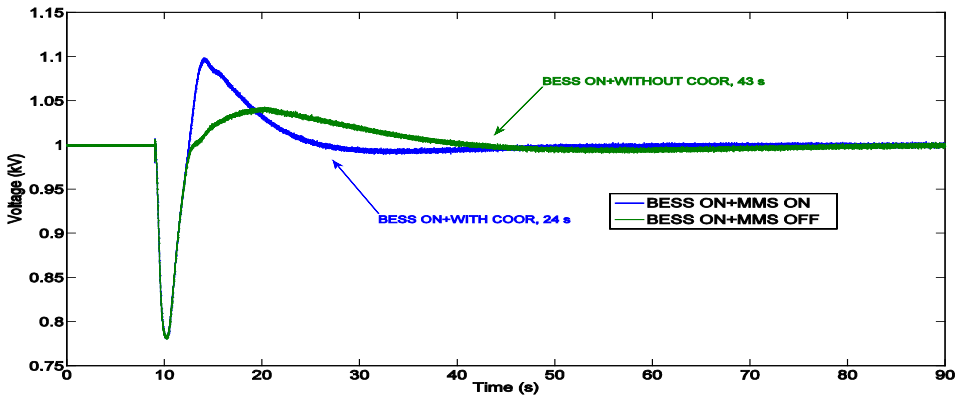

Figure 5-7 : Voltage response with (green)/without (blue) secondary control of MMS

It is observed that all dispatchable DG units are switched on to V-f mode to control the voltage by sharing or rescheduling between three units based on their participation factors. It can also be seen that the voltage dropped to 0.78 pu and recovered to the operational range after 24 s (i.e. settled at 1 pu.) in **Figure 5-7**. Therefore, the BESS can improve voltage performance of the system.

Likewise, in **Figure 5-8**, the frequency response with the secondary control of MMS is shown with legend BESS ON+ MMS ON (green curve) and the frequency response without the secondary control of MMS is shown with legend BESS ON + MMS OFF (blue curve), respectively. As it can also be seen in **Figure 5-8** that the frequency dropped to 48.99 Hz and recovered by the BESS at 24 s. Also, the secondary control of the MMS is capable of reducing the frequency excursions considerably and keeping it within permissible limits by load sharing actions taken by three dispatchable DG units. Clearly, the voltage and frequency of the system is well maintained by the primary control action of the BESS and the secondary control action of the MMS. The time intervals between 10 s to 20 s show the contribution of the primary frequency control and the time intervals between 20 s to 60 s highlight the interests of the secondary frequency control. The frequency is still kept in a very narrow range.

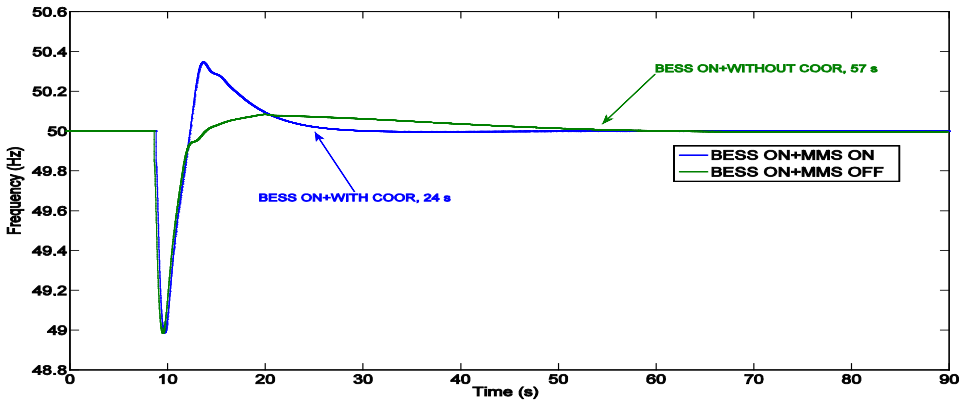

Figure 5-8 : Frequency response with (green)/without (blue) secondary control of MMS

In **Figure 5-9**, the energy requirement from the BESS (i.e. 3.47 kwh to 1.11 kwh) is also greatly reduced with all dispatchable DG units participating in secondary frequency control. The shaded area in the figure represents the total energy contributions from three dispatchable DG units. The power outputs of DG units are shown in the **Table 5-1**.

Table 5-1 : Power output for dispatchable DG units

Unit	Participation Factor	Power Output (MW)
DG 1	*0.3333*	*2.347*
DG2	*0.3333*	*2.347*
DG3	*0.3334*	*2.351*

In this case, the MMS was activated which in return calls the RTDS dynamic simulation computation module. This computation module runs dynamic simulations for a given sample time intervals. At the end of each dynamic simulation, the integral and absolute value of frequency deviation is read from the RTDS's output file. Using this information, new power set points are computed and stored in the RTDS's information file for the next dynamic simulation. This process is repeated up to frequency stabilization or a maximum simulation time.

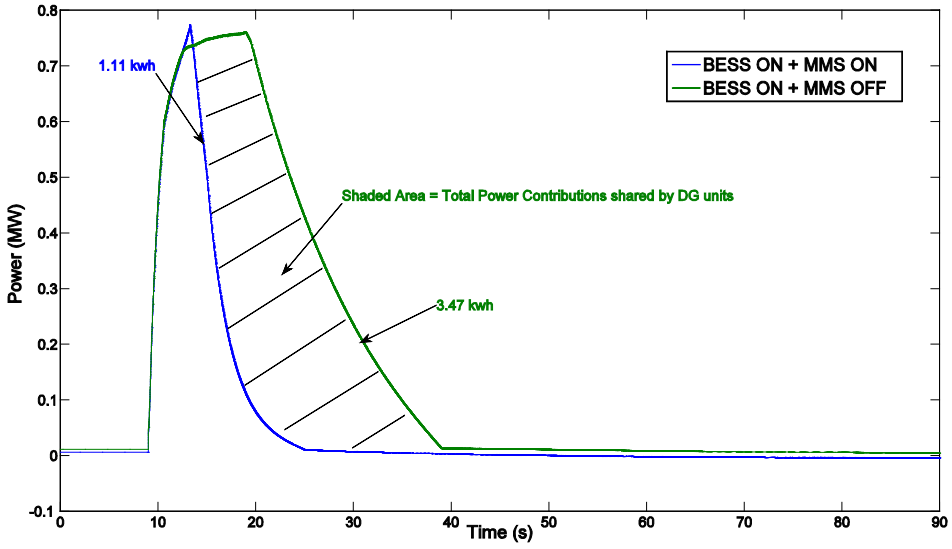

Figure 5-9 : Power output of BESS

5.4.1.2 Simulation Case II

The results obtained with wind speed variation are presented in the next four figures. In this particular case, the wind speed was modified from 12m/s to 10m/s during simulation in order to simulate a drop in wind power production as shown in **Figure 5-10** (a). The BESS ensures that the frequency and voltage remain within threshold limits of the system as evident from **Figure 5-10** (b) and (c). Also, it is observed that only small amounts of BESS capacity (0.195 MW) can improve the response of the modeled system as evident from the **Figure 5-10** (d).

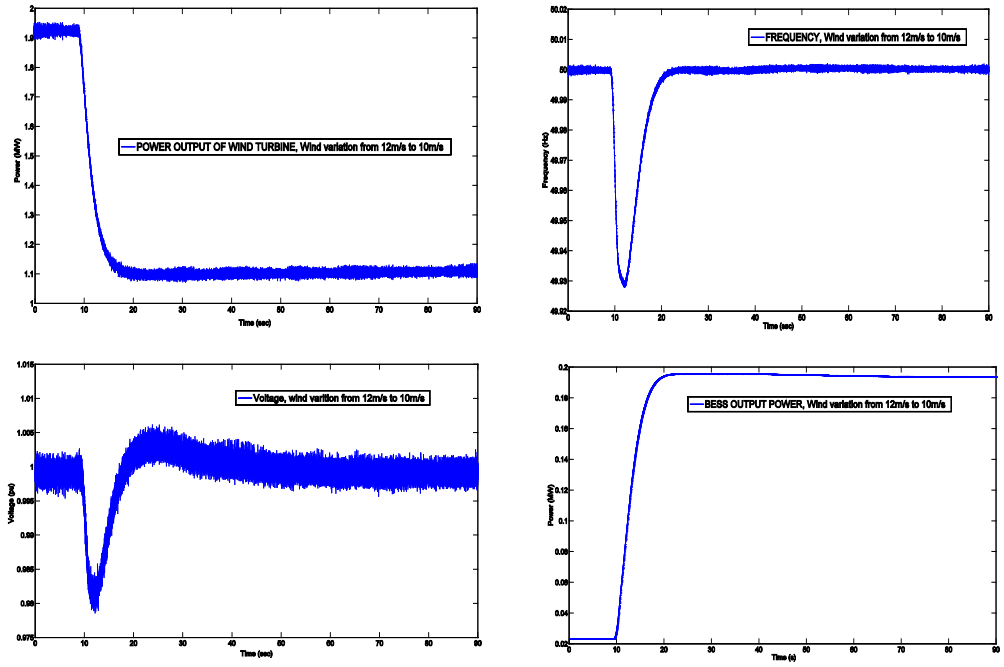

Figure 5-10 : Response of wind speed variation (a) wind turbine P_{out}, (b) frequency response, (c) voltage response, and (d) BESS P_{out} , left to right direction

5.4.2 Test Case 2 (Bornholm System)

To further investigate the performance of the proposed coordinated control strategy, four simulation cases were performed. The frequency and voltage response is conducted with/without an option of the secondary control of MMS after switching to islanding operation as the first case. The simulation with and without the BESS regulation is considered as a second case. The two remaining cases are the wind speed variation and a sudden load step disturbance. The initial condition for each case is that the load is balanced with the production at exactly 50 Hz. This system initially has about 21.8 MW load. The centralized MMS control is continuously monitoring the voltage and frequency to respond to any disturbance. A 3-phase fault disconnecting from the Swedish is applied at ($P_{scr} = 1pu,\ \delta_0 = 0, initial\ power\ flow\ of\ 1.57\ MW$) at t = 10 s.

5.4.2.1 Simulation Case I

The simulation sequence is described as follows;

- Step 1. Loss of 1.57 MW power from the external grid
- Step 2. Created an imbalance in the islanded system
- Step 3. Observe voltage & frequency drop
- Step 4. BESS activated as a primary control
- Step 5. With/without the secondary control of MMS
- Step 6. Voltage & frequency recover

The main focus of the case is to explain the role of BESS as a primary frequency control and the dispatchable DG units acting as secondary frequency control. In **Figure 5-11** (a), the power output of BESS changes from zero to a certain value in order to maintain the frequency and the voltage as a fast-acting primary control during islanding operation. The output power of two DG units also changed from initial values to new power set points calculated by secondary control of MMS, as shown in **Figure 5-6**, Section 5.3.2. The MMS detects the change in the power output of the BESS and assigns the total power difference to DG units. This secondary control can greatly reduce the consumption of the stored energy of BESS without degrading the control performance and ensure the maximum controlling reserve. It is clearly observed that only small amounts of BESS (i.e. 0.045 MW) can improve the response of the Bornholm as shown in **Figure 5-11** (a, blue curve). The BESS does not need to contribute or compensate the complete power mismatch. The shaded area in the figure represents the total energy contributions from two DG units. The power outputs of DG units are shown in the **Table 5-2**. The injected power of BESS is shown with legend BESS ON + MMS ON (blue curve) and the injected power BESS without the secondary control of MMS is shown with legend BESS ON + MMS OFF (green curve), respectively. In **Figure 5-12** (b) and (c), the voltage and frequency response are shown with legend BESS ON + MMS ON (blue

curve) and with legend BESS ON + MMS OFF (green curve), respectively. The energy contributions from two DG units are represented in **Figure 5-12** (d) and (e).

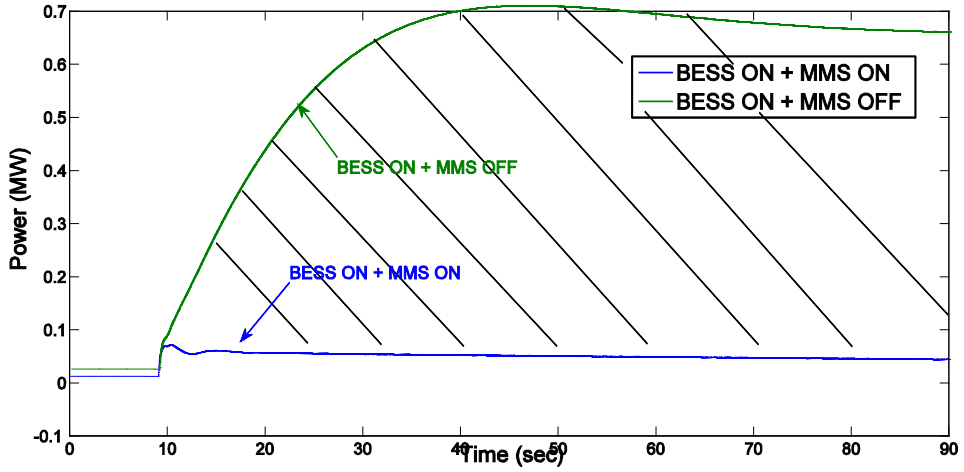

(a)

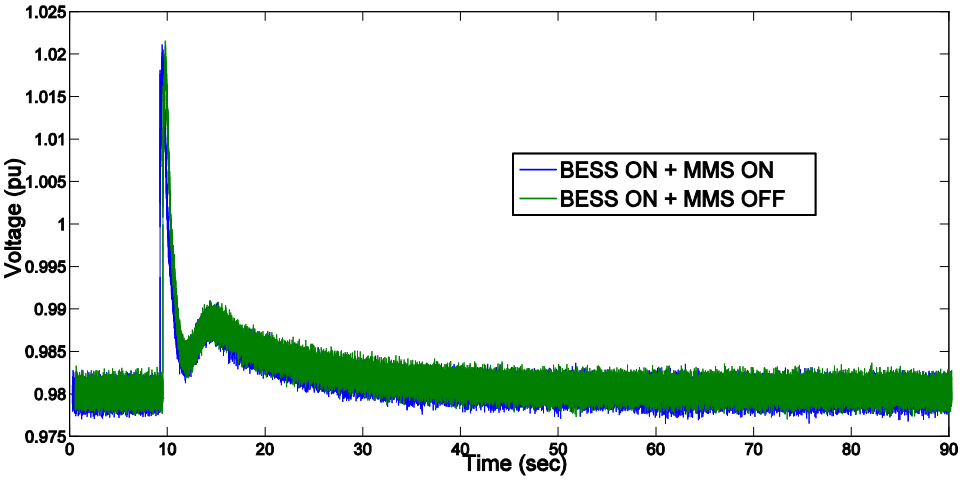

(b)

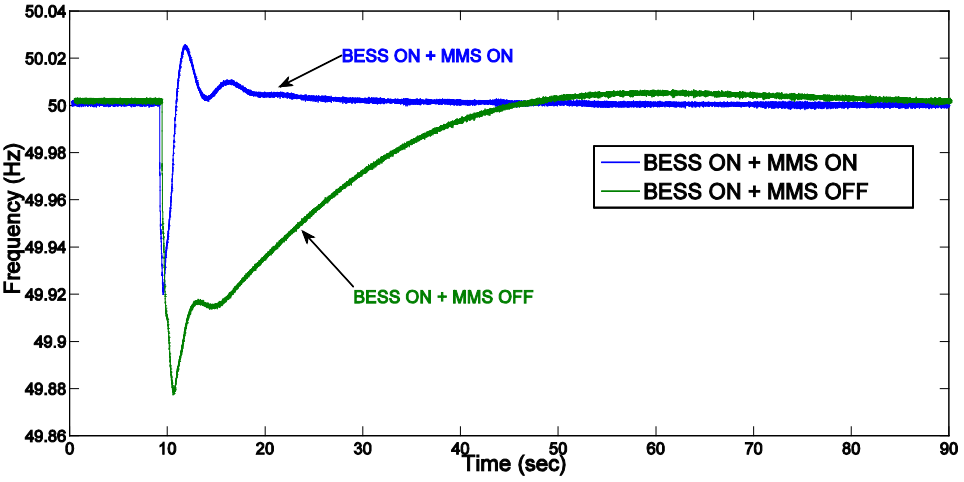

(c)

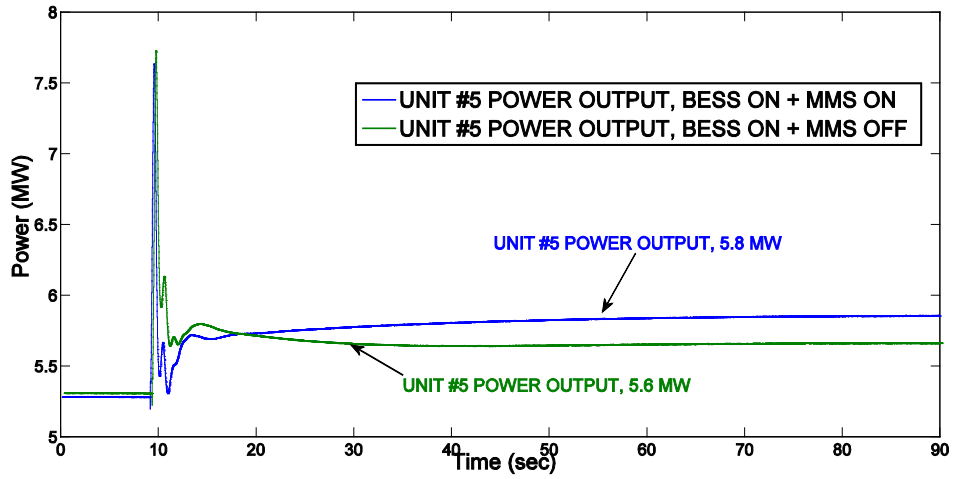

(d)

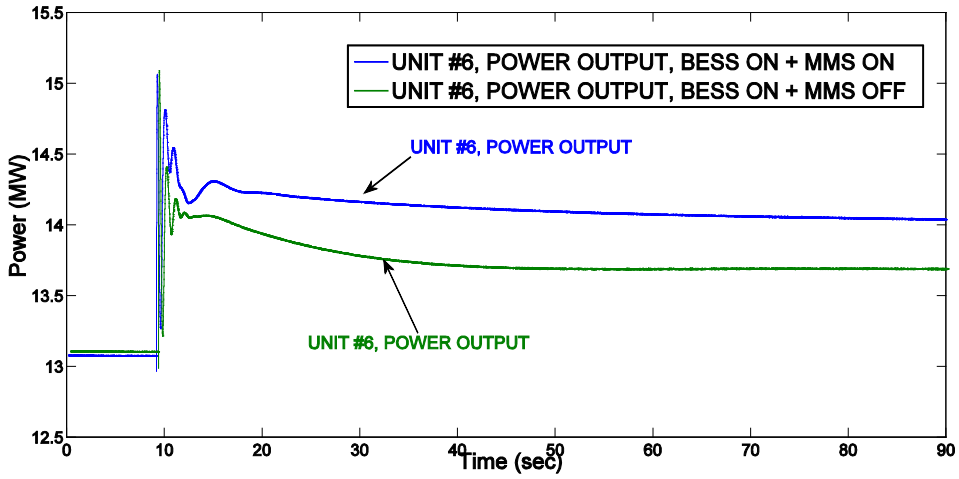

(e)

Figure 5-11 : BESS regulation & coordinated control on & off option (a) BESS P_{out}, (b) voltage, (c) frequency, (d) Unit #5 P_{out}, (e) Unit #6 P_{out}

Table 5-2 : Power contribution for DG units

Unit	Participation Factor	Power Output (MW)
Unit 5	*0.3858*	*0.588*
Unit 6	*0.6142*	*0.937*

Likewise, it is observed that the two DG units are switched on to V-f mode to control the overall island frequency by sharing or rescheduling between two units based on their participation factors. The output power of two DG units increased from initial values to new values to consequently correct the frequency offset. It can be seen that the frequen-

cy dropped to 49.92 Hz and recovered to the nominal value after 20 s. Due to its secondary control of MMS, the frequency is still kept in a very narrow range. The time intervals between 10 s to 20 s show the contribution of the primary frequency control and the time intervals between 30 s to 60 s highlights the interests of the secondary frequency control. Overall, the five sets of results in the **Figure 5-11** show a good agreement with the previous simulation results in Section 5.4.2.1. The BESS ensures that the frequency remains within threshold limits as evident from the frequency response in **Figure 5-11** (c). Obviously, the maximum frequency after islanding event was less severe with the secondary control than that of without the secondary control. From comparison of **Figure 5-11**, it is clear that the proposed control strategy with BESS and the secondary control of MMS is superior to achieve the better frequency regulation performance.

5.4.2.2 Simulation Case II

In this case, the frequency and voltage response is also conducted with and without the BESS regulation. Both case had no secondary control. In **Figure 5-12** (a) and (b), the frequency and voltage response with BESS is shown with legend BESS ON + MMS (blue curve) and with legend BESS OFF + MMS OFF (green curve), respectively. As it can also be seen from **Figure 5-12** (a, blue curve) that the frequency dropped to 49.88 Hz and recovered to the nominal value after 55 s. Due to the absence of the secondary control, the frequency is slowly recovered as opposed to the results obtained in the first case (i.e. much faster, 30 s). Nonetheless, the stability of the system is well maintained by the primary control action of BESS. The power injections from two DG units are represented in **Figure 5-12** (c) and (d). Obviously, the frequency deviation was less severe with BESS than that of without the BESS.

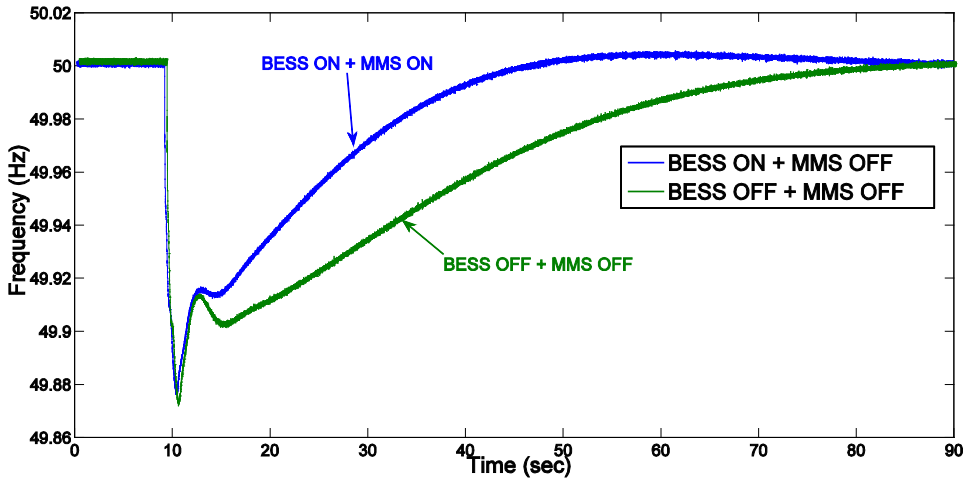

(a)

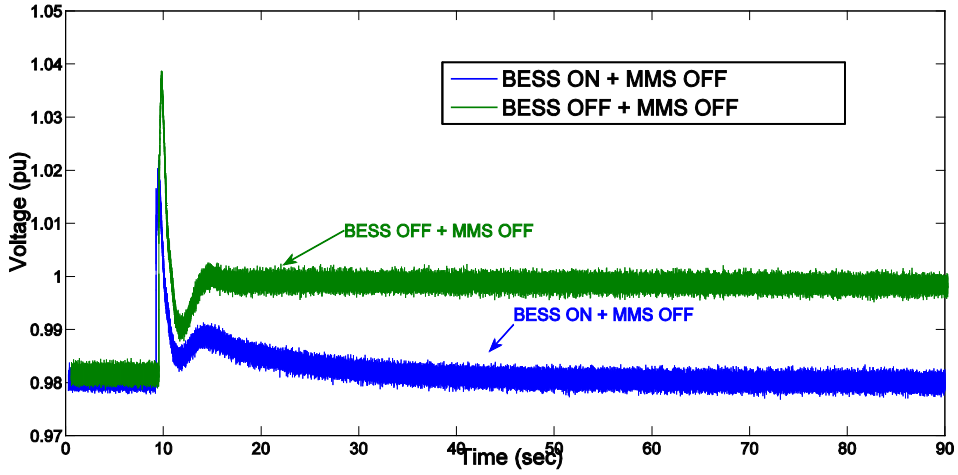

(b)

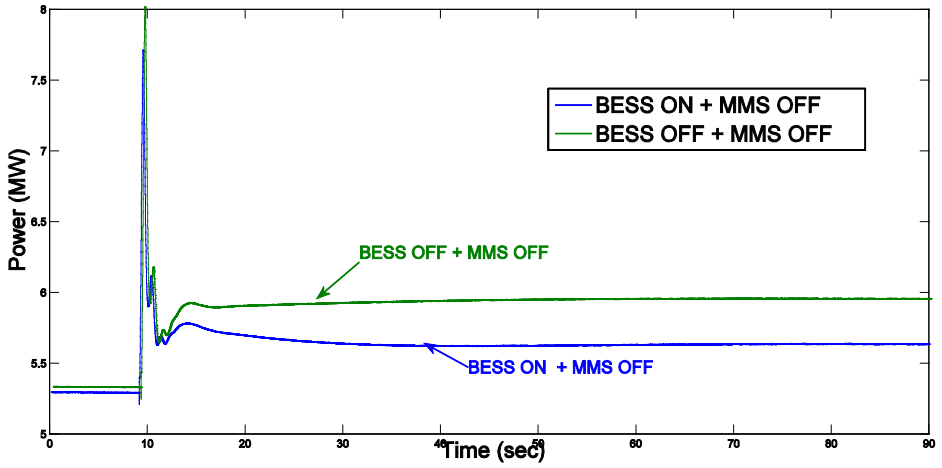

(c)

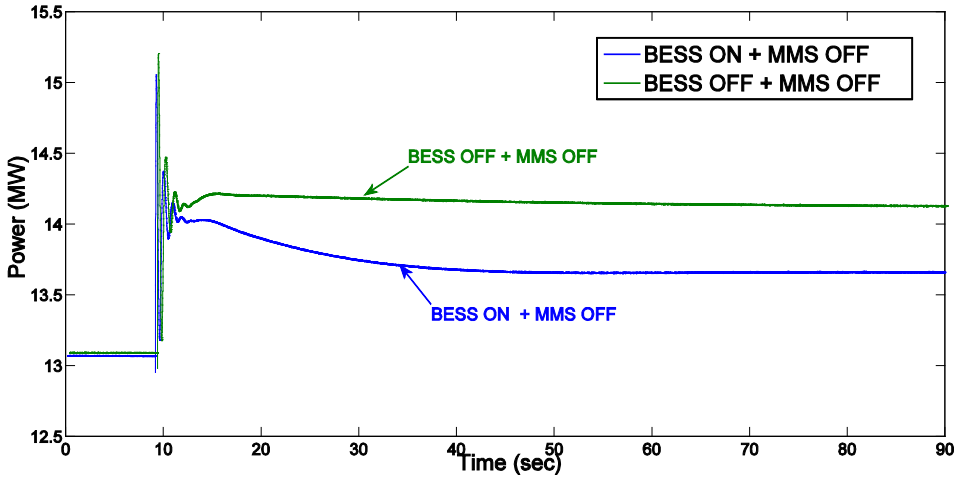

(d)

Figure 5-12 : BESS regulation with and without coordinated control (a) frequency, (b) voltage, (c) Unit #5 P_{out}, (d) Unit #6 P_{out}

5.4.2.3 Simulation Case III

The results obtained with wind speed variation are presented in the next figures. In this particular case, the wind speed was modified from 12 m/s to 15 m/s while simulation in order to simulate an increase in wind power production as shown in **Figure 5-13** (f). The BESS ensures that the frequency and voltage remain within threshold limits during islanding operation as evident from the **Figure 5-13** (b) and (c). Also, it is observed that the BESS reduced its output power from 0.045 MW to 0.035 MW since more wind is available as evident from the wind turbine output in the **Figure 5-13** (a). Consequently, the power requirements from two DG units are also greatly reduced as shown in the **Figure 5-13** (d) and (e).

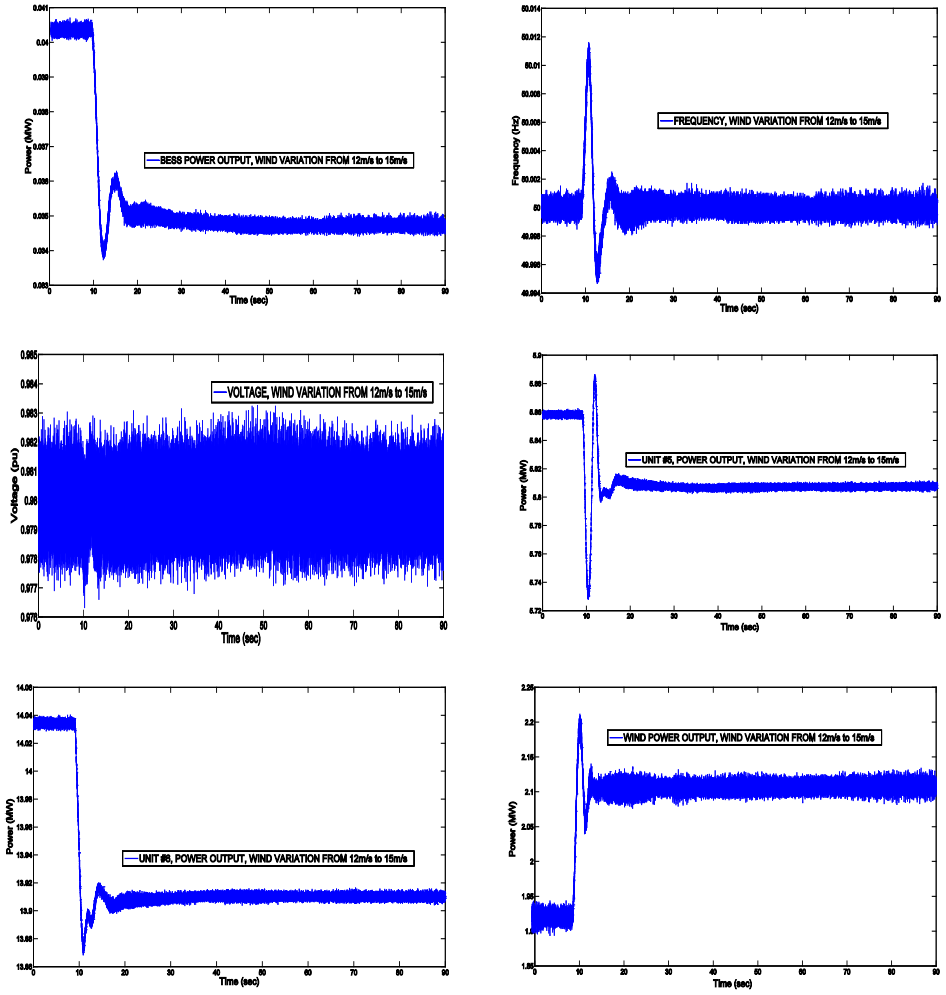

Figure 5-13 : Response of wind speed variation (a) BESS P_{out}, (b) frequency, (c) voltage, (d) Unit #5 P_{out}, (e) Unit #6 P_{out}, and (f) wind P_{out}

5.4.2.4 Simulation Case IV

The main results obtained with a sudden load step disturbance are presented in the next figures. The load was varied from 6.01 MW to 8.01 MW, while the simulation is running, in order to simulate an increase in load demand as shown in **Figure 5-14** (d). The BESS ensures that the frequency and voltage remain within threshold limits during islanding operation as evident from the **Figure 5-14** (b) and (c). Also, it is observed that the BESS increased its output power from 0.045 MW to 0.105 MW since there was a 2 MW shortfall in electrical power as evident from the **Figure 5-14** (a). The difference was covered by the two DG units, as shown in the **Figure 5-14** (e) and (f).

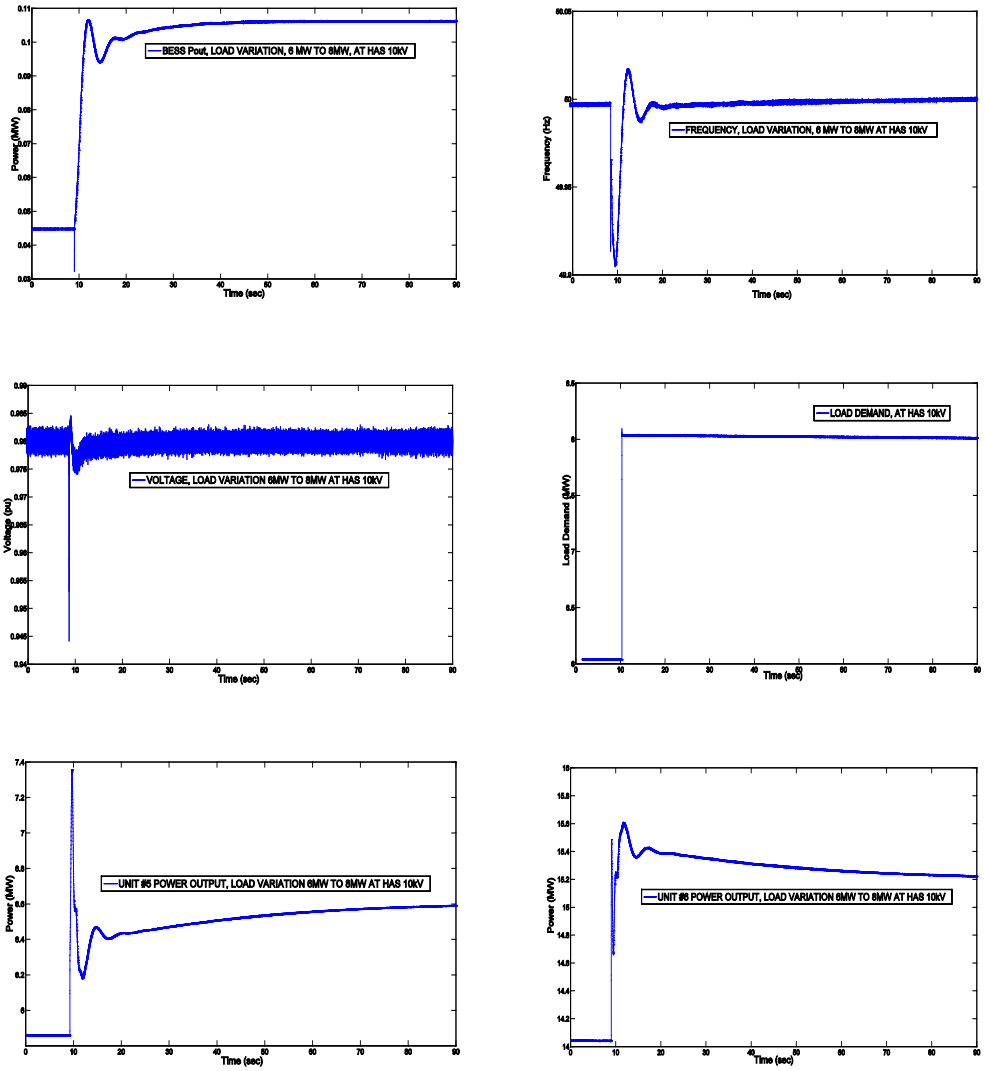

Figure 5-14 : Response of load variation (a) BESS P_{out}, (b) frequency, (c) voltage, (d) load demand (e) Unit #5 P_{out}, and (f) Unit #6 P_{out}

5.5 Summary and Discussion

Use of an effective coordinated control strategy between ESS and other DG units may ensure that ESS provides the required services in the most optimal way. This chapter presents a coordinated frequency control strategy between a small-sized BESS and the AGC participating DG units to improve the frequency regulation performance. Particularly, the BESS is among the most efficient and compatible technologies because of its fast operation with a high power level. In the proposed strategy, the charging and discharging operation is performed on the BESS to balance the total power generation with the total power demand. However, a small-sized BESS is assumed; therefore, the continuous charging and discharging operations are not available all the time on the BESS because the stored energy level hits its capacity limit. To avoid this undesirable effect and to perform the continuous frequency regulation on the BESS, the power outputs of the dispatchable DG units can be coordinated to share the load following burden of the BESS and to keep the stored energy level on the BESS within the prespecified level. The power contribution from the DG units increases whenever the stored energy level on the BESS decreases. On the other hand, the power generation from the DG units decreases whenever the stored energy level on the BESS increases. By the proposed coordination, the frequency regulation performance is highly improved in the event of islanding operation. The BESS is designed to provide frequency support as a fast-acting primary control, and the secondary control of the MMS acts as a supplementary to help maintaining the constant frequency. To demonstrate the efficiency of the proposed control strategy, a real-time digital simulation is carried out for each test case. The simulation results indicate the advantages of the proposed control strategy. It is observed that only small amount of BESS capacity can improve the system frequency and the secondary regulation control can also reduce the consumption of the stored energy of BESS without degrading the proposed control performance. Clearly, it is shown how a relatively simple BESS control algorithm may be used to enable stable operation of ADNs. Hence, the results indicate the efficiency of the BESS for real-time applications and its suitability for the cases considered. In addition, the simulation results presented can quantify BESS performance both in EMS for real-time operation and in system planning for future RES connections. However, there are a number of challenges that require further improvement as future work. These are concerned with a dedicated state of charge (SOC) control scheme, the use of high time resolution wind data, improvement of coordinated control strategies, and the controller optimization. Specially, the current BESS model can take energy from the grid when the frequency is too high and return that energy to the grid when the frequency begins to sag. The current implementation can provide a few minutes of energy, but overall system management, including shifting peak loads, and supporting renewables, will require longer durations of storage and therefore re-engineering of conventional storage systems to handle greater energy and power ratios. The outcome of such optimization is a smart charge and discharge schedule for the BESS.

6 Fuzzy Logic based Secondary Frequency Control for Islanding Operation of ADNs

This chapter presents a new application of FLC to an islanded system for improving the system frequency performance. The concept of control strategy is similar to the previous chapter. However, the BESS will not only be involved in primary frequency control, but also in the secondary frequency control. In this case, a large-sized BESS is assumed. Therefore, the continuous charging and discharging operations are available in both grid-connected and islanding operation. The hierarchical control structure has two levels: MMS (central) and local controller (LC). The new fuzzy-logic based secondary frequency control between a BESS and dispatchable DG units in the high level of the MMS is proposed. The effectiveness of proposed fuzzy-logic based secondary frequency control is illustrated by using a test case (i.e. a typical microgrid). The simulation results show that the frequency regulation performance is highly improved in the event of islanding operation. The chapter is organized as follows: Section 6.1 presents the basic concept of fuzzy logic. The new fuzzy-logic based secondary frequency control between a BESS and dispatchable DG units in the high level of the MMS and control system topology are introduced in Section 6.2 and Section 6.3. As the core of the control strategy, the design procedure of FLC is briefly discussed in Section 6.4. The description of the test case is including in Section 6.5. The simulation results are presented in Section 6.6. In the end, a brief summary is included in Section 6.7.

6.1 Introduction

The concept of fuzzy logic was firstly developed by Lotfi Zadeh in 1965 to address uncertainty and imprecision which widely exists in engineering problems. Zadeh presented fuzzy logic not as a control methodology, but as a way of processing data by allowing partial set membership. However, this approach to set theory was not applied to control systems until the 70's due to insufficient small-computer capability prior to that time. In this context, fuzzy logic is a problem-solving control system methodology and provides a simple way to arrive at a definite conclusion based upon imprecise or even missing input information. Fuzzy logic is also expressed by means of the human language rather than attempting to model a system mathematically. It uses an imprecise but very descriptive language to deal with input data more like a human operator. Based on fuzzy logic, a fuzzy controller converts a linguistic control strategy into an automatic control strategy, and fuzzy rules are constructed by expert experience or knowledge database

[90]. The first application of fuzzy control comes from the work of Mamdani and Assilian in 1975, with their design of a FLC for a steam engine [91]. The objective of the controller was to maintain a constant speed by controlling the pressure on pistons by adjusting the heat supplied to a boiler. Since then, a vast number of FLC have been developed for consumer products and industrial processes.
Recently, because of simplicity and robustness, fuzzy logic is used in almost all fields of science and technology, including solving a wide range of control problems in power system operation and control. Unlike the traditional control theorems, the FLC is not so sensitive to variations of system structure, parameters and operation points and can be easily implemented in a large scale non-linear system.
Several studies have been reported for the fuzzy-logic based frequency control schemes in the literature [92] - [95]. There are many possible FLC structures for frequency control purposes, some differing significantly from each other by the number and type of inputs and outputs, or less significantly by the number and type of input and output fuzzy sets and their membership functions, or by the type of control rules, inference engine, and defuzzification method. FLC can be regarded as a nonlinear static function that maps controller's inputs onto controller's outputs. A controller is used to control some system or plant. The system has a desired response that must be maintained under whatever inputs are received. However, the inputs to the system can change the state of the system which will cause a change in system response. The task of the controller is to take corrective action by providing a set of inputs that ensures the desired response. Motivated by the above observations, a new fuzzy-logic based secondary frequency control is designed and implemented for further improving the system frequency performance in the event of islanding operation.

6.2 Control System Topology

Similarly, the concept of control strategy described in the previous chapter 5 is used. However, the BESS will not only be involved in primary frequency control, but also in the secondary frequency control. In this case, a large-sized BESS is assumed. Therefore, the continuous charging and discharging operations are available in both grid-connected and islanding operation. As mentioned, the hierarchical control structure has two levels: MMS (central) and LC. Two operation modes is performed through a local controller at DG units, a RES, a BESS and a central controller MMS [44]. The MMS is a supervisory centralized controller that includes several key functions (such as economic managing functions and control functionalities). For dispatchable DG units, it can exchange information with LCs and decide the power output set points. For RES, in some extreme situations (e.g. the wind power is larger than the load demand and BESS reaches its maximum limit), MMS can down regulate the RES. The hierarchical control structure is illustrated in **Figure 6-1**.

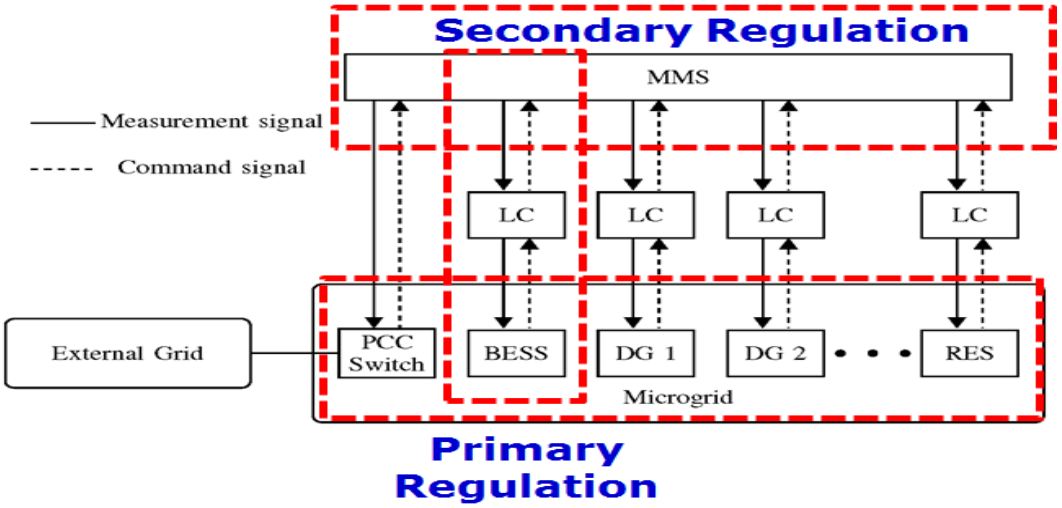

Figure 6-1 : Hierarchical control structure of microgrid

6.3 Coordinated Control Strategy

The main concept of the control strategy is the coordination between the BESS and other dispatchable DG units. Through this control strategy, following control objectives are achieved.

- Grid-connected operation - Smoothing power output at PCC

The grid-connected operation is briefly discussed since the main focus is on the islanding operation. In grid-connected operation, the frequency and voltage of the microgrid are closely related to the external grid and can be considered to operate in a tight range. So, it is unnecessary to regulate the dispatchable DGs. In order to maximize the use of wind power, the LC regulates wind turbine to operate following the maximum power point tracking (MPPT). Therefore, the main objective of MMS is adjusting the BESS to smooth the fluctuations at the PCC, p_{PCC} for the external grid. Furthermore, the BESS will be charged if the charging level is low (i.e. SOC < 50%).

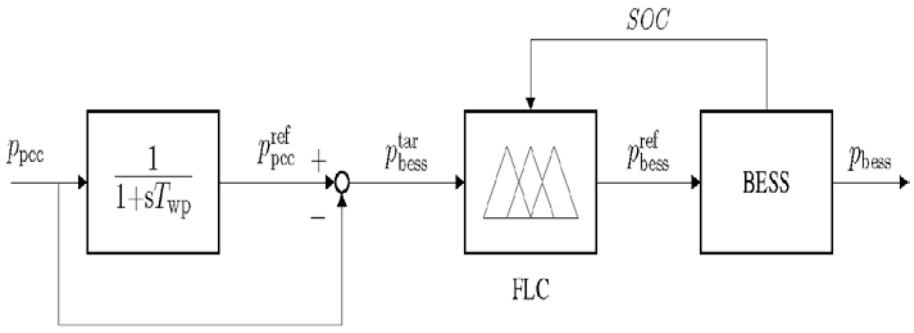

Figure 6-2 : Smoothing control for grid-connected operation

As shown in **Figure 6-2**, the output reference value of PCC, $p_{\text{pcc}}^{\text{ref}}$ is derived through a first-order filter with a smoothing time constant T_{wp}. The difference between p_{pcc} and $p_{\text{pcc}}^{\text{ref}}$ is set to be the target power of BESS ($p_{\text{bess}}^{\text{tar}}$). To ensure that the BESS can operate properly, SOC should be taken into consideration. The FLC is used to enhance the smoothing output and secure the battery charging level. Both $p_{\text{bess}}^{\text{tar}}$ and SOC are regarded as inputs for FLC and the practical reference value ($p_{\text{bess}}^{\text{ref}}$) can be derived and given to the BESS. As a result, the BESS will supply or absorb the real power accordingly.

- Islanding operation - Maintaining the frequency and voltage

In islanding operation, quality of the frequency and voltage in the microgrid are the key issues of concern. They mainly depend on the control performance of the BESS. The reactive power of the BESS is not bound to the battery capacity, so the voltage level could be controlled continuously. Hence, the main focus is on the frequency control. The main cause of the frequency deviation is the imbalance between generation and load. When the deviation exceeds a predefined threshold, the primary control acts to halt the frequency decline or rise. The time scale is in the order of seconds. During this period, BESS will respond and fill the gap between generation and load. Then, the secondary control restores frequency to the nominal value. It adjusts the load reference set point of the governor of dispatchable DG units. The time scale is in the order of minutes. In this study, BESS could also be involved in the secondary control due to the large capacity (60 kWh). The specific parameters are listed in Section 6.5, **Table 6-1**. The controller for islanding operation is illustrated in **Figure 6-3**.

Table 6-1 : Model parameters

Item	Description and Parameters
DG units	DG1: 20 kW DG2: 50 kW
RES	Wind power 30 kW, power profile is illustrated below.
Battery	Total capacity: 60 kWh Capacity per cell: 100 Ah Voltage when the cell is empty ($u_{\min}$): 12V Voltage when the cell is full ($u_{\max}$): 13.85V Amount of cells in parallel: 10 Amount of cells in row: 5 Internal Resistance per cell: 0.001Ω
Load	Load 1: 50 kW Load 2: 50 kW Load 3: 10 kW
Transformer	3-phase 22.9/0.38 kV, 200 kVA, Leakage impedance 6%
Line	R : 0.1878 Ω/km, X : 0.0968 Ω/km

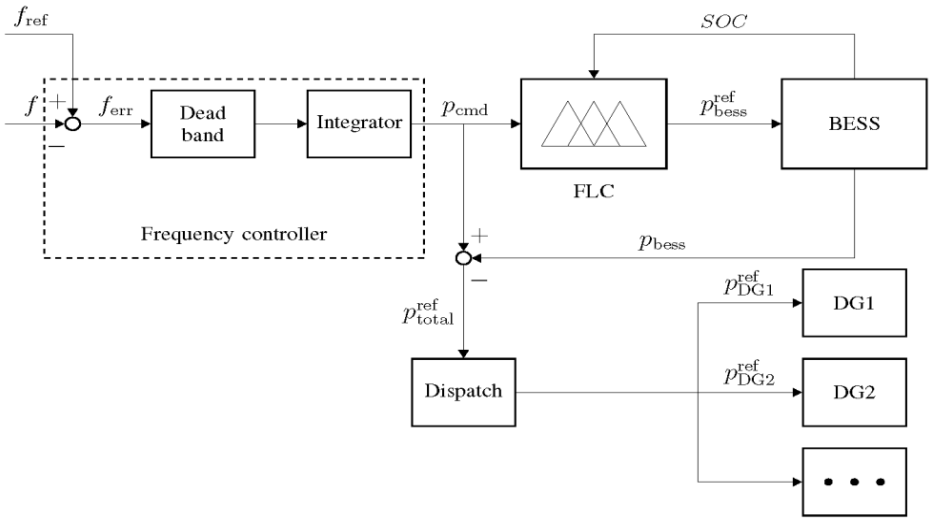

Figure 6-3 : Secondary frequency control for islanding operation

The participation factor is dependent on the SOC and power output (p_{cmd}) command, which can be derived from the frequency controller. p_{cmd} is further allocated by the dispatch function block to generate the load reference set point for each DG unit. Each participation factor (pf_i) can either be based on the nominal power or available power. In this study, it is proportional to the nominal power p_{nomi} . The calculated relations are listed in equations (1) – (3).

$$p_{DGi}^{ref} = pf_i \cdot p_{total}^{ref} \qquad (1)$$

$$pf_i = \frac{p_{nomi}}{p_{total\_nomi}} \qquad (2)$$

$$p_{total\_nomi} = \sum_{i-1}^{n} p_{nomi} \qquad (3)$$

The details of the FLC are described in the following Section 6.4.

6.4 FLC Design Procedures

The design of FLC involves four main parts as shown in **Figure 6-4**.

- Fuzzification: The process of converting a real number into a fuzzy number is called fuzzification. This involves reading, measure and scaling the control variables are used as FLC inputs. The various inputs considered are the equation (4) and equation (5).

- Knowledge Base: This includes defining the membership functions for each input to the FLC and designing necessary rules which specify FLC output using fuzzy variables.

- Inference Engine: This is a mechanism which simulates human decisions and influences the control actions based on fuzzy logic.

- Defuzzification: This is a process which converts FLC output (i.e. fuzzy number) to a real numerical value.

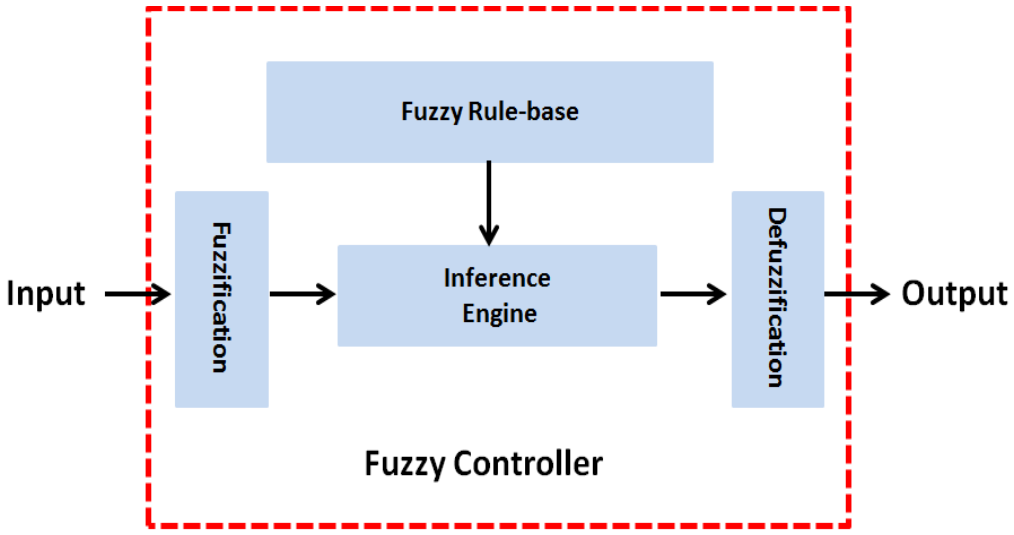

Figure 6-4 : General configuration of FLC

As mentioned in the previous section, the FLC adjusts output power reference $p_{\text{bess}}^{\text{ref}}$ based on the charging level of BESS (SOC) and target power ($p_{\text{bess}}^{\text{tar}}$) to secure its operation range. The proposed control strategy can be formulated as follows equations (4) - (6). The equation (6) shows the "Fuzzification" part. Fuzzy rules proposed for the FLC in **Table 6-2** corresponds to "Knowledge Base" part. Based on the design, the 3D graphic of fuzzy rule surface can be created. **Figure 6-6** shows the generated control signal according to the default mechanism of fuzzy logic tool in Matlab.

$$p_{bess}^{min} \leq p_{bess} \leq p_{bess}^{max} \quad (4)$$

$$SOC_{min} \leq SOC \leq SOC_{max} \quad (5)$$

$$p_{bess}^{ref} = f_{fuzzy}\,(p_{bess}^{tar}, SOC) \quad (6)$$

The FLC part employs two inputs and has a single output. Each input and output has membership function. In general, a membership function of a linguistic variable is represented. The selected membership functions (fuzzy sets) for FLC is shown in **Figure 6-5**. For the input *SOC*, there are five memberships adopted: VS (very small), S (small), M (middle), B (big) and VB (very big). For the input $p_{\text{bess}}^{\text{tar}}$, there are seven memberships adopted: NB (negative big), NM (negative middle), NS (negative small), ZO (zero), PS (positive small), PM (positive middle), PB (positive big). For the output $p_{\text{bess}}^{\text{ref}}$, there are seven memberships and their names and descriptions are same as $p_{\text{bess}}^{\text{tar}}$. Fuzzy rules for $p_{\text{bess}}^{\text{ref}}$ is listed in **Table 6-2**. This set is actually a visual representation of all the possible combinations of the linguistic variables plus the corresponding FLC action. The relevant surface is shown in **Figure 6-6**.

Table 6-2 : Fuzzy rules proposed for the FLC

$p_{\text{bess}}^{\text{tar}}$ / SOC	NB	NM	NS	ZO	PS	PM	PB
VS	NB	NB	NB	NM	NM	NS	ZO
S	NB	NB	NM	NM	NS	ZO	PS
M	NM	NM	NS	ZO	PS	PM	PM
B	NS	ZO	PS	PM	PM	PB	PB
VB	ZO	PS	PM	PM	PB	PB	PB

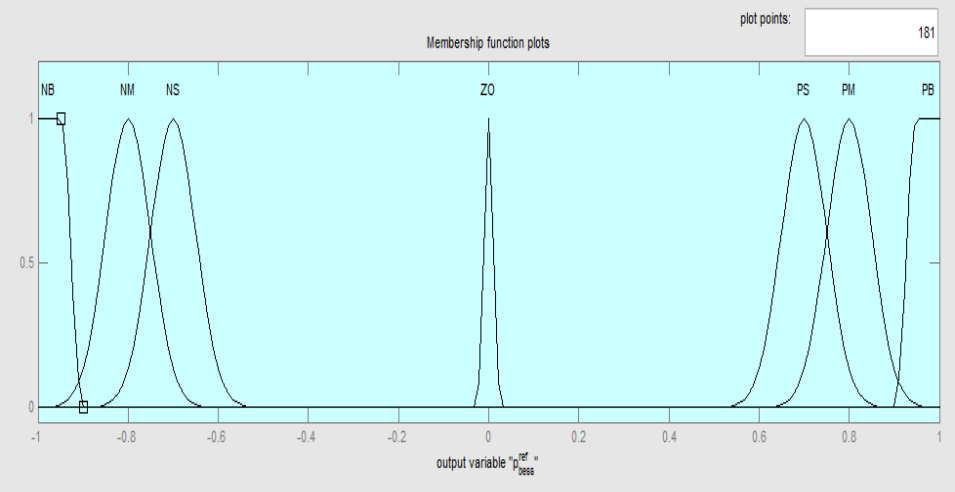

Figure 6-5 : Membership function for the fuzzy variables of the FLC

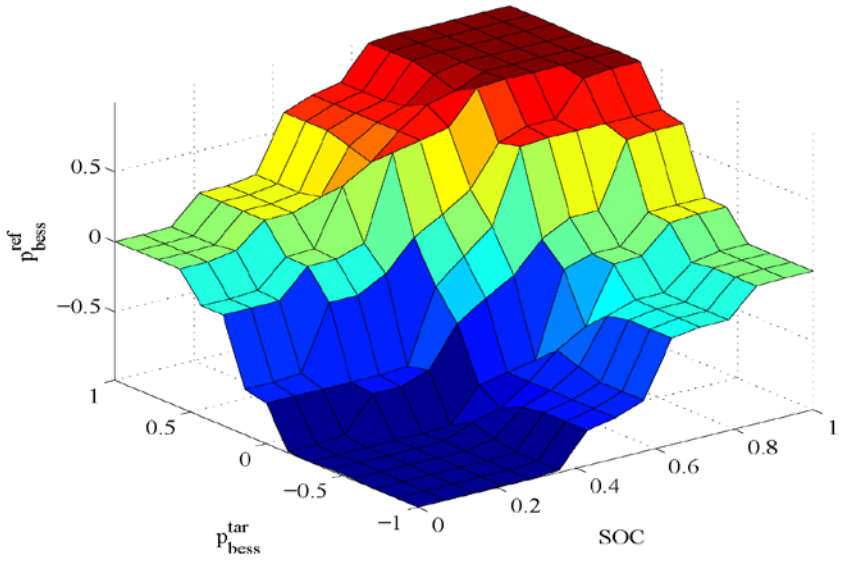

Figure 6-6 : Fuzzy rule surface

6.5 Description of Test Case

A typical configuration of the microgrid system introduced in [61] is adopted as the test case. This system is composed of two DG units, a RES, a BESS, a distribution line and three loads, as depicted in **Figure 6-7**. The parameters of these components are listed in **Table 6-1** in the previous section 6.3. The normal operation range of the BESS is set between 20% and 80%. In grid-connected operation, BESS will be charged to a high level (SOC > 50%). The cut-off time, when the PCC switch opens, is at t = 1000 s. The total simulation time is 2500 s. In order to test the response of the designed FLC to different charging levels, two cases with different initial SOC are defined (Case 1: SOC = 50%; Case 2: SOC = 70%).

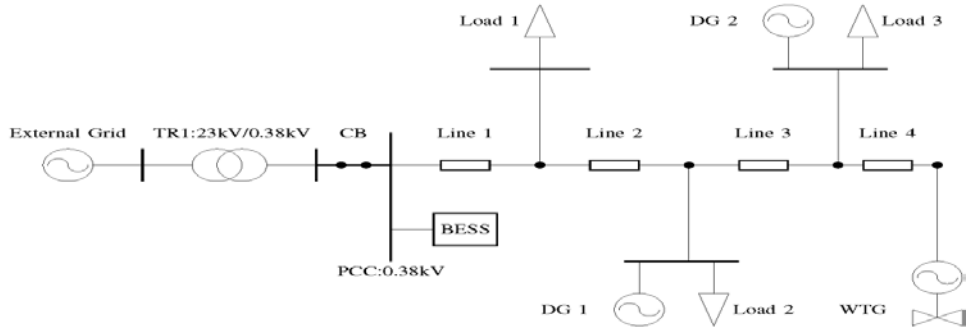

Figure 6-7 : Single line diagram of test case

6.6 Simulation Results

The measurements are read into the wind and load models. The profiles are plotted in **Figure 6-8**. The total load consumption varies from 100kW to 110kW and the total wind power varies from 5kW to 35kW. The wind penetration level is about 30%. For brevity, the simulation result of the grid-connected operation is not included, but it will be interpreted in summary and discussion part in section 6.7.

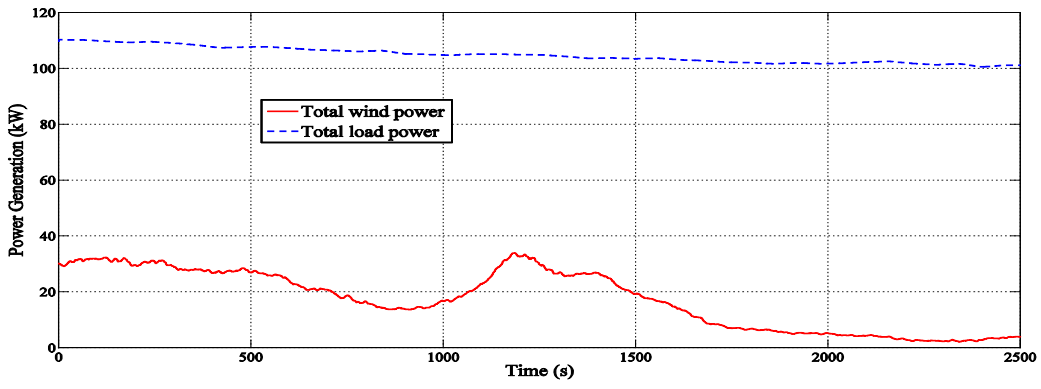

Figure 6-8 : Wind and load profile from BPA

From t = 1000 s to t = 2500 s, the system operates in islanding operation. The main objective of the control strategy is stabilizing voltage and frequency. The voltage and frequency deviation waveforms are illustrated in **Figure 6-9** and **Figure 6-10**, respectively. When the PCC switch opens, the voltage fluctuates for a very short period and is quickly damped out after several cycles, then gets into the steady state after about 0.5 s.

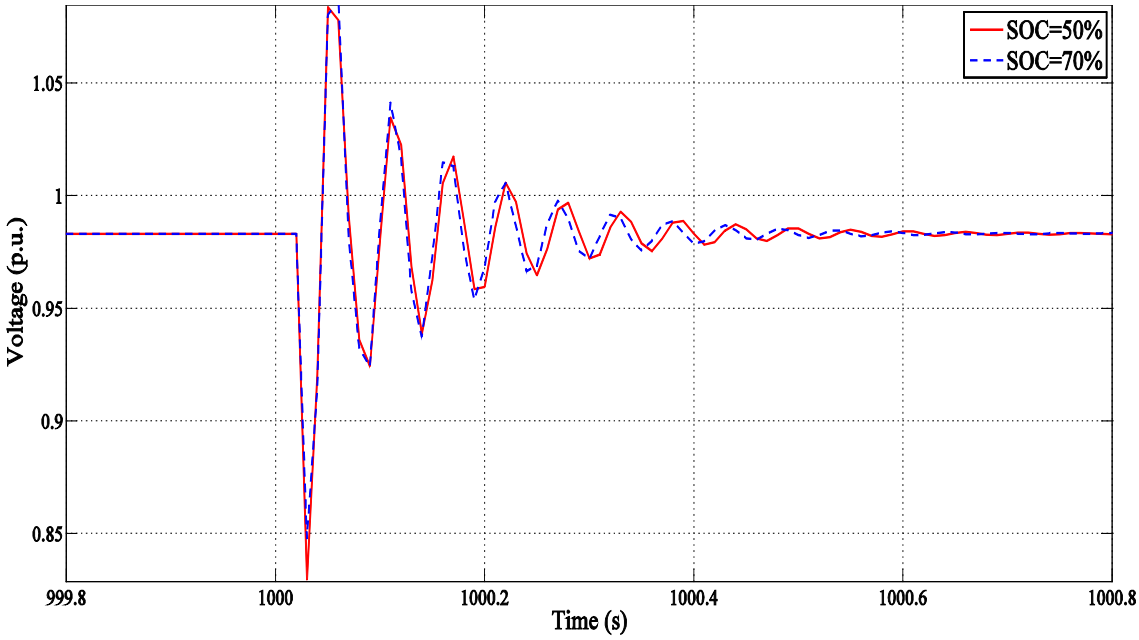

Figure 6-9 : Voltage response at PCC

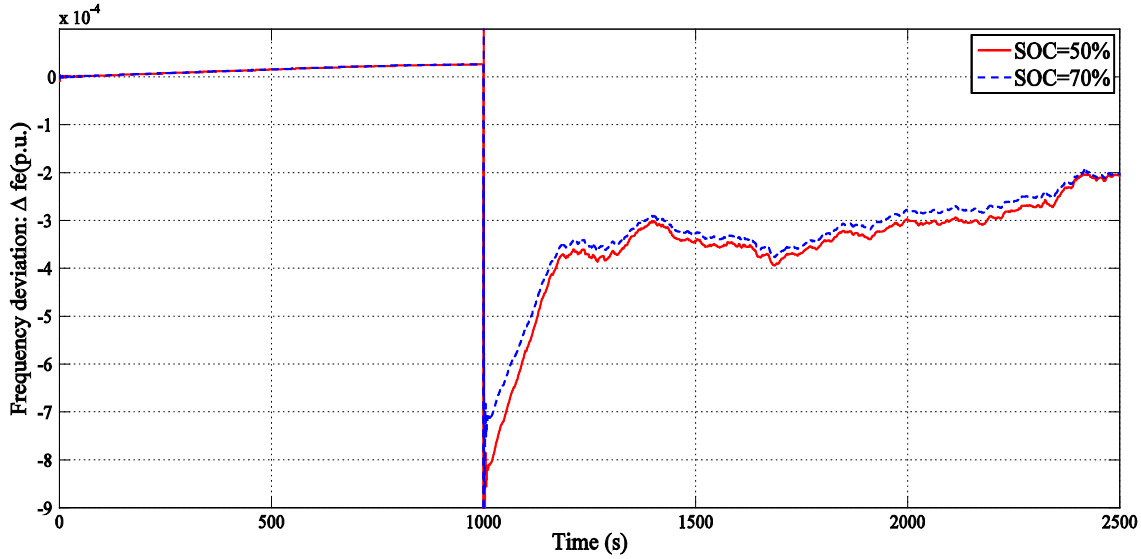

Figure 6-10 : Frequency response at PCC

The recovery of frequency can clearly be divided into two parts according to the waveform. From t = 1000 s to t = 1100 s, the frequency increases rapidly due to the fast response of BESS (**Figure 6-11** (a), (b)). This time frame belongs to primary frequency control period. Also, MMS starts to regulate the dispatchable DG units to compensate active power. From t = 1200 s to t = 2000 s, the system is in the secondary control period. More power is distributed for the DG units. The power distribution factors are different: pf1: pf2 = 1:3, the DG generations are plotted (**Figure 6-11** (c), (d)). Since the charging level is still high, BESS is still involved in the secondary frequency control part. The time span is dependent on the target input power and SOC level. Obviously, BESS with lower charging level will decreases much faster. The gap is filled by DG units. At about 2400s (t = 1200 s to t = 2400 s), the frequency returned back to the normal range (0.99 pu–1.01 pu, dead band is set to ±0.01 pu) as shown in **Figure 6-10**.

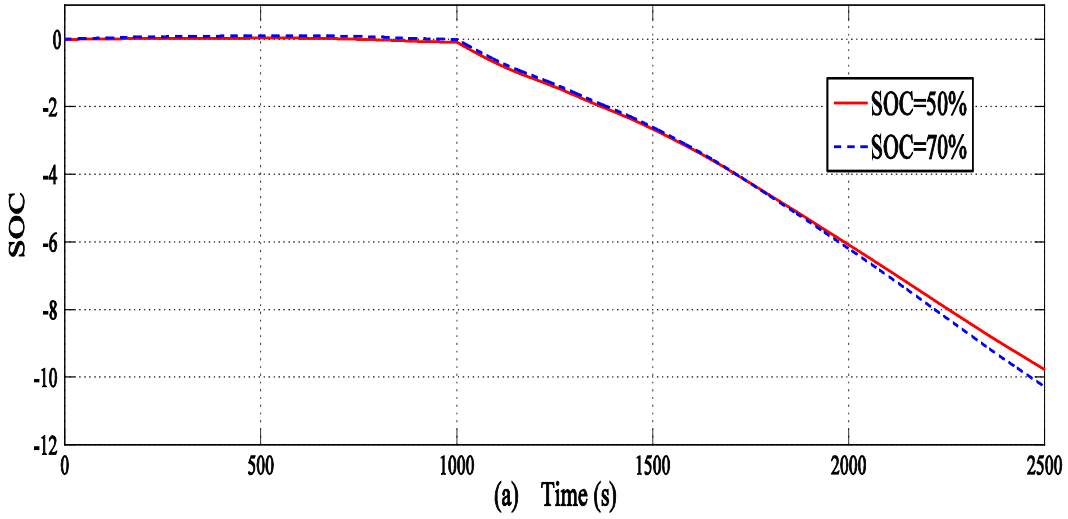

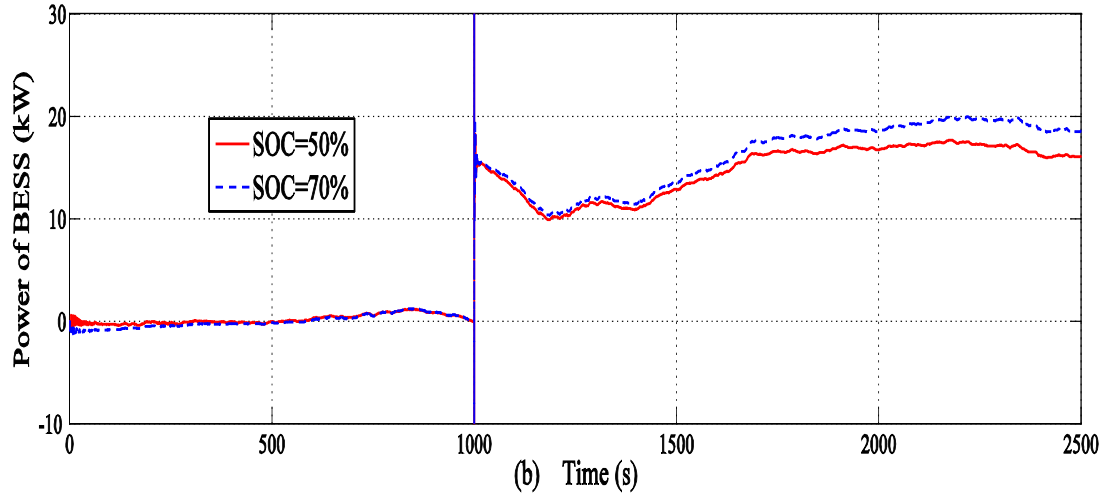

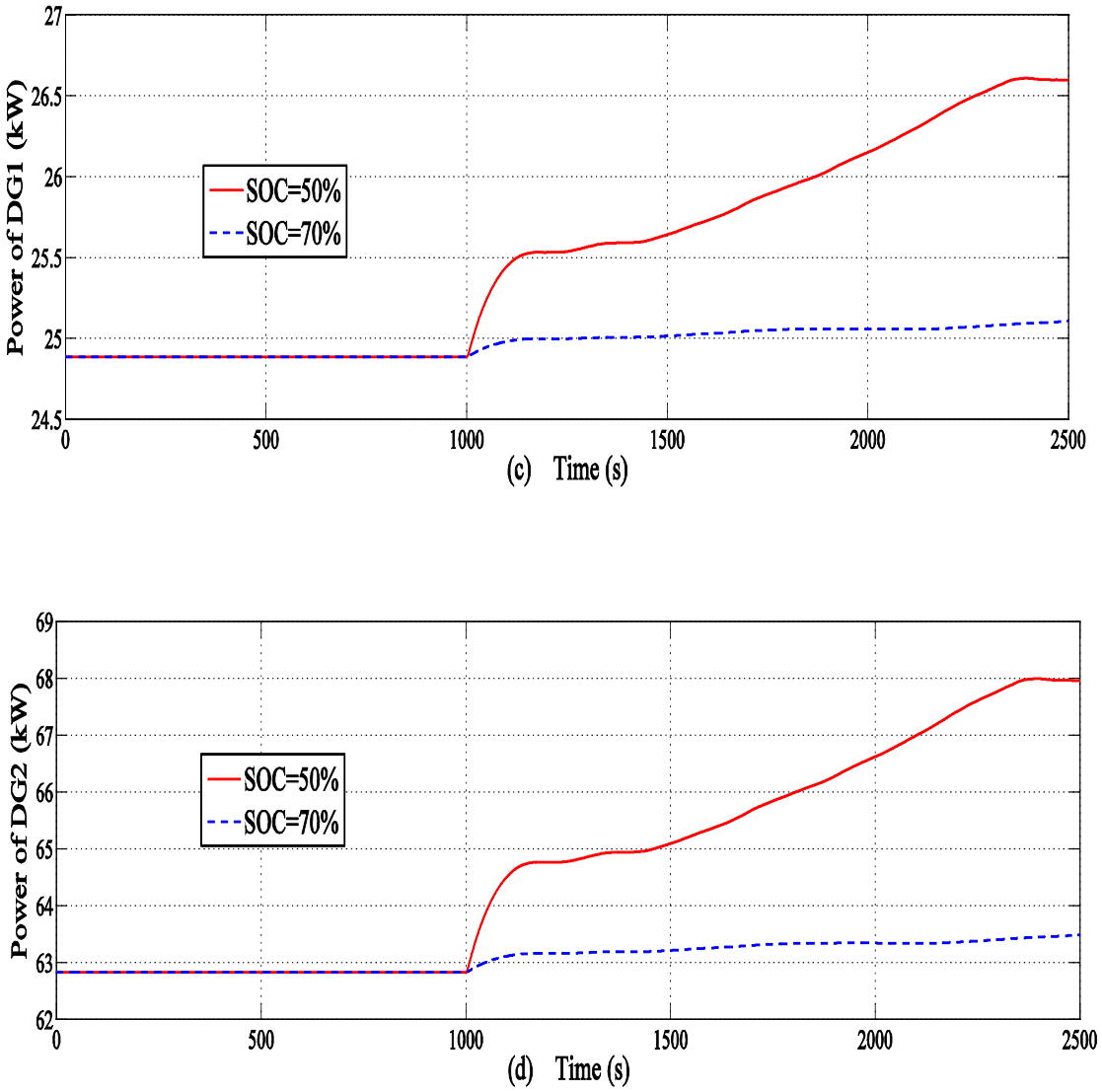

Figure 6-11 : Islanding operation

6.7 Summary and Discussion

Two perspectives are considered. First, control method for timely management of BESS SOC and effective smoothing of wind power generation real-time power output fluctuations are required. Second, the BESS with larger capacity is estimated to be utilized in the future, it will not only be involved in primary frequency control but also in the secondary frequency control. This requires a suitable control strategy that can effectively regulate power output levels and system frequency. The new FLC strategy between a BESS and dispatchable DG units in the high level of the MMS is proposed for further improving the system frequency performance (islanding operation) as well as reducing output power fluctuations (grid-connected operation). In the proposed strategy, the BESS is able to provide a fast charging and discharging operation, the variations of power from the wind turbine units can be absorbed through the charging or discharging operation of the BESS. This enables the BESS to balance the total power generation with the total power demand. For the situation, if the wind power generation changes slowly, SOC levels are almost stable for both two initial SOC cases (i.e. SOC = 50%, SOC = 70%). On the other hand, if wind output decreases, the BESS supplies power to the external grid. Due to different SOC levels, BESS with higher charging level will compensate more power. It indicates that the proposed FLC strategy could efficiently in a timely manner adjust the stored kW hours of power during the BESS's high charging phase, and thereby could augment the performance of the microgrid without adding energy storage capacity. In addition, a large-sized BESS is assumed; therefore, the continuous charging and discharging operations are available on the BESS to be involved in primary frequency control as well as in the secondary frequency control. To perform the continuous frequency regulation on the BESS, the power outputs of the dispatchable DG units (i.e. operating close to their maximum capacities, but still room left for the secondary frequency control) can also be coordinated to share the load following burden of the BESS and to keep the stored energy level on the BESS within the prespecified level. Therefore, through this proposed FLC strategy, the power contribution from the DG units increases whenever the stored energy level on the BESS decreases. On the other hand, the power generation from the DG units decreases whenever the stored energy level on the BESS increases. The simulation results clearly indicate the superiority of the proposed FLC strategy. The fluctuation of output power at PCC is reduced to a great extent while managing battery SOC within a specified target region. The frequency is kept stable and its regulation performance is highly improved in the event of islanding operation. As the core of the control strategy, the design of FLC is verified. Coordination control strategy is rather simple, but the control effect is very good. It gives a new thinking way to increase the quality of coordinated control strategy. The design procedure of the FLC may be applied to other systems, possibly with more complex structure and with careful examination of its potential properties.

7 Multi-agent based Secondary Frequency Control for Islanding Operation of ADNs

This chapter presents a multi-agent based secondary frequency control strategy for islanding operation of ADNs. As mentioned, the ADNs consist of RESs such as wind generation units, DG units, and BESS. The power generation from the wind generation units depends on environmental factors, such as wind velocity. Therefore, complete regulation of the power from these units is quite difficult. Contribution of BESS to the frequency regulation in coordination with AGC participating DG units is addressed in Chapter 5, and the application of fuzzy logic control is discussed in Chapter 6. Similarly, in this chapter, the BESS is coordinated with DG units to propose a new multi-agent based secondary frequency control strategy. In the proposed strategy, the BESS provides the primary frequency regulation, while the DG units provide a secondary frequency regulation. Namely, a coordinated AGC between the BESS and the DG units has been proposed for balancing the total power generation and the total power demand in islanding operation. The control strategy is developed using an agent based paradigm. The proposed multi-agent system (MAS) consists of several types of agents: monitoring agents for transferring the required information through the network, control agents for the charging/discharging operation on the BESS and also for the power regulation on the DG units, and finally, a directory facilitator (DF) agent for continuously monitor the state of the distribution system, identify and respond to any changes or transitions, etc. Hence, multi-agent based simulation platform is also implemented using libraries from the Java Agent Development Framework (JADE). These agents can communicate through the DNP protocol to achieve a desirable secondary frequency performance. Moreover, PSO technique is employed to search globally optimal parameters of the secondary controller in the AGC scheme. The modified IEEE 9-bus system, agent system, and especially its middleware based on the DNP protocol have been used for bi-communication between the RTDS platform and the multi-agent framework. A real-time laboratory experimental setup is constructed in order to investigate the efficiency of the proposed control strategy. The application results show that the proposed multi-agent based secondary frequency control strategy provides a desirable performance, in comparison to PI control design when islanding event is applied to the test system. The various sections are organized as follows. Section 7.1 gives a background of the multi-agent technology applied to the power system optimization and some references are also included. Section 7.2 discusses multi-agent control structure and three types of agents. The descriptions of the three main agents and its communication are included in Section

7.3. In Section 7.4, a stochastic approach, PSO technique is employed to search globally optimal parameters of the secondary controller in the AGC scheme. In Section 7.5, shows an overview of the real-time experimental setup. The simulation has been performed to demonstrate the efficiency of the proposed multi-agent based secondary frequency control for islanding operation of ADNs. The simulation results are presented in Section 7.6 and discussed in Section 7.7.

7.1 Introduction

Smart grid is made possible by applying sensing, measurement, and control techniques with two-way communications to electricity production, transmission, distribution, and consumption parts of the power system. Two-way communication is necessary for system users, operators, and automated devices to have the knowledge of power system condition in order to respond for the changes in system dynamically. Current approach of using a central SCADA system and several smaller distributed SCADA systems is no longer sufficient for large complex smart grid operations. As a consequence, an approach that provides adaptable local control and intelligent decision making is required. Such an issue is particularly important for ADN operation since DGs, energy storage units, and loads under active demand side management are key resources to tackle frequency control. In case of a separation from the HV system, some sort of frequency control is mandatory to guarantee that, at least, part of the system can be operated in islanding operation. Intelligent MAS is a promising technology for implementing such a system because it provides a common communication interface for all elements, and has the potential to provide autonomous intelligent control actions in a distributed nature. MAS provides platform for modeling autonomous decision making entities in decentralized fashion and can be used to implement smart grid concepts for the operation of ADNs. The MAS philosophy and its potential value to the power systems are discussed in [96] - [98]. In recent literature, many researchers have investigated the application of MAS technology with different characteristics and intelligent cores for the frequency control schemes and operation of microgrids [97]. A multi-agent based frequency control scheme for islanded systems with DERs such as PV units, wind units, diesel units, and energy storage is presented [99] - [100]. The addressed scheme has been proposed through the coordination of controllable diesel units and the energy storage with small capacity. All the required information for the proposed frequency control is transferred between the diesel units and the energy storage through computer networks. A secondary frequency controller is needed to maintain the system frequency at the desired nominal value. Many efforts have been dedicated to design novel control strategies for microgrid operation, especially in islanding operation to correctly manage a microgrid during its transition from a grid-connected to an islanding operation, as well as during its autonomous operation [28], [61], [101] - [107]. In [108], control strategies named single master operation and multiple master operation were tested for microgrid island-

ing operation. Also, different PSO based controllers are commonly used in several literatures as the control strategy for LFC [109] - [118]. PSO is a population-based evolutionary technique that has many key advantages over other optimization techniques, and is not only well suitable for scientific research, but also electric power systems applications. Furthermore, PSO has been proven to be an efficient tool both in terms of speed and optimization capability, and robustness. It is a trend to incorporate the multi-agent technology into power system optimization [72], [112], [119] - [125]. Motivated by the above observations, the secondary frequency control strategy is developed using an agent based paradigm and PSO is adopted due to its applicability, speed and optimization capability, and robustness. The algorithm used in this work is based on the previous author's research [72] on improving the efficiency via agent based PSO.

7.2 Proposed MAS Structure

The proposed structure consists of a number of agents. Each agent represents some of the physical components in the distribution system. Each zone has two agents (control and monitoring) that communicate with each other to control the whole system and a corresponding DF agent. The placement of agents is shown in **Figure 7-1**. Moreover, there are DG agents and load agents depending on the zone. The test case used for the experiment purpose is shown in **Figure 7-2** which is the same test case used in Chapter 5. It consists of a section of typical medium voltage (11 kV) distribution system. It includes 3 DG agents, 4 load agents and 3 DF agents. The system is divided into three zones based on the availability of DG. There is no DG available in the zone 1. The zone 2 has two DGs, whereas the zone 3 has one DG. Corresponding DF agents are responsible for all the balancing and assigning new tasks in their respective zones. **Table 1** describes different possible states, roles, capabilities and control actions for the three kinds of agents. The aim of MAS is to define a distributed mapping function from agents to roles, based on current state and capabilities of agents.

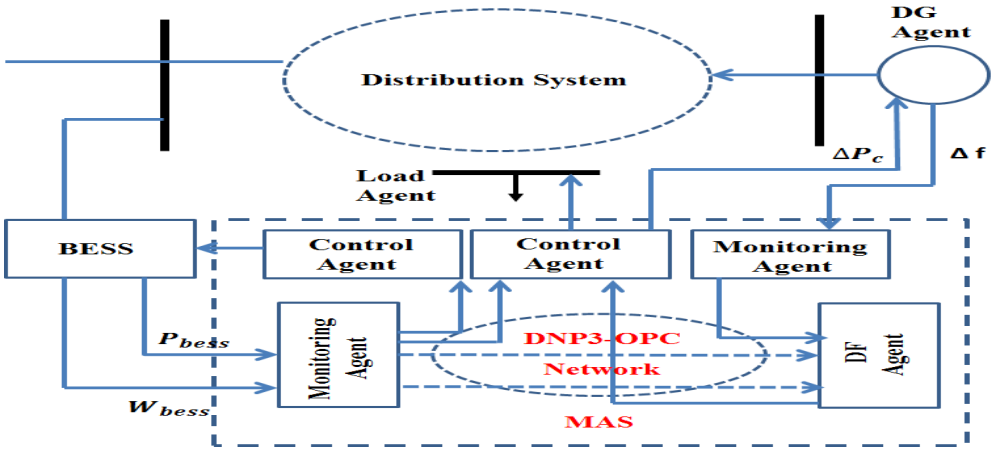

Figure 7-1 : An overview of different agents

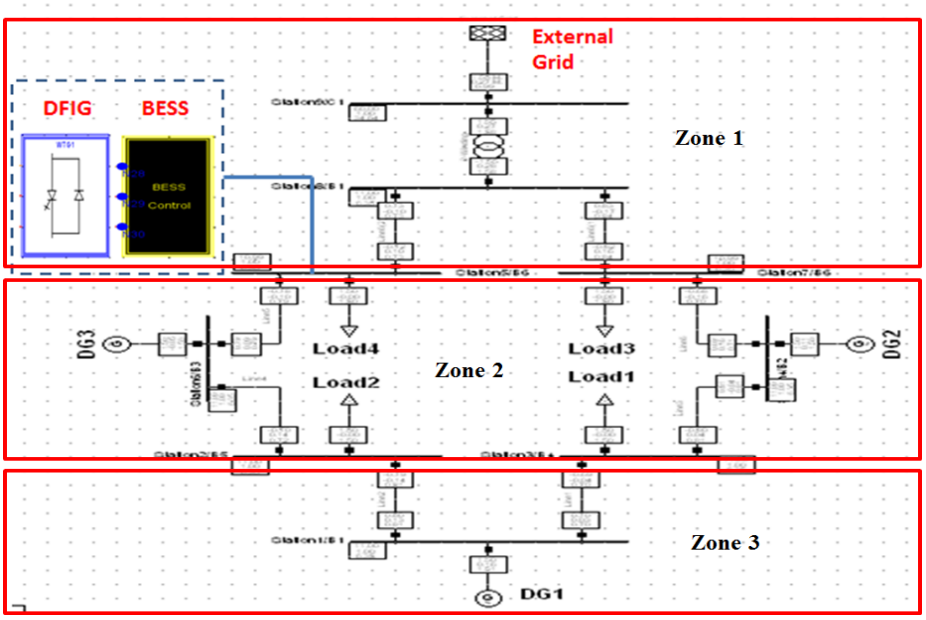

Figure 7-2 : Test case used for experiment consisting of 3 zones

Table 7-1 : Description of agents, states, roles, capabilities and related actions

Agents	States	Roles	Capabilities	Actions
DG	High Average Low Disconnected	Generator Regulator	Produce power and Frequency control	P+ P- Disconnect (Re)connect
DF	Disconnection Reconnection Fault State changes	Directory Facilitator Identify Decision	Monitor current and voltage	Calculation Negotiation
Load	Critical Non-critical	Connected Disconnected	Auto Shed	(Re)connect Disconnect

However, defining proper control plans and assigning specific roles to agents are two different tasks. Accomplishment of a specific control plan requires successful execution of a number of roles. A set of such roles defines a proper control plan. A transition function maps a role set (i.e. a control plan to specific situations). The detail description of this mapping process based on domain rules [127] how they determine the role sets are out of the scope of this chapter. Such transitions are defined during the design phase. The DF agent determines best situation to control plan mapping every time there is a new situation. The decision of assigning specific roles to agents is taken dynamically through explicit communication. This is done in a distributed manner through an auc-

tion mechanism. For example, a fault scenario on the external grid in zone 1, DF agent analyzes the current islanding situation and determines a best control plan that maps to the current situation. Then, DF agent communicates with DG and load agents for specific role assignment in chosen control plan. DG and load agents calculate their local cost functions based upon their current states and capabilities. Based upon the value of this cost functions, DG and load agents send bids to DF agents. As a consequent, DF agent responds and assigns a role to every agent in the selected control plan. **Figure 7-3** shows the process of control plan determination and role assignment.

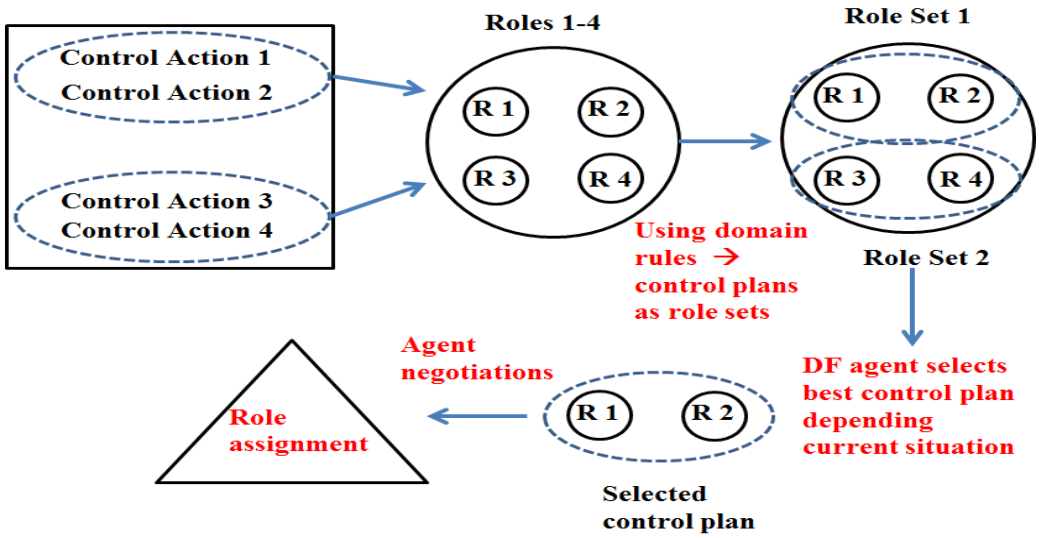

Figure 7-3 : Control plan and role assignment process in agents

7.3 Agent Decision Models and Communication

This describes the three main agents that incorporate in the MAS are given below.

7.3.1 DF Agent

The DF agent has a central role in proposed structure. They continuously monitor the state of the distribution system, identify and respond to any changes or transitions. If the fault is detected in any of the zones, the DF agent will calculate energy balancing and assign new roles to DGs and loads. This requires calculation of total generation and consumption of energy and negotiation with DG and load agents for participation in balancing. DG and load agents calculate local cost functions based upon their current state and capabilities and communicate it with DF agent. The DF agent based upon the value of cost function of each of these agents assigns them new roles. Thus, the job of

DF agent is to determine a mapping function that takes current state and maps roles to specific agents based upon their capabilities.

$$f_{tr} = (S_{cur}, T_i CP_{ini}) = CP_{fn} \quad (1)$$

where $f_{tr}$is a function that takes current state S_{cur} and a transition property T_i, to map chosen control plan CP_{ini} into a final control plan CP_{fn} with all roles assigned to specific agents. T_i are the transition properties (i.e disconnection, reconnection, faults, state changes) which trigger a change in the current control plan.

7.3.2 DG Agent

DG agents represent each DG in distribution system. Each DG agent, on receiving message from DF agent, calculates its cost function. The cost function of DG agent is based upon its current state, e.g. active power set point capabilities, and ability to control frequency, etc. The cost function of a DG agent is defined as:

$$\delta_c (S_{cur}, C_{cur}) = U_{role} \quad (2)$$

The cost function is a function that maps the current state of DG agent S_{cur} and current capabilities C_{cur} into a role utility U_{role}. After calculating the cost function, DG agent sends a bid based on the value of this cost function. The DF agent cumulates bids from all DG agents and sends back a message with a new role. DG agent on receiving this message takes up the new role and starts to execute actions.

7.3.3 Load Agent

Load agents represent distributed loads in distribution system. Each load agent, on receiving message from DF agent, calculates its cost function. The cost function of the load agent is based upon its current state, e.g. critical/non-critical and capabilities. The cost function of load agent is defined as:

$$\delta_c (S_{cur}, C_{cur}) = U_{role} \quad (3)$$

Similarly, the cost function is a function that maps the current state of load agent S_{cur} and current capabilities C_{cur} into a role utility U_{role}. After calculating the cost function, load agent sends a bid based upon value of this cost function to DF agent. DF agent cumulates all load agents and sends back a message with a new role. Load agent on receiving this message takes up the new role.

7.3.4 Agent Communication

Real-time communication between the multi-agent software platform and RTDS is achieved by implementing a middleware based upon OPC and DNP protocols [72], [128]. This middleware is implemented using JADE and fully conforms to the OPC standard. Through an OPC server, software agents can connect to respective device models in the RTDS and perform control actions, e.g. changing the set point of a DG, opening and closing of a breaker during simulations, etc. Each agent in the software platform creates its own instance of connection and has an individual channel of control commands, which ensures that decentralized nature and robustness of the control mechanism is not compromised [129]. This will be further explained later in Section 7.5.

7.4 Particle Swarm Optimization

PSO is a population based stochastic optimization technique developed by Dr. Eberhart and Dr. Kennedy in 1995 as a new heuristic method, inspired by social behavior of bird flocking or fish schooling [130]. It belongs to the class of direct search methods that can be used to find a solution to an optimization problem in a search space. In the PSO method, each particle *i* (*i* = 1, ..., N) in the population is characterized by three vectors (x_i, v_i, p_i) which represent their temporal position $x_i = (x_{i1}, \dots \dots . . x_{in})$, velocity $v_i = (v_{i1} \dots \dots \dots v_{in})$ and the best position $p_i = (p_{i1}, \dots \dots p_{in})$. The fitness of each particle is given by the function value of $f(x_i)$. In this study, the load setting points of governors for DG units will be optimized. Hence, the lower the function value the better the fitness. Each particle stores its best position called *pbest* which gives the best fitness in memory. Furthermore, the best position found by all particles in the population (global best position) can be represented as *gbest* [109] - [110], [131]. In each step, the best particle, global position, and corresponding objective function values should be saved. For the next iteration, each particle *i* move around the search space at iteration *k*, and renews its velocity component v_i^{k+1} using its previous *pbest, gbest* and current velocity , v_i^k at iteration *k*. The position, velocity corresponding to the *k* th dimension of ith particle can be updated using the following equation. During this time of iteration (*t*), the particles update the speed of the previous speed with the new speed determined by equation (4). The new position is determined by the sum of the previous position and the new velocity as shown in equation (5).

$$v_i^{k+1} = v_i^k + c_1 r_1 \left(p_i^k - x_i^k\right) + c_2 r_2 \ \left(p_g^k - x_i^k\right) \quad (4)$$

where c_1 and c_2 are the acceleration constants, and r_1 and r_2 are the uniform random numbers in the interval [0, 1]. If v_i^k is larger than a predefined velocity v_{max} called maximum velocity, it is set to v_{max}. Similarly, if it is smaller than $-v_{max}$, it is fixed to $-v_{max}$. Then, the particle changes its position by the 'equation of motion'.

$$x_i^{k+1} = x_i^k + v_i^{k+1} \qquad (5)$$

Using the concept described in **Figure 7-4**, at given current position and velocity of particle, the change of velocity (v^{mod}) is determined based on *gbest* and *pbest*. Then, the new velocity (v^{k+1}) can be calculated by summation of current velocity (v^k) and the change of velocity (v^{mod}). Finally, new position is updated by equation (5).

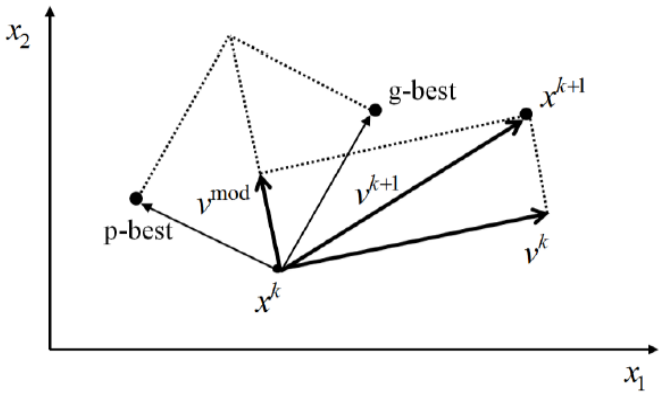

Figure 7-4 : Update the position and velocity of each particle

The process of searching optimal value by PSO is as follow and the flowchart of verification is also depicted in **Figure 7-5**.

1. Initialize all particles via a random solution.
2. Evaluate the performance F(x^k) of each particle using its current position, (x^k).
3. Compare the performance of each particle to its best performance (*pbest*) :
   If F(x^k) < *pbest*,then
   (a) *pbest* = F(x^k)
   (b) $x^{pbest} = x^k$
4. Compare the performance of each particle to its global best performance (*gbest*):
   If F(x^k) < *gbest*,then
   (a) *gbest* = F(x^k)
   (b) $x^{gbest} = x^k$
5. Update the velocity of each particle according to equation (4).
6. Update and move each particle to a new position according to equation (5).
7. Stop the process if the stop criterion is satisfied. Otherwise, go to step 2.

The variables are used in PSO are summarized in **Table 7-2**.

Table 7-2 : Variables used in PSO algorithm

Variable	Definition
x_i	*Position of ith particle*
v_i	*Velocity of ith particle*
pbest	*Best position particle i achieved based on its own experience*
gbest	*Best particle position based on overall swarm's experience*
w	*Inertia Weight*
c_1 & c_2	*Acceleration constants*
r_1 & r_2	*Uniform random numbers*
k	*Iteration index*

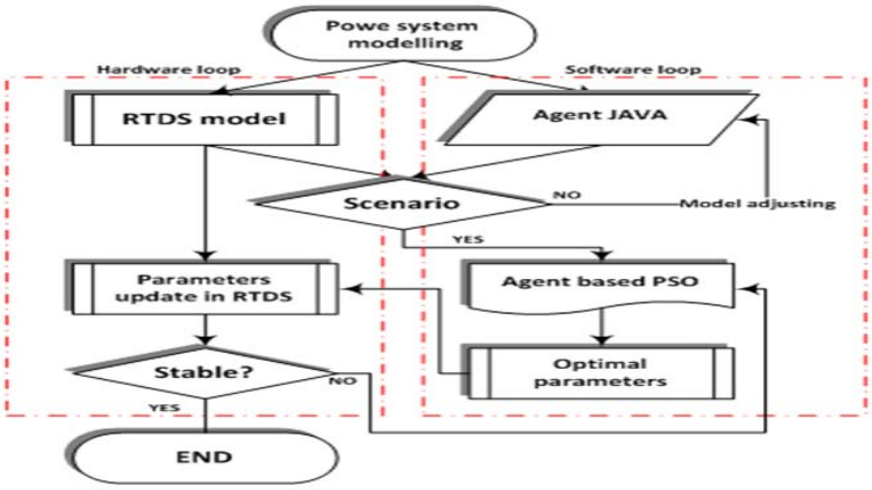

Figure 7-5 : Flowchart of the parameter optimization in MAS and RTDS verification

Based upon formulation, the objective function is to minimize the cost of providing regulation power from DGs (DG_{i1}..... DG_{in}) in two dimensions of P and Q in the islanded system. For this purpose, the PSO will attempt to search globally optimal parameters of the secondary controller in the AGC scheme. In particular, the load setting points of governors for DG units, K_i … K_{in}will be optimized based on their cost functions where K_i is individual load set point for a single DG in distribution system. The algorithm will start with a randomly selected value and traverse through a swarm of candidate solutions.

$$X_{ik}\ (K_{i1}(p_i, q_i), K_{i2}\ (p_i, q_i), \ldots\ldots K_{in}\ (p_i, q_i)) \qquad (6)$$

The PSO generates the optimal values of the controller parameters simultaneously by minimizing the objective function above. The entire approach is verified by the RTDS and its parameter optimization process is shown in **Figure 7-5**. The proposed multi agent based secondary frequency control strategy provides a desirable performance, in comparison to PI control design [132] - [133]. The PSO parameters were set to$c_1 =$

2.05 and $c_2 = 2.05$, which are the typical value of PSO. The 30 of population size and 20 of maximum iteration were used. In the table, iteration means the average iteration of 20 runs which is satisfied with convergence criteria of 10^{-3}. The optimization parameters of PSO are listed in **Table 7-3**. After the optimization by PSO, the K_i is determined at 0.6259.

Table 7-3 : Parameters used for PSO

PSO parameters	Value / Type
Iteration	*20*
Population	*30*
c_1 & c_2	*2.05, 2.05*
r_1 & r_2	*0.4, 0.6*

7.5 Real-Time Laboratory Experiment

7.5.1 SIL Test Platform

The real-time experimental setup is comprised of the RTDS, Matrikon OPC server for SCADA DNP, and agent JAVA as illustrated in **Figure 7-6**. The RTDS is equipped with analogue and digital I/O cards to enable the data exchange between the RTDS and external systems. In addition, the RTDS has one gigabit transceiver network (GTNET) interface card which enables the RTDS to communicate with external systems with DNP and IEC 61850 protocols. The Matrikon OPC server for SCADA DNP is a communication gateway which provides OPC access to devices compatible with the DNP protocol. Hence, data can be exchanged between the RTDS and agent JAVA over a LAN using the DNP-OPC protocol [134] - [136]. Since it is a closed loop testing, the practical communication latency for the RTDS and OPC is already embedded.

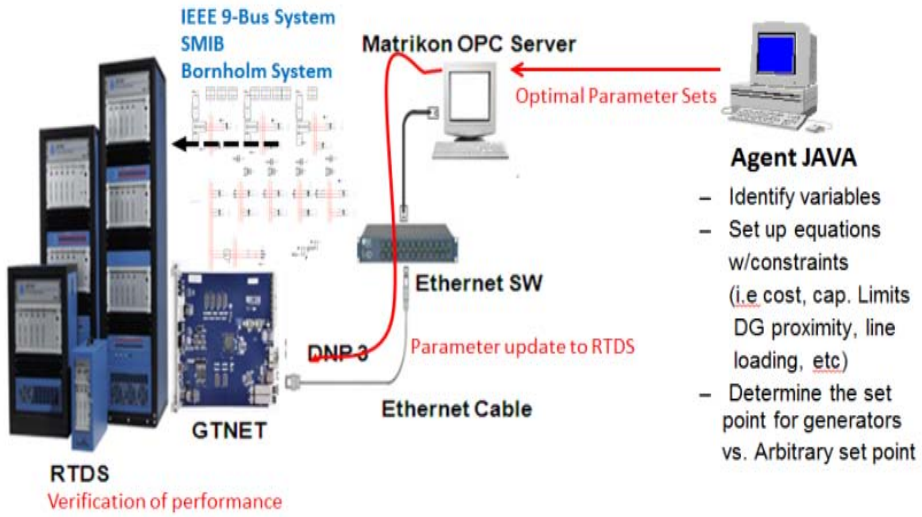

Figure 7-6 : Hardware & software setup: RTDS (left) and Java (right) in a complete SIL environment.

7.5.2 Communication Test between the RTDS and the Matrikon OPC

In order to verify the data exchange between the RTDS and the Matrikon OPC server for SCADA DNP, a communication test has been carried out. A small test case is built to verify the data exchange for analogue and binary variables between the RTDS and the Matrikon OPC server. The test case is shown in **Figure 7-7**.

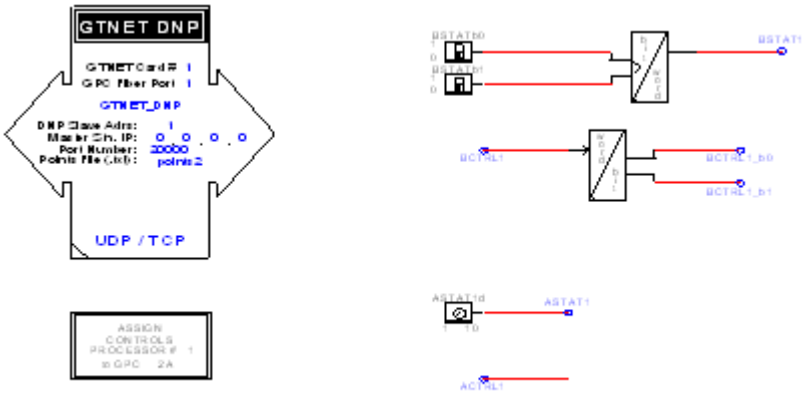

Figure 7-7 : Simple communication test case implemented in RTDS

The RTDS is connected to the Matrikon OPC server for SCADA DNP through an Ethernet network. The Matrikon OPC Explorer is used to view the values of status variables from the RTDS and to change the values of control variables to the RTDS. In order to avoid the ambiguity, terms of ‘status’ and ‘control’ are used to represent the variables from the RTDS and to the RTDS, respectively. In the test case, one analogue status variable and one analogue control variable are defined to test the analogue data exchange; two binary status variables and two binary control variables are defined to test the binary data exchange. The defined variables are listed in **Table 7-4**.

Table 7-4 : Variables used in the test case

Variable Name	Variable Type
BSTATb0	Binary Status Variable
BSTATb1	Binary Status Variable
BCTRL1_b0	Binary Control Variable
BCTRL1_b1	Binary Control Variable
ASTAT1	Analog Status Variable
ACTRL1	Analog Control Variable

The values of binary and analog status variables will be transported from the RTDS to the Matrikon OPC server and the values of binary and analog control variables will be transported from the Matrikon OPC server to the RTDS. In the Matrikon OPC Explorer, tags for all variables have to be defined. The used tags are listed in **Table 7-5**.

Table 7-5 : Tags used in the Matrikon OPC Explorer

Tag Name	Value
AnalogInput 030.0.x	Analog status value
AnalogOutput 040.0.x	Analog control value
AnalogOutputBlockShortFP 041.3.x	Analog control setting
BinaryInput 001.0.x	Binary status value
BinaryOutput 010.0.x	Binary control value
ControlBlockRelay 012.1.x	Binary control setting

The AnalogInput 030.0.x tag is used to get the analog status values from the simulated power system in the RTDS. The AnalogOutput 040.0.x tag is used to change the analog control values to the simulated power system which will be the set points for the control variables. The AnalogOutputBlockShotFP 041.3.x is used to change the value of AnalogOutput 040.0.x. The BinaryInput 001.0.x tag is used to get the binary status values from the simulated power system in the RTDS. The BinaryOutput 010.0.x is used to change the binary control values in the simulated power system. The ControlBlockRelay 012.1.x is used to change the value of BinaryOutput 010.0.x. The status and control values in the RTDS and the Matrikon OPC Explorer are shown in **Figure 7-8** and **Figure 7-9,** respectively. The status and control values should match. For example, Runtime meter values (i.e. 4, red circle) match with the AI status (i.e. ASTAT1.0) in **Figure 7-8**.

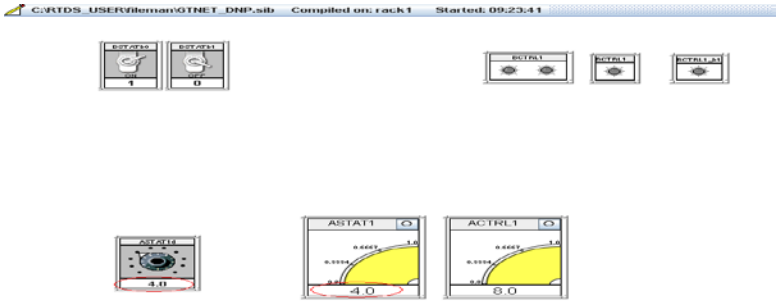

Figure 7-8 : Status and control values in the RTDS communication test case

Contents of 'Group0'

Item ID	Access Path	Value	Quality
Rtds.Rtdshost.Rtdsdnp3.AnalogInput 030.0.0		7	Good, non-specific
Rtds.Rtdshost.Rtdsdnp3.AnalogOutput 040.0.0		3	Good, non-specific
Rtds.Rtdshost.Rtdsdnp3.AnalogOutputBlockShortFP 041.3.0		0	Good, non-specific
Rtds.Rtdshost.Rtdsdnp3.BinaryInput 001.0.0		True	Good, non-specific
Rtds.Rtdshost.Rtdsdnp3.BinaryInput 001.0.1		True	Good, non-specific
Rtds.Rtdshost.Rtdsdnp3.BinaryOutput 010.0.0		True	Good, non-specific
Rtds.Rtdshost.Rtdsdnp3.BinaryOutput 010.0.1		True	Good, non-specific
Rtds.Rtdshost.Rtdsdnp3.ControlBlockRelay 012.1.0		3,1,0,0,0	Good, non-specific
Rtds.Rtdshost.Rtdsdnp3.ControlBlockRelay 012.1.1		3,1,0,0,0	Good, non-specific

Figure 7-9 : Status and control values in Matrikon OPC Explorer

The test results show that both analog and binary status values can be obtained from the simulated system in the RTDS and the values of control variables can be sent back to the simulated system in the RTDS. Therefore, with the system setup as such, the functionality of agent based controller can be tested.

7.5.3 Modified IEEE 9-Bus Test System

The modified IEEE 9-bus system from chapter 5 is used and the details are given in Section 5.2.1. For brevity, only the AGC scheme is presented as shown in **Figure 7-10**, measures the system frequency and changes load settings of DGs via the AGC signal. All the relevant parameters are also given in [72], [74].

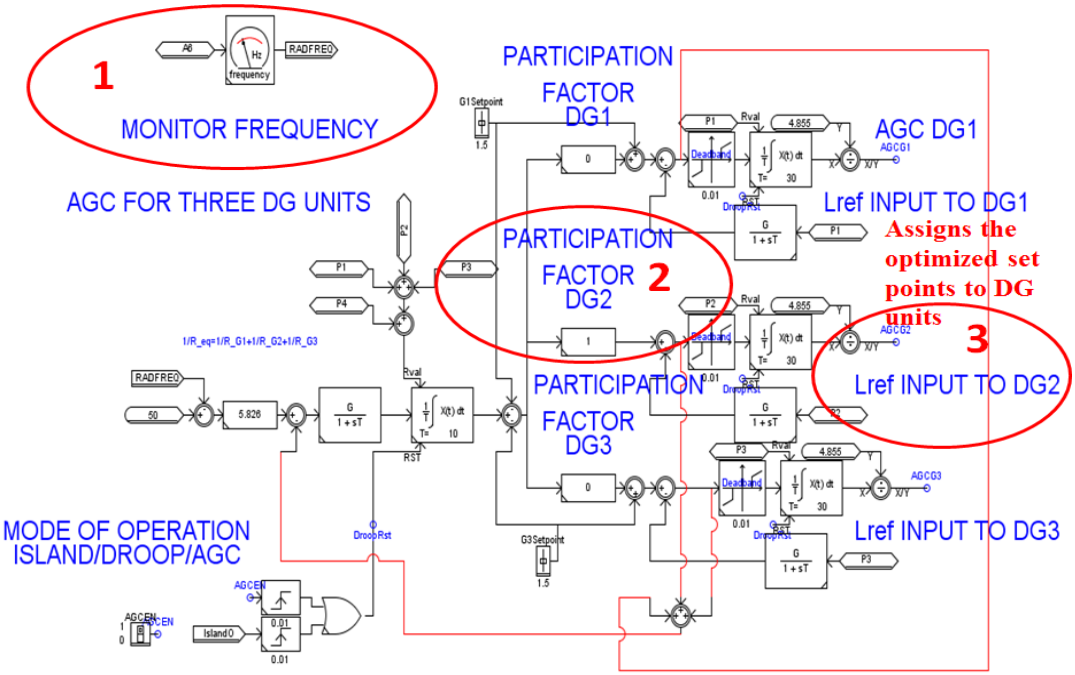

Figure 7-10 : RTDS model of AGC scheme to control the speed of DGs

7.6 Simulation Results

In order to further assess the effectiveness and robustness of the proposed multi agent based secondary frequency control, simulation is carried out. Initially, the test system is balanced and all voltages at the nodes of all loads are at 1pu. Corresponding agents are continuously monitoring the voltage & frequency to respond to any disturbance. A 3-phase fault is applied at the nominal operating conditions (P_{scr} = 1pu, δ_0 = 0, initial power flow of 2.5MW) at t = 10 s. The following case is considered.

7.6.1 Case I: One DG Unit Providing AGC

In this case, only one DG is providing regulation service as defined by the equation (1) in Section 7.3.3. The corresponding DG provides an extra active power for balancing in the islanded system. The execution sequence is described as follows;

- Step1. Loss of 2.5 MW power from the external grid
- Step2. Created an imbalance in the islanded system
- Step3. Load agents observe voltage & frequency drop
- Step4. Load agents contact DF agent for any available regulation service
- Step5. DF agents informs the current service availability and provides its reference
- Step6. Load agents request DG #2 agent for provision of service
- Step7. DG #2 agent accepts the request and provides the service by increasing its active power (i.e. PSO optimization process starts as SIL)
- Step 8. Voltage & frequency recover at the nodes of all loads

The distribution system is divided into three zones as described and shown in **Figure 7-2**. Each zone has a number of agents that communicate with each other. These agents were simulated using JADE. The size of the messages is about 1500 bytes. The typical time it takes to send a message and have it received by another agent is around 1 to 200 milliseconds. The time depends on the network conditions and the process running inside the algorithm. For example, messages will take longer if the corresponding agents need to compute an optimization problem and then send the results to other agents. This analysis was implemented in a relatively small case; thus, if these results are extrapolated to larger systems, the simulation time increases as well as the complexity of the problem. For these larger cases, it is better to simulate different zones of the system in different processors so that each processor can parallelize the solution of the algorithm. This concept aligns with the RTDS's parallel processing technique. Each subsystem is simultaneously solved by different processors. The DG agents would know at a specific time the amount of power that can be controlled depending on their current status, e.g. active power set point capabilities, and ability to control frequency. These DG agents

communicate with other agents for exchange data. In reality, the device could be the smart meter that is part of the advance meter infrastructure (AMI). Using data obtained from the AMI smart meter, the DG agent knows the amount of power that can be controlled during islanding operation. The AMI data would be collected by three agents (i.e. DG, load, DF) that exchange information among themselves and others. For example, two types of different control can be performed through this process. One is to inject power by DG units and the other is the disconnection of loads for shedding purposes, but only for specific situations such as the line overload. General approach is to use the strategy based upon on-line measurement of the loads and load frequency characteristics. Load with smaller frequency dependency are shed first, and with larger frequency dependency are shed later. However, the treatment of load shedding is not fully implemented in the simulation. Furthermore, equipment currently available in the market can shed a load within 80 ms is the best option. Hence, it will not be discussed and remains as a future work. Based on the information collected from each agent, the corresponding zone agent (DG and/or load) performs a local cost function to determine the amount of power that needs to deliver to alleviate and stabilize the frequency. Also the zone agent negotiates with other zone agents in the distribution system if a solution is not obtained. In this case, agents can communicate with each other through a secure DNP-OPC communication channel between the RTDS and Agent JAVA to achieve a desirable AGC performance. Based on the proposed control strategy, DF agent uses the received data from DG/load agents to provide the generation participation factors, role assignment and appropriate control action signal, through a simple AGC scheme. Using this information in the process of PSO optimization step 7, new power set points are computed and sent to the RTDS for the next dynamic simulation. This process is repeated up to frequency stabilization or a maximum simulation time.

In **Figure 7-11**, the frequency response without AGC (no control, has a steady-state error) for islanding operation is shown with legend AGC OFF (green line) and the frequency response with proposed multi agent based secondary frequency control is shown with legend AGC ON (blue line), respectively.

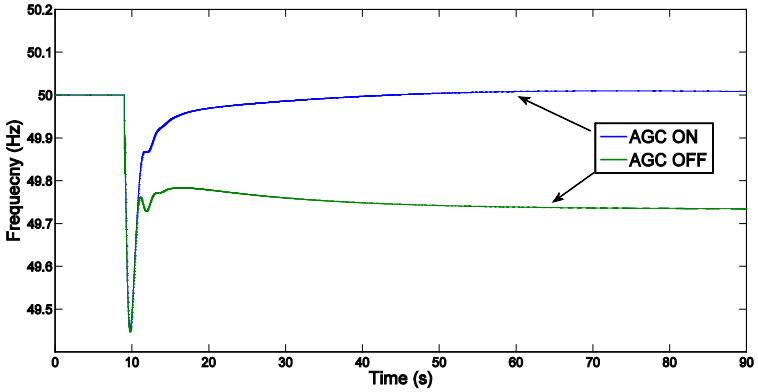

Figure 7-11 : Comparison between AGC on and AGC off

The control strategy is to use one DG as the master controller while the other remains as the slaves. The master DG is switched on to V-f mode after islanding to control the overall island voltage and frequency while the other slave DGs are maintained at fixed generation (i.e. 1.5 MW). As it can be seen from **Figure 7-12** that the frequency dropped to 49.45 Hz and then recovered by the activation of secondary frequency control strategy. Similarly, the voltage dropped to 0.8728 pu and recovered to the operational range after 60 s. The response of active and reactive power output of DG#2 is shown in **Figure 7-13** (a) and (b). The master controller is capable of reducing the voltage and frequency excursions considerably and keeping them within permissible limits. It should be noted that the reactive power set points for DG is not considered by the agent.

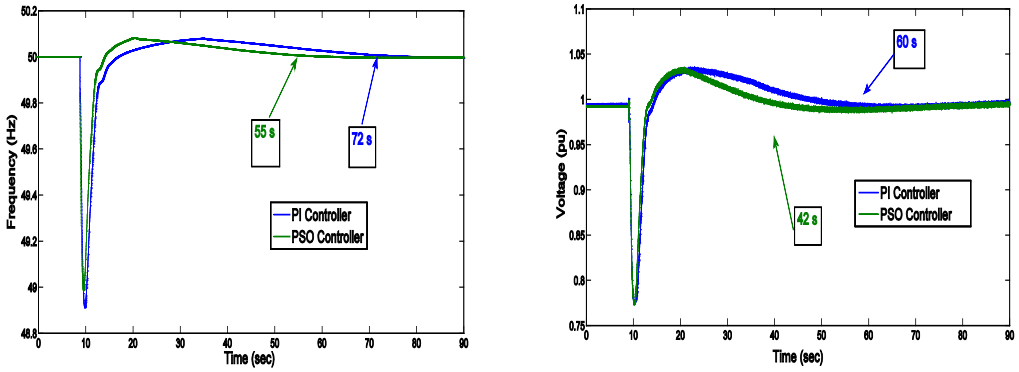

(a) (b)

Figure 7-12 : Monitored changes in frequency waveforms (a) and voltage (b) at bus 5

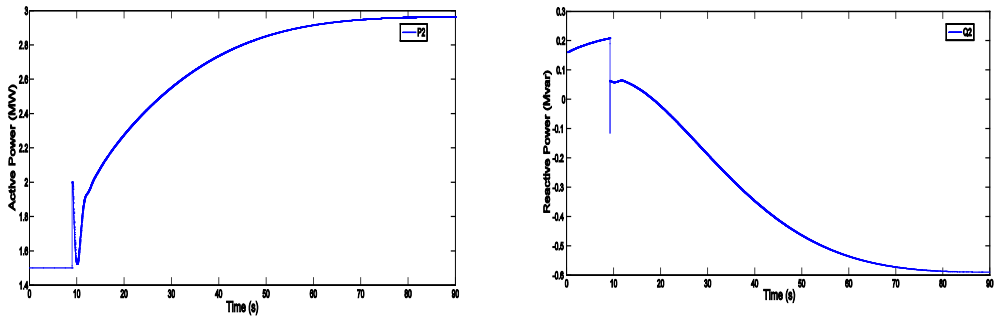

(a) (b)

Figure 7-13 : Monitored active and reactive power output of DG#2 (DG#1 and DG#3 are not participating in secondary frequency control)

Figure 7-14 shows the communication of agents during the simulation. It can be seen that the load agent sends a request message to the DF agent for regulation service. The DF agent sends back a message with the available service information. Load agent sends a request message to DG agent for provision of this service. The content of request is the optimized load set point for DG#2 to increase the active power in order to stabilize the frequency. Finally, DG #2 agent replies with an 'agree' message.

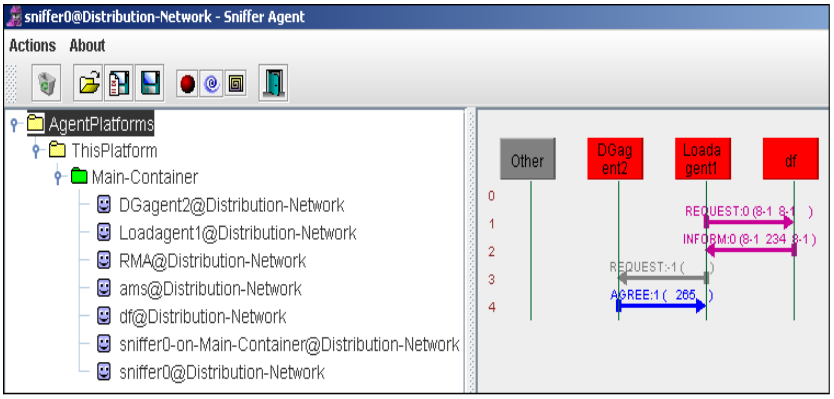

Figure 7-14 : Agent communication

7.7 Summary and Discussion

An intelligent multi-agent based secondary frequency control for the islanding operation of ADN is proposed. A real-time digital simulation of the test case is carried out and optimization of the parameters of the AGC is achieved in a simple manner through the effective application of PSO. Based on the proposed control strategy, DF agent uses the received data from DG and load agents to provide the generation participation factors, role assignment and appropriate control action signal, through a simple AGC scheme. The outcome of simulation results show that the proposed multi-agent based secondary frequency control strategy performs well, in comparison to the performance of PI control design even in the existence of the communication delay time through existing computer network. It must be noted that there always exists the communication delay time for transferring the required information on the network. The estimated communication delay time is around 40 to 50 ms for the proposed multi-agent AGC system during the tests. There exists no significant degradation of control performance by the existing communication delay. However, for the longer communication delay, the control performance might be degraded or deteriorated not to be able to perform the proper AGC. When considering the actual installation of the proposed multi-agent based AGC scheme, the stable operation of the proposed AGC scheme might be required for the communication delay up to 0.1s.

Also, the MAS are implemented in foundation for intelligent physical agents (FIPA) compliant JADE open source platform. The distribution system is successfully monitored, controlled and operated by means of the developed MAS. The developed MAS in this research are scalable, robust and easily reconfigurable. Therefore, the developed MAS can be easily extended for managing and controlling different kind of DG units by extending the functions of the agents and creating additional agents in the system. Hence, the results indicate the efficiency of the proposed multi-agent based secondary frequency control strategy with PSO technique for real-time applications. Nevertheless, there are a number of challenges, specific to the proposed multi-agent based secondary frequency control strategy that requires further investigation as future work. These are concerned with the scalability such as multi-set of DG units and loads, coordination strategies, and improvement on SIL optimization procedure using agent java in real-time simulation environment. In addition, communication is very costly if a direct communication link is lost from the central coordinating agent to the bottom agents, then the task cannot be performed, so the AGC is terminated. Therefore, agents must maintain coordination when communication is unavailable. Or, agents may not be able to share all the information with other agents all the time due to the limitations of the communication channel and computational device. The usual delay attached with communication links, and sensor measurements is around 50 ms to 1 s. To solve this problem, a hierarchical control structure should be considered which has the upper controller and the decentralized controller using only locally measured frequency deviation.

8 Conclusion and Future Work

This PhD project is intended to develop effective frequency control strategies for the islanding operation of an ADN or a small island distribution system. The coordinated control strategy consists of a primary control action of the BESS and a secondary control action of the MMS is proposed. Also, the design of FLC and multi-agent based control are introduced for improving secondary frequency control performance. These contributions are summarized in Section 8.1. Finally, a discussion on the future works and research needs is highlighted in Section 8.2.

8.1 Conclusion

The main contributions and findings of the thesis are as follows:

In **chapter 4**, a reliable real-time model of the Bornholm distribution system is constructed using the RTDS. The resulting model is capable of performing dynamic simulations of the islanded Bornholm distribution system to investigate the frequency regulation performance. The role of AGC model in connection with the Bornholm distribution system to manage the islanded system is emphasized. The simulation models, the typical data, and the scenarios used are also introduced. The outcome of simulation results have shown that the contribution to AGC is effective for a successful islanding manoeuvre performed under different power levels. The simulation results show the secondary frequency control loops properly act to maintain system frequency and exchange powers close to the scheduled values by sending a corrective signal to the DG units in proportion to their participation in the AGC system. The participation factor for DG unit 5 is 0.3858, while the larger participation belongs to DG unit 6. Simulation results for the Bornholm distribution system show a good agreement with the previous PF simulation study conducted. In addition, an equivalent generic model of Bornholm distribution system is also constructed, which can be used as a benchmark model for smart grid testing purposes. The algorithm used is based on the dynamic reduction of power systems using relation factors combining with FDNE feature available in the RTDS. The dynamic reduction technique uses a coherency based reduction of the electromechanical model of the power system to be equivalence. The low frequency behaviour is being modelled by dynamic reduction technique. A FDNE is placed in parallel with this model to accurately capture the high frequency behaviour. An improved equivalent approach is presented, which reduces a large power network into a small manageable equivalent

model with reduced hardware costs. Moreover, the generic parameter sets are developed for further process which later combines with above two processes into form a simpler equivalent. The system parameters are identified, averaged and randomized based on the complete data of the Bornholm distribution system using Matlab's NORMRND function. By using a modified procedure, an equivalent generic model of the Bornholm distribution is successfully constructed. Its scale is reduced within the hardware capacity (i.e. greatly reduce the computational effort by a factor of 6 and allows the RTDS to handle very large system with much less hardware, 23% less process usages) for the RTDS. The application results exhibit a desirable performance and good agreement between the RTDS Full model original and the RTDS equivalent. Two resultant curves match to a very high degree of accuracy, which demonstrates the confidence that the proposed equivalent approach has been performed properly. It can be concluded that the equivalent system retains the dynamic response of the original system accurately. The algorithm is capable of creating equivalents of real distribution system, thereby in the future, bringing entire Danish systems containing thousands of buses into the realm of real time digital simulation.

In **chapter 5**, the simplified battery model with a small internal resistance and a CVS is adopted and has been modeled in the RTDS in order to investigate the role of the BESS as a primary frequency regulator during islanding transition. The charging and discharging operation is performed on the BESS to balance the total power generation with the total power demand. However, a small-sized BESS is assumed; therefore, the continuous charging and discharging operations are not available all the time on the BESS because the stored energy level hits its capacity limit. To avoid this undesirable effect and to perform the continuous frequency regulation on the BESS, a coordinated control strategy between a BESS and dispatchable DG units is also formulated. Particularly, this control strategy consists of a primary frequency control action of the BESS and a secondary frequency control action of the MMS. The MMS detects the change of the power output of the BESS and tries to return the power output of the BESS to reference value by assigning total power difference to the dispatchable DG units (i.e. governor's load reference points) to share the load following burden of the BESS and to keep the stored energy level on the BESS within the prespecified level. The power contribution from the DG units increases whenever the stored energy level on the BESS decreases. On the other hand, the power generation from the DG units decreases whenever the stored energy level on the BESS increases. The effectiveness of the proposed primary frequency control strategy is illustrated by using two test cases (i.e. IEEE 9-bus and Bornholm distribution system). Both simulation results indicate the advantages of the proposed control strategy and the frequency regulation performance is highly improved in the event of islanding operation. It is observed that only small amount of BESS capacity can improve the system frequency as a fast-acting primary control, and the secondary control of the MMS can also reduce the consumption of the stored energy of BESS (i.e.

maximum controlling reserve) without degrading the proposed control performance. Clearly, it is shown how a relatively simple BESS control algorithm may be used to enable stable operation of ADNs. However, the battery is assumed to be fully charged all the time meaning that the BESS did not have proper SOC taken into account. Hence, a dedicated SOC control scheme, the use of high time resolution wind data, improvement of coordinated control strategies, and the controller optimization remain as future work. Nevertheless, the results indicate the efficiency of the BESS for real-time applications and its suitability for the cases considered. In addition, the simulation results presented can quantify BESS performance both in EMS for real-time operation and in system planning for future RES connections.

In **chapter 6**, a new fuzzy logic based secondary frequency control strategy between a BESS and dispatchable DG units in the high level of the MMS is proposed for further improving the system frequency performance (islanding operation) as well as reducing RES output power fluctuations (grid-connected operation). The proposed FLC strategy can be formulated using the 4 main processes, namely fuzzification, knowledge base, inference engine, and defuzzification process. The process of converting a real number into a fuzzy number is called fuzzification. The two inputs SOC and $p_{\text{bess}}^{\text{tar}}$ are considered as FLC inputs. Fuzzy rules proposed for the FLC can be generated based on knowledge base and inference engine processes. This selected membership functions is all the possible combinations of the linguistic variables. Defuzzification process is taken which converts FLC output (i.e. fuzzy number) to a real numerical value. The practical reference value ($p_{\text{bess}}^{\text{ref}}$) can be derived and given to the BESS. As a result, the BESS will supply or absorb the real power accordingly. Hence, the variations of power from the wind turbine units can be absorbed through the charging or discharging operation of the BESS. This enables the BESS to balance the total power generation with the total power demand. For grid-connected situation, if the wind power generation changes slowly, SOC levels are almost stable for both two initial SOC cases (i.e. SOC = 50%, SOC = 70%). On the other hand, if wind output decreases, the BESS supplies power to the external grid. It was observed that due to different SOC levels, BESS with higher charging level compensated more power. It indicates that the proposed FLC strategy could efficiently in a timely manner adjust the stored kW hours of energy during the BESS's high charging phase, and thereby could augment the performance of the microgrid without adding energy storage capacity. In addition, since a large-sized BESS is assumed; therefore, the continuous charging and discharging operations are available on the BESS to be involved in primary frequency control as well as in the secondary frequency control. To perform the continuous frequency regulation on the BESS, the power outputs of the dispatchable DG units (i.e. operating close to their maximum capacities, but still room left for the secondary frequency control) can also be coordinated to share the load following burden of the BESS and to keep the stored energy level on the BESS within the prespecified level. For islanding operation, the recovery of frequency is very prompt

due to the fast response of BESS. This time frame belongs (i.e. t = 1000 to t = 1100) to primary frequency control period. Also, MMS starts to regulate the dispatchable DG units to compensate active power. From t = 1200 s to t = 2000 s, the system is in the secondary control period. It was observed that more power is distributed from the DG units. Since the charging level is still high, BESS is still involved in the secondary frequency control part. The time span is dependent on the target input power and SOC level. Obviously, BESS with lower charging level will decreases much faster. The gap is filled by DG units. At about 2400s (t = 1200 s to t = 2400 s), the frequency returned back to the normal range. Overall, the simulation results clearly indicate the superiority of the proposed FLC strategy. The fluctuation of output power at PCC is reduced to a great extent while managing battery SOC within a specified target region. The frequency is kept stable and its regulation performance is highly improved in the event of islanding operation. As the core of the control strategy, the design of FLC is verified through time domain simulation. Coordination control strategy is rather simple, but the control effect is very good. It gives a new thinking way to increase the quality of coordinated control strategy. Moreover, the design procedure of the FLC may be applied to other systems, possibly with more complex structure and with careful examination of its potential properties.

In chapter 7, an agent based paradigm is adopted and utilized for the development of the control strategy. An intelligent multi-agent based secondary frequency control for the islanding operation of ADN is proposed. The real-time experimental setup is constructed comprising the RTDS, Matrikon OPC server for SCADA DNP, and agent JAVA. Hence, data can be exchanged between the RTDS and agent JAVA over a LAN using the DNP-OPC protocol. This was verified by a small test case and the data transfer was successful even in the existence of the communication delay time through existing computer network. Since it was a complete SIL testing, the practical communication latency for the RTDS and OPC was already embedded. The proposed MAS structure consists of a number of agents. Each agent represents some of the physical components in the test system consisting of three zones. Each zone has several agents (control, monitoring, DG, load, etc.) that communicate with each other to control the whole system and a corresponding DF agent. The proposed MAS were implemented in foundation for intelligent physical agents (FIPA) compliant JADE open source platform. The test system (i.e. divided into 3 zones) was successfully monitored, controlled and operated by means of the developed MAS. The aim of MAS was to define a distributed mapping function from agents to roles, based on current state and capabilities of agents. Simulation has been performed. A three phase fault scenario on the external grid in zone 1 was applied. Corresponding DF agent responded and analyzed the current islanding situation and determined a best control plan that maps to the current situation. Then, DF agent communicated with DG and load agents for specific role assignment in chosen control plan. DG and load agents calculated their local cost functions based upon their

current states and capabilities. Based upon the value of this cost functions, DG and load agents sent bids to DF agents. All bids are accumulated and negotiation took place. As a consequent, DF agent again assigned a role to every agent in the selected control plan. In this case, only DG #2 was able to provide regulation service, so DG#2 accepted the request. At this moment, optimization of the parameters of the secondary controller was achieved in a simple manner through the effective application of PSO technique**.** The PSO parameters were set to $c_1 = 2.05$ and $c_2 = 2.05$, which are the typical value of PSO. The 30 of population size and 20 of maximum iteration were used. The outcome of simulation results show that the proposed multi-agent based secondary frequency control strategy performs well, in comparison to the performance of PI control design without PSO. It must be noted that there always exists the communication delay time for transferring the required information on the network. The estimated communication delay time was around 40 to 50 ms for the proposed multi-agent AGC system during the tests. There was no significant degradation of control performance by the existing communication delay. However, for the longer communication delay, the control performance might be degraded or deteriorated not to be able to perform the proper AGC. When considering the actual installation of the proposed multi-agent based AGC scheme, the stable operation of the proposed AGC scheme might be required for the communication delay up to 0.1s. In addition, the developed MAS in this research are scalable, robust and easily reconfigurable. Therefore, the developed MAS can be easily extended for managing and controlling different kind of DG units by extending the functions of the agents and creating additional agents in the system. Hence, the results indicate the efficiency of the proposed multi-agent based secondary frequency control strategy with PSO technique for real-time applications. Nevertheless, there are a number of challenges, specific to the proposed multi-agent based secondary frequency control strategy that requires further investigation as future work. These are concerned with the scalability such as multi-set of DG units and loads, coordination strategies, load shedding schemes and improvement on SIL optimization procedure using agent java in real-time simulation environment. Moreover, communication is very costly if a direct communication link is lost from the central coordinating agent to the bottom agents, then the task cannot be performed, so the AGC is terminated. Therefore, agents must maintain coordination when communication is unavailable. Or, agents may not be able to share all the information with other agents all the time due to the limitations of the communication channel and computational device. The usual delay attached with communication links, and sensor measurements is around 50 ms to 1 s. To solve this problem, a hierarchical control structure should be considered which has the upper controller and the decentralized controller using only locally measured frequency deviation.

8.2 Future Work

The thesis is completed by opening several interesting research directions and issues since there are some assumptions and limitations of the proposed approach in this thesis, which make it difficult to directly apply the proposed approach in practice. Some particular cases need explanations. Below is the list of topics outlined as proposals for future work.

- There are a number of challenges specific to the proposed FLC and multi-agent based control strategies that require further investigation as future work. One of them is the scalability. What if there are multi-set of DG/BESS units and loads? In this study, an aggregated BESS is only considered. Hence, the system is operated in constant frequency and voltage control mode. However, if multiple BESSs are introduced, the control mode of BESS should be changed to a droop control mode. Likewise, the secondary control loop has to be modified to regulate the frequency and voltage instead of regulating the active and reactive power output of BESS. Thus, a more appropriate secondary control strategy should be needed. Also, the response times and internal characteristics of the various components (DG units with different response characteristics, etc.) in the system may cause instability or secondary control can't perform in an effective way. Hence, coordination or advanced dispatch strategies for handling these issues need to be pursued in the future.

- In this thesis, the coordination control strategy is proposed with the assumption that there is at least one conventional synchronous machine based dispatchable DG unit. However, the control strategy should be different in the case of all inverter based DG units. For that reasons, the local control strategy of DG unit is different and at least one DG unit should act as a voltage source inverter (VSI). Hence, a new coordinated control strategy between VSIs should be considered.

- The current rudimentary implementation of BESS can provide a few minutes of energy, but overall grid management, will require longer durations of storage and therefore re-engineering of conventional storage systems to handle the above issue. The outcome of such optimization is to develop a smart SOC schedule (i.e. detailed modeling of the PI controller with a constraint on the capacity of the BESS in order to secure continuous stable operation) for the BESS.

- The growing expansion of renewable energy with a number of large-scale WPPs expected to be dispersed throughout the system. Since the power coming from some wind turbine, is stochastic, it is difficult to straightly use their kinetic energy storage in AGC. Further studies are needed to coordinate the timing and size of the kinetic energy discharge with the characteristics of DG units.

- The developed AGC scheme using the BESS validated its efficacy under islanded distribution system and showed a great performance for alleviating frequency deviations. However, the development of advance voltage control scheme is also needed that can be combined together with the existing frequency stabilizing scheme. These studies are not presented, as the main purpose of this study is to develop effective frequency control strategies for the islanding operation of ADNs.

- The future ADNs must be able to handle complex interactions between control areas, DG units, and some types of controllable demand, while maintaining security of supply. These efforts are directed at developing monitoring/measurement and control technologies in order to guarantee quality service and to achieve optimal performance during islanding operation. A much greater extent than is the case today. An advanced fast hardware measurement devices are definitely needed to realize smooth islanding operation.

- The goal, as always, is to provide more efficient operation, in this case, be able to transit smoothly into islanding operation mode. At present, islanding operation is still not likely to be attractive, but may be commercially viable in the future (i.e. in terms of improved reliability of power supply, power quality, additional revenues, and maintain the security of power supply, etc.) In this regard, the economic feasibility of islanding operation needs to be investigated taking into account costs associated with outage, extra equipment and revenue generated from islanding operation. It is highly recommended to address the appropriate procedures/guidelines (i.e. or even to address the lack of information included in the current regulatory or standard regarding intentional islands). Future work is needed on defining changes and recommendations that would be required to facilitate safe reliable operation of islanding.

9 References

[1] N. Jenkins, "Embedded generation," *IEE-95*, pp. 468-475, 2000.

[2] T. Ackermann, G. Andersson, L. Soder, "Distributed generation : a definition," *Electric Power Systems Research*, pp. 195-204, 2001.

[3] T. Ackermann, G. Andersson, L. Soder, "Distributed resources and re-regulated electricity markets," *Electric Power Systems Research*, pp. 1148-1159, 2007.

[4] R.A. Walling, "Distributed generation islanding-implications on power system dynamic performance," IEEE Power Engineering Society Summer Meeting, vol. 1, 2002, pp. 92–96.

[5] W. El-Khattam, M.M.A. Salama, "Distributed generation technologies, definitions & benefits," Electric Power System Research, vol. 71, 2004, pp. 119-128.

[6] Zeineldin H., Marei M. I., El-Saadany E. F., Salama M.M.A, "Safe controlled islanding of inverter based distributed generation," *IEEE Power Electronics Specialists Conference*, June 2004.

[7] Dimeas A. L., Hatziargyriou N. D., "Operation of a multiagent system for microgrid control," *IEEE Transactions on Power Systems*, vol. 20, No. 3, Aug., 2005.

[8] Piagi P., Lasseter R. H., "Autonomous control of microgrids," *IEEE Power Engineering Society Meeting*, 2006.

[9] Pecas Lopes J. A., Moreira C. L., Madureira A. G., "Defining control strategies for microgrids islanded operation," *IEEE Transactions on Power Systems*, vol. 21, No. 2, May 2006.

[10] Zeineldin H., El-Saadany E. F., Salama M.M.A, "Distributed generation microgrid operation: control and protection," *IEEE Power Systems Conference, Advance Metering, Protection, Control, Communication, and Distributed Resources*, March 2006.

[11] Jayawarna N., Wut X., Zhangt Y., Jenkins N., Barnes M., "Stability of a microgrid," *IET International Conference on Power Electronics, Machines and Drives*, March 2006.

[12] Barklund E., Pogaku N., Prodanovic M., Hernandez-Aramburo C., Green T.C., "Energy management system with stability constraints for stand-alone autonomous

microgrid," *IEEE International Conference on System of Systems Engineering*, April, 2007.

[13] De Brabandere K., Vanthournout K., Driesen J., Deconinck G., Belmans R., "Control of microgrids," *IEEE PES General Meeting*, June 2007.

[14] Seung Tae, Cha, Qiuwei W., Arshad S., Jacob Ø., and Yi D., "Modeling and Control of Sustainable Power Systems, Towards Smarter and Green Electric Grids, Green Energy & Technology," ISBN 978-3-642-22903-9, Chapte 3, Springer, 2011

[15] www.pikeresearch.com.

[16] IEA, "Distributed Generation in Liberalized Electricity Market," online. Available: http://iea.org/textbase/nppdf/free/2000/distributed2002.pdf, 2002

[17] N. Acharya, P. Mahat, and N. Mithulananthan, "An Analytical Approach for DG Allocation in Primary Distribution Network," *Int. J. Elect. Power Energy Syst.*, vol. 28, no. 10, pp. 669-678, Dec. 2006.

[18] D. C. Mayor, R. Picos, and E. G. Moreno, "State of the Art of the Virtual Utility: the Smart Distributed Generation Network," *Int. J. Energy Research*, vol. 28, pp. 65-80, 2004.

[19] Pukar Mahat, "Control and Operation of Islanded Distribution Systema," Dept. Energy Techloogy, Aalborg University, Ph.D thesis, Sept 2010.

[20] DTI, "Islanded Operation of Distribution Networks," URN Number: 05/591, Crown Copyright, 2005

[21] F. Castro-Sayas and G. D. Clarke, "The costs and benefits of embedded generation islanding operation," http://webarchive.nationalarchives.gov.uk/tna/ and http://www.dti.gov.uk/renewables/publications/pdfs/kel00284.pdf/, 2002 [14 June 2010].

[22] IEEE Std 1547.4™-2011, IEEE guide for design, operation, and integration of distributed resource island systems with electric power systems, by the IEEE standards coordinating committee 21 on fule cells, photovoltaics, dispersed generation, and energy storage, July 2011.

[23] IEC 61727 Standard, Photovoltaic (PV) systems - Characteristics of the utility interface, December 2004.

[24] K. Christensen, et. al., "Technical Regulation for Thermal Power Station Units of 1.5 MW and higher," Energinet.dk, Fredericia, Denmark, Regulation for grid connection TF 3.2.3, 2008.

[25] P. P. Barker and R. W. de Mello, "Determining the Impact of Distributed Generation on Power Systems: Part 1 – Radial Distributed Systems," *IEEE Power Eng. Soc. Summer Meeting*, 2000, vol. 3, pp. 1645-1656.

[26] S. P. Chowdhury, S. Chowdhury, P. A. Crossley, and C. T. Gaunt, "UK scenario of islanded operation of active distribution networks with renewable distributed generators," *Renewable Energy*, vol. 34, no. 12, pp. 2585-2591, Dec. 2009.

[27] H. Shayeghi, H. A. Shayanfar, A. Jalili, "Load frequency control strategies: A state-of-the-art survey for the researcher," *Energy Conversion and Managemen, Elsevier*, pp. 344-353, 2008.

[28] Nuno Jose Gil, J. A. Pecas Lopes, "Hierarchical frequency control scheme for islanded multi-microgrids operation," *IEEE Powertech*, 2007

[29] A. Suwannarat, B. Bak-Jensen, Z. Chen, "Power system operation with large scale wind power integration," *IEEE Powertech*, 2007

[30] P. Lund, S. Cherian, T. Ackermann, "A Cell Controller for autonomous operation of a 60 kV distribution area," *International Journal of Distributed Energy Resources*, pp. 83-100, 2006.

[31] Gauthier Delille, Bruno Francois, Gilles Malarange, "Dynamic frequency control support: a virtual inertia provided by distributed energy storage to isolated power systems," *IFAC World Congress*, 2010.

[32] Yu Chen, Zhao Xu, Jacob Østergaard, "Security of Assessment for Intentional Island Operation in Modern Power System," Electric Power System Research, vol. 71, pp. 1849-1857, 2011

[33] R.H. Lasseter, "Microgrids and Distributed generation," *Journal of Energy Engineering, American Society of Civil Engineers*, Sept, 2008

[34] California Energy Commission, "Integration of Distributed Generation : The CERTS Microgrid Concept, " Report, pp. 500-503, 2003.

[35] Pecas Lopes J. A., Moreira C. L., Madureira A. G., "Defining control strategies for microgrids islanded operation," *IEEE Transactions on Power Systems*, vol. 21, No. 2, May 2006.

[36] B. Krrroooposki, et al., "Making Microgrids Work," *IEEE Power & Energy Magazine*, May/June, 2007

[37] F. Katiraei, et al., "Planned Islanding on Rural Feeders – Utility Perspective," *IEEE PES General Meeting*, July, 2008

[38] J. Peralta, H. Iosfin, X.B.C. Tang, "Hydro Perspective on Distribution Islanding for Customer Reliability, " *CIGRE Symposium-Integration of Wide-Scale Renewable Resources into the Delivery System*, July, 2009.

[39] X. Xiong and W. Li, "A new under-frequency load shedding scheme considering load frequency characteristics," in *Proc. Int. Conf. Power System Technology*, pp. 1 - 4, Oct. 2006.

[40] Antikainen, J., Repo, S. & Järventausta, P.: Designing intended island operation in distribution networks, International Journal of Distributed Energy Resources, 2010.

[41] W. Lachs, D. Sutanto, "Application of battery energy storage in power systems," *International Conference on Power Electronics and Drive Systems*, pp. 700-705, 1995

[42] A. Joseph, M. Shahidehpour, "Battery energy storage systems in electric power systems," *IEEE Power Engineering Society General Meeting Conf.*, pp. 1-8, 2006

[43] D. Kottick, M. Blau, D. Edelstein, "Battery energy storage for frequency regulation in an island power system," *IEEE Transactions on Energy Conversion*, vol. 8, No. 3, pp. 455-459, Sept. 1993.

[44] Jong Yul Kim, Seul Ki Kim and June Ho Park, "Contribution of an energy storage system for stabilizing a microgrid during islanded operation," *Journal of Electrical Engineering & Technology*, vol. 4, No. 2, pp. 194-200, 2009.

[45] Jong Yul Kim, "Cooperative control strategy of energy storage system and microsources for stabilizing the microgrid during islanded operation," Dept. Electrical Eng., Pusan National University, Ph.D thesis, Dec. 2010.

[46] Seung Tae, Cha, Haoran Z., Qiuwei Wu, Arshad Saleem, Jacob Østergaard "Coordinated control scheme of battery energy storage system and distributed generations for electric distribution grid operation ," *IEEE Industrial Electronics Society, 2012*

[47] Seung Tae, Cha, Haoran, Z., Qiuwei W., Jacob, Ø., T. Nielsen, H. Madsen, "Evaluation of Energy Storage System to Support Danish Island Grid of Bornholm Power Grid," *IEEE International Power and Energy Conference (IPEC)*, 2012

[48] N. K. Stanton, J. C. Giri, Anjan Bose, "Power System Stability : New Opportunities for Control, Chapter in stability and control of dynamical systems and applications," Boston, 2003

[49] H. Bevrani, T. Hiyama, "Intelligent Automatic Gneration Control," CRC Press, 2011

[50] T. Ackermann, "Wind Power in Power Systems, " *Wiley,* 1st Edition, 2005.

[51] T. K. Nagsarkar and M. S. Sukhija, "Power System Analysis," New Delhi, *Oxford University Press*, 2007

[52] H. Bevrani, "Robust Power Sytem Frequency Control," New York, *Springer*, 2009

[53] P. Kundur, "Power System Stability and Control," *McGraw-Hill*, 1994

[54] M. Shaidehpour, H. Yamin, Z. Li, "Market Operation in Electric Power Systems:

Forecasting, Scheduling, and Risk Management," New York, *John wiley & Sons*, 2002

[55] NERC Operating manual, Princeton, 2002

[56] N. Jaleeli, L. S. Vanslyck, "NERC's new control performance standards," *IEEE Transaction Power Systems*, pp. 1092-1099, 1999.

[57] S. A. Nirenberg and D. A. McInnis, "Fast acting load shedding", *IEEE Trans. Power Systems*, vol. 7, no. 2, pp. 873-877, May 1992.

[58] J. G. Thompson and B. Fox, "Adaptive load shedding for isolated power systems," *IEEE Proc. Gen., Transm. Distrib.*, vol. 141, no.5, pp. 491-496, Sept. 1994.

[59] V. N. Chuvychin, N. S. Gurov, S. S Venkata, and R. E. Brown, "An adaptive approach to load shedding and spinning reserve control during under-frequency conditions," *IEEE Trans. Power Sys.*, vol. 11, no. 4, pp. 1805-1810, Nov. 1996.

[60] L. Zhang and J. Zhong, "UFLS design by using f and integrating df/dt," in *Proc. IEEE Power Eng. Soc. Power Systems Conf. Expo.*, pp. 1840-1844, 2006.

[61] J. Y Kim, H. M. Kim, S. K. Kim, J. H. Jeon, H. K. Choi, "Designing an energy storage system fuzzy PID controller for microgrid islanded operation," *International Journal of Energies*, Vol. , No. 4, pp. 1443-1460, 2011.

[62] P. Piagi and R. H. Lasseter, "Industrial application of microgrids," *Power System Engineering Research Center (PSERC)*, 2001.

[63] Yu Chen, "Control Architecture for Intentional Islanding Operation in Distribution Network with High Penetration of Distributed Generation," Dept. Electrical Eng., Technical University of Denmark, Ph.D thesis, May. 2010.

[64] Yu Chen, Z. Xu, Jacob Østergaard, "Frequency analysis for planned islanding operation in the Danish distribution system – Bornholm," *UPEC, 2008*.

[65] Yu Chen, Z. Xu, Jacob Østergaard, "PMU frequency data processing for a planned islanding operation in Bornholm," *Nordic Wind Power Conference (NWPC)*, 2009.

[66] Vladislav A., John Eli N., Jacob Østergaard, and Arne H. N., "Wind power system of the Danish island of Bornholm: Model set-up and determination of operation regimes," *World Energy Conference*, June 2009.

[67] Vladislav A., John Eli N., Jacob Østergaard, and Arne H. N., "State-estimation of wind power system of the Danish Island of Bornholm," *Nordic Wind Power Conference (NWPC)*, Sept., 2009.

[68] Jacob Østergaard, John Eli N., "The Bornholm power system - An overview," *Nordic Wind Power Conference (NWPC)*, Sept., 2009.

[69] Edward James S., Mikael Togeby, "Security of supply for Bornholm - Integration of fluctuating generation using coordinated control of demand and wind turbines," Ea Energy Analyses, Oct 2007.

[70] Vladislav A., John Eli N., Jacob Østergaard, and Arne H. N., "Technical aspects of status and expected future trends for wind power in Denmark," *Wind Energy*, vol. 10, No. 1, pp. 31-49, 2007.

[71] Seung Tae Cha, "RTDS implementation of Bornholm power system - distribution system modeling and analysis," Dept. Electrical Eng., Technical University of Denmark, Lyngby, Internal Report, pp. 1-58, Nov. 2010.

[72] Seung Tae, Cha, Arshad Saleem, Qiuwei Wu, Jacob Østergaard, "Multi-agent based controller for islanding operation of active distribution networks with distributed generation," *International Conference on Electric Utility Deregulation and Restructuring and Power Technologies (DRPT)*, pp. 803-810, July 2010.

[73] Seung Tae, Cha, Qiuwei W., and Jacob Ø., "A Generic Danish Distribution Grid Model for Smart Grid Technology Testing," *IEEE PES Innovative Smart Grid Technologies (ISGT)*, Oct., 2012.

[74] Seung Tae, Cha, Qiuwei W., and Jacob Ø., "Frequency Stabilizing Control Scheme for a Danish Island Grid," *IEEE PES Innovative Smart Grid Technologies (ISGT)*, Oct., 2012.

[75] Christian T. Blach, "Study of frequency control for islanding operation of active distribution systems," Dept. Electrical Eng., Technical University of Denmark, Lyngby, Bachelor thesis, 2011.

[76] P. M. Anderson, A. A. Fouad, "Power system control and stability," *Iowa State University Press*, Iowa 1994.

[77] Rasmus H. Rasmussen, Theis N. Nielsen, Guang-Ya Yang, G. Rodrigo G. Valle, and Jacob Østergaard, "Dynamic equivalent model of a Danish island for MV and LV studies," *IEEE ISGT Europe*, pp. 1-4, 2011.

[78] M. Artenstein, A. Giusto, "Equivalent model of the Argentinian electrical power system for stability analysis of the Uruguayan network," *IEEE Transmission & Distribution Conference and Exposition*, pp. 1-5, 2008.

[79] Yong Hak Kim, Seung Tae, Cha, J.W Lee, T.K. Kim, J. B. Choo, and H.K Nam, "Construction of largest equivalent systems for power system simulator," pp. 79-91, *European Transactions on Electrical Power*, 2005.

[80] Xi Lin, A. M. Gole, and Ming Yu, "A wide-band multi-port system equivalent for real-time digital power system simulators," *IEEE Transactions on Power Systems*, vol. 24, No. 1, pp. 237-249, 2009.

[81] Yuefeng Liang, Xi Lin, A. M. Gole, Ming Yu, "Improved coherency-based wide-band equivalents for real-time digital simulators," *IEEE Transactions on Power Systems*, vol. 26, No. 3, pp. 1410-1417, 2011.

[82] H. J. Kim, G. Jang, and K. Song, "Dynamic reduction of the large-scale power systems using relation factor," *IEEE Transactions on Power Systems*, vol. 19, No. 3, pp. 1696-1699, 2004.

[83] RTDS, FDNE : An Introduction Manual, 1-18 and RTDS User's Manual

[84] R. Podmore, "Identification of coherent generators for dynamic equivalents," *IEEE Transactions on Power Systems*, vol. 97, pp. 1344-1354, 1978.

[85] A. J. Germond and R. Podmore, "Dynamic aggregation of generating unit models," *IEEE Transactions on Power Systems*, vol. 97, pp. 1060-1069, 1978.

[86] Yu Chen, "Control architecture for intentional islanding operation in distribution network with high penetration of distributed generation," Dept. Electrical Eng., Technical University of Denmark, Lyngby, Ph.D thesis, May 2010.

[87] K. Yamashita, O. Sakamoto, Y. Kitauchi, T. Nanahara, T. Inoue, H. Fukuda, T. ShiOhama, "Development of a Frequency-stabilizing Scheme for Integrating Wind Power Generation into a Small Island Grid" in *Proc. IEEE Power Eng. Soc. Power Sys tems Conf. Expo.*, pp. 1840-1844, 2006.

[88] California Energy Commission, Navigant Consulting Inc., "The Value of Distri bution Automation," *IEEE Power Eng. Soc. Power Systems Conf. Expo.*, pp. 1840-1844, 2006.

[89] G. V. K. Murthy, "Reliability Improvement of Radial Distribution System with Distributed Generation," *International Journal of Engineering Science and Technology (IJEST)*, pp. 4003-4011, Vol. 4 No.09, Sept 2012.

[90] Online : http://www.seattlerobotics.org/encoder/mar98/fuz/flindex.html.

[91] E.H. Mamdani, S. Assilian, "An Experiment in Linguistic Synsthesis with a Fuzzy Logic Controller," *International Journal of Man-Machine Studies*, vol. 7, No. 1, pp. 1-13, 1975.

[92] C. F. Juang, C. F. Lu, "Load Frequency Control by Hybrid Evolutionary Fuzzy PI Controller," *IEE Generation Transmission and Distribution*, pp. 196-204, 2006.

[93] A. Feliachi, D. Rerkpreedapong, "NERC compliant Load Frequency Control Design using Fuzzy Rules," *Electric Power Systems Research*, Vol. 73, pp. 101-106, 2005.

[94] C. S. Rao, S. S. Nagaraju, P. S. Raju, "Automatic Generation Control of TCPS based Hydrothermal System under Open Market Scenario: A Fuzzy Logic Approach," *Electric Power Energy Systems*, Vol. 31, pp. 315-322, 2009.

[95] J. Y Kim, "Designing an energy storage system fuzzy PID controller for microgrid islanded operation", *International Journal of Energies*, Vol. , No. 4, pp. 1443-1460, 2011.

[96] Simens Smart Grid Innovation Contest, MAS for Operation of Smart Grid, http://www.smartgridcontest.com/idea.php?id=63#.

[97] S. D. J. McArthur, E. M. Davidson, V. M. Catterson, A. L. Dimeas, N. D. Hatziargyriou, F. Ponci, T. Funabashi, "Multi-Agent Systems for Power Engineeing Applications, Part I. Concepts, Applications and Technical Challenges," *IEEE Transaction Power System*, pp 1743-1752, 2007.

[98] S. D. J. McArthur, E. M. Davidson, V. M. Catterson, A. L. Dimeas, N. D. Hatziargyriou, F. Ponci, T. Funabashi, "Multi-Agent Systems for Power Engineeing Applications, Part II. Technologies, Standards and Tools for Multiagent Systems," *IEEE Transaction Power System*, pp 1753-1759, 2007.

[99] H. Bevrani, "Robust Power Sytem Frequency Control," New York, *Springer*, 2009

[100] T. Hiyama, D. Zuo, T. Funabashi, "Multi-agent based automatic generation control of isolated stand alone power system," *International Conference on Power System Technology*, 2002

[101] T. Hiyama, D. Zuo, T. Funabashi, "Multi-agent based control and operation of distribution system with dispersed power sources," *IEEE PES, Transmission and Distribution Conference and Exhibitionon*, 2002

[102] S. Conti, A. M. Greco, N. Messina, U. Vagliasindi, "Generator control systems in intentionally islanded MV microgrids", *in proceedings of International Symposium on Power Electronics, Electrical Drives, Automation and Motion (SPEEDAM)* , 2008.

[103] Pradit Fuangfoo, Thongchai Meenual, W. J. Lee, "PEA guidelines for impact study and operation of DG for islanding operation," *IEEE Transactions on Industry Applications*, vol. 44, No. 5, pp. 1348-1353, 2008.

[104] Irvin J. Balaguer, Q. Lei, S. Yang, U. Supatti, F. Z. Peng, "Control for grid-connected and intentional islanding operations of distributed power generation," IEEE Transactions on Industrial Electronics, vol. 58, No. 1, pp. 147-157, 2011.

[105] Irvin J. Balaguer, U. Supatti, Q. Lei, N. S. Choi, F. Z. Peng, "Intelligent control for islanding operation of microgrids", *in proceedings of ICSET* , 2008.

[106] S. P. Chowdhury, S. Chowdhury, C. F. Ten, P. A. Crossley, "Operational and control of DG based power island in smart grid environment", *in proceedings of CIRED* , 2008.

[107] Cheng Ting Hsu, Chao S. Chen, "Islanding operations for the distribution systems with dispersed generation systems", *in proceedings of IEEE PES*, 2005.

[108] Puka Mahat, Z. Chen, B. Bak-Jensen, "Control and operation of distributed generation in distribution systems," *Electric Power System Research*, pp. 1-8, 2010

[109] Pecas Lopes J. A., Moreira C. L., Madureira A. G., "Defining control strategies for microgrids islanded operation", *IEEE Transactions on Power Systems*, vol. 21, No. 2, pp 916-924, May 2006.

[110] Muhamad Haddin, Soebagio, Adi Soeprijanto, "Gain coordination of AVR-PSS and AGC based on particle swarm optimization to improve the dynamic stability of the power system," *International Journal of Academic Research*, vol. 3, no. 3, 2011, pp. 462-470.

[111] A. Soundarrajan, S. Sumathi, C. Sundar, "Particle swarm optimization based LFC and AVR of autonomous power generating system," *IAENG International Journal of Computer Science*, vol. 37, no. 1, 2010, pp. 37-1-10 online publication.

[111] Haluk Gozde, M. Cengiz Taplamacioglu, "Automatic generation control application with craziness based particle swarm optimization in a thermal power system," *Electric Power System Research*, pp. 8-16, 2011

[112] M. R. AlRashidi, M. E. El-Hawary, "A survey of particle swarm optimization applications in electric power systems," *IEEE Transactions on Evolutionary Computation*, vol. 13, no. 4, 2009, pp. 913-918.

[113] Saumya Kr. Gautam, Nakul Goyal, "Improved particle swarm optimization based load frequency control in a single area power system", *in proceedings of Annual IEEE India Conference (INDICON)* , 2010.

[114] M. A. Hassan and M. A. Abido, "RTDS implementation of the optimal design of grid-connected microgrids using particle swarm optimization", *in proceedings of European Association for the Development of Renewable Energies, Environment and Power Quality (EA4EPQ)* , 2012.

[115] Seyed A. Taher, Reza Hematti, A. Abdolalipour, Seyed H. Tabei, "Optimal decentralized load frequency control using HPSO algorithms in deregulated power systems," *American Journal of Applied Sciences*, vol. 5, no. 9, 2008, pp. 1167-1173.

[116] Haluk Gozde, M. Cengiz Taplamacioglu, Ilhan Kocaarslan "A swarm optimization based load frequency control application in a two area thermal power system," *Electric Power System Research*, pp. 124-128, 2010

[117] Ranuva N. Rao, P. R. Krishna Reddy, "PSO based tuning of PID controller for a load frequency control in two area power system," *International Journal of Engineering Research and Applications (IJERA)*, vol. 1, Issue 3, pp. 1499-1505

[118] T. Hiyama, D. Zuo, T. Funabashi, "Multi-agent based automatic generation control of isolated stand alone power system," in Proc. of *International Conference on Power System Technology (PowerCon)*, vol. 1, pp. 139-143, 2002

[119] S. Shangxiong, "A particle swarm optimization algorithm based on multi-agent system," in Proc. International Conference on Intelligent Computation Technology & Automation, 2008, pp. 802-805.

[120] M. A. Mazurowski, J. M. Zurada, "Solving multi-agent control problems using particle swarm optimization," IEEE Swarm Intelligence Symposium, 2007, pp. 1-7.

[121] Stephen D. J. McArthur, Euan. M. Davidson, Victoria M. Catterson, "Building multi-agent systems for power engineering applications," *IEEE PES Multi-agent Systems*, 2006

[122] Euan. M. Davidson, Victoria M. Catterson, "Multi-Agent Systems for Power Engineering Applications - Part I: Concepts, Approaches, and Technical Challenges," *IEEE Transactions on Power Systems*, pp. 1743-1752,Nov 2007.

[123] Euan. M. Davidson, Victoria M. Catterson, "Multi-Agent Systems for Power Engineering Applications - Part II: Technologies, Standards, and Tools for building multiagent systems," *IEEE Transactions on Power Systems*, pp. 1753-1759, Nov 2007.

[124] A. L. Dimeas, "Operation of a Multiagent System for Microgrid Control," *IEEE Transactions on Power Systems*, Aug 2005.

[125] Nguyen, Multi-agent system based active distributuion networks, Dept. Electrical Eng., Technische Universiteit Eindhoven, Ph.D thesis, 2010.

[126] F. Zambonelli, N. R. Jennings, M. Wooldridge, "Organization rules as an Abstraction for the Analysis and Design of Multi-Agent Systems," *International Journal of Software Engineering and Knowledge Engineering*, pp. 303-328, June, 2001.

[127] Arshad Saleem, Kai H., M. Lind, "Agent services for situation aware control of power systems with distributed generation", *IEEE PES*, 2009.

[128] Jignesh M. Solanki, Noel N. Schulz, "Agent services for situation aware control of power systems with distributed generation," IEEE PSCE , 2009, pp. 1735-1740.

[129] Eberhart, R. and Kennedy, "Particle swarm optimization," IEEE International Conference on Neural Networks, vol. IV, 1995, pp. 1942-1948.

[130] PSO Tutorial, http://www.swarmintelligence.org/tutorials.php.

[131] F. Daneshfar, "Automatic generation control using multi-agent systems", Dept. Electrical and Computer Eng., University of Kurdistan, Sanandj, Iran, M.S thesis, 2009.

[132] T. Hiyama, D. Zuo, T. Funabashi, "Multi-agent based control and operation of distribution system with dispersed power sources," *in Proc. of IEEE PES Transmission & Distribution Conference and Exhibition (TDCE)*, 2002

[133] Seung Tae, Cha, Jacob, Ø., Qiuwei W., and Francesco M., "A Real Time Simution Platform for Power System Operation", in proceedings of the 8th IEEE International Power and Energy Conference (IPEC), 2010.

[134] Matrikon OPC Server for SCADA DNP 3.0 User Manual.

[135] RTDS User Manual, Chapter 9 GTNET DNP and Power System Users Manual, Chapter 2 RTDS General Operation

Appendix A - 60 kV / 10 kV Substations in Bornholm

Below is the list of Bornholm distribution system's 60/10 kV substations.

Year	Name	Number of TRs	TR (MVA)	Number of 10 kV Feeders
1959	Olsker	2	8.0	6
1959	Bodilsker	2	14.0	6
1967	Aakirkeby	2	16.0	10
1974	Østerlars	1	6.3	4
1977	Snorrebakken	1	10.0	6
1980	HALSE	2	20.0	7
1981	Nexø	2	20.0	6
1983	Rønne Syd	1	10.0	4
1984	Allinge	2	20.0	4
1988	Svaneke	1	10.0	6
1988	Viadukten	1	10.0	7
1989	Rønne Nord	1	10.0	6
1990	Poulsker	1	10.0	5
1994	Vesthavnen	1	10.0	4
1998	Gudhjem	1	4.0	4
1998	Værket	2	41.0	9
		23	**219.3**	**94**

Appendix B - Generation Units in Bornholm

Below is the summary of installed wind turbine types in Bornholm distribution system.

Year	Capacity (kW)	Voltage (kV)	Manufacturer	Type	Location
1992	225	0.4	Vestas	Vestas27	Rutsker
1992	225	0.4	Vestas	Vestas27	Rutsker
1992	225	0.4	Vestas	Vestas27	Rutsker
1996	225	0.4	Vestas	V29/225/690	Bodilsker
1996	225	0.4	Vestas	V29/225/690	Bodilsker
1996	225	0.4	Vestas	V29/225/690	Bodilsker
1980	55	0.4	V Windmatic	Unknown	Klemensker
1982	30	0.4	Nordtank	NT 22/7.5	Bodilsker
1988	130	0.4	Windmatic	WM 20S	Nyker
1988	130	0.4	Windmatic	WM 20S	Nyker
1989	18	0.4	Reymo DK	Reymo 18.5	Vestermarie
1999	660	10.0	Vestas	V47/660	Rutsker
1999	11	0.4	Gaia-Møllen	Unknown	Østermarie
2002	30	0.4	Vestas	HVK 10	Rutsker
2002	660	10.0	Vestas	V47-660-2G	Olsker
2002	900	10.0	NegMicon	NM 52/900	Bodilsker
2002	900	10.0	NegMicon	NM 52/900	Bodilsker
2002	900	10.0	NegMicon	NM 52/900	Bodilsker
2002	800	10.0	Nordex	N50/800	Knudsker

Year	Capacity (kW)	Voltage (kV)	Manufacturer	Type	Location
2002	800	10.0	Nordex	N50/800	Knudsker
2002	800	10.0	Nordex	N50/800	Knudsker
2002	1,300	10.0	Nordex	N60/1300	Rutsker
2002	1,300	10.0	Nordex	N60/1300	Rutsker
2002	1,300	10.0	Nordex	N60/1300	Rutsker
2002	1,300	10.0	Nordex	N60/1300	Åker
2002	1,300	10.0	Nordex	N60/1300	Åker
2002	1,300	10.0	Nordex	N60/1300	Åker
2002	1,300	10.0	Nordex	N60/1300	Åker
2002	1,300	10.0	Nordex	N60/1300	Åker
2006	1,750	10.0	Vestas	V66-1.75MW	Rutsker
2006	1,750	10.0	Vestas	V66-1.75MW	Rutsker
2006	1,750	10.0	Vestas	V66-1.75MW	Rutsker
2006	2,000	10.0	Vestas	V80-2MW	Åker
2006	2,000	10.0	Vestas	V80-2MW	Åker
2006	2,000	10.0	Vestas	V80-2MW	Åker
	29,824				

Below is the summary of the generating units in Bornholm distribution system.

	Rønne Unit 5	**Rønne Unit 6**
Year	1974	1995
Capacity	25 MW	37 MW
Manufacturer	Brown Boveri	Brown Boveri
Rated Voltage	10.5 kV	10.5 kV
Rated Frequency	50 Hz	50 Hz
Rated Speed	3,000 rmp	3,000 rpm
Rated Power / pf	29.4 MVA / 0.85 pf	46.8 MVA / 0.85 pf

The parameters used for the generator and associated controls are listed in the following tables.

Unit 5 – Generator Parameters

lf_rtds_sharc_sld_MACV31

SIGNAL NAMES FOR RUNTIME AND D/A: MAC
D/A CHANNEL ASSIGNMENTS (Continued): MAC
ENABLE D/A OUTPUT (MAX = 12 SIGNALS): MAC | D/A CHANNEL ASSIGNMENTS: MAC
SIGNAL MONITORING IN RT AND CC: MAC
MACHINE ZERO SEQUENCE IMPEDANCES | OUTPUT OPTIONS
MACHINE ELECT DATA: GENERATOR FORMAT
MECHANICAL DATA AND CONFIGURATION | MACHINE INITIAL LOAD FLOW DATA
GENERAL MODEL CONFIGURATION | PROCESSOR ASSIGNMENT

Name	Description	Value	Unit	Min	Max
Xa	Stator Leakage Reactance	0.1	p.u.	0.01	
Xd	D-axis: Unsaturated Reactance	1.57	p.u.	0.1	
Xd'	D: Unsaturated Transient Reactance	0.16	p.u.	0.05	
Xd"	D: Unsaturated Sub-Trans. Reactance	0.125	p.u.	0.02	
Gfld	D: Real Component of Transfer Admit.	100.0	p.u.	0.0	100.0
Bfld	D: Imag Component of Transfer Admit.	100.0	p.u.	0.0	100.0
Xq	Q-axis Unsaturated Reactance	2	p.u.	0.1	
Xq'	Q: Unsaturated Transient Reactance	0.3	p.u.	0.05	1.0e6
Xq"	Q: Unsaturated Sub-Trans. Reactance	0.2	p.u.	0.02	
Ra	Stator Resistance	0.004	p.u.	0.00125	
Tdo'	D: Unsat. Transient Open T Const.	5.3969	sec	0.001	
Tdo"	D: Unsat. Sub-Trans. Open T Const.	0.064	sec	0.001	
Tqo'	Q: Unsat. Transient Open T Const.	0.55	sec	0.001	4.0
Tqo"	Q: Unsat. Sub-Trans. Open T Const.	0.075	sec	0.001	

Update | Cancel | Cancel All

Unit 5 – AVR Parameters

rtds_sharc_ctl_EXST2

CONFIGURATION | DATA

Name	Description	Value	Unit	Min	Max
Tr	Time Constant Tr	0.05	sec	0.0	
Ka	Gain Ka	1.0			
Ta	Time Constant Ta	1.0	sec	0.0	
Vrmx	Upper Limit VRmax	1	pu		
Vrmn	Lower Limit VRmin	-1	pu		
Ke	Constant Ke	0.0			
Te	Time Constant Te	1.0	sec	0.001	
Kf	Feedback Gain Kf	0.0			
Tf	Feedback Time Constant Tf	1.0	sec	0.001	
Kp	Constant Kp	0.0			
Ki	Constant Ki	1.0			
Kc	Constant Kc	1.0			
Efmx	Upper Limit EFDmax	1.5	pu		

Update | Cancel | Cancel All

Unit 5 – Governor Parameters

rtds_sharc_ctl_IEEEG1

CONFIGURATION | DATA

Name	Description	Value	Unit	Min	Max
K	Constant K	10.8416			
T1	Time Constant T1	0.001	sec	0.001	
T2	Time Constant T2	0.5	sec	0.001	
T3	Time Constant T3	0.1	sec	0.001	
Uo	Upper Rate Limit	1	pu/sec		
Uc	Lower Rate Limit	-1	pu/sec		
Pmx	Upper Limit Pmax	1	pu		
Pmn	Lower Limit Pmin	0	pu		
T4	Time Constant T4	0.2	sec		
K1	Constant K1	1			
K2	Constant K2	0.0			
T5	Time Constant T5	0	sec		
K3	Constant K3	0.0			
K4	Constant K4	0.0			
T6	Time Constant T6	0	sec		
K5	Constant K5	0			
K6	Constant K6	0.0			
T7	Time Constant T7	0	sec		
K7	Constant K7	0			
K8	Constant K8	0.0			

Update | Cancel | Cancel All

Unit 6 – Generator Parameters

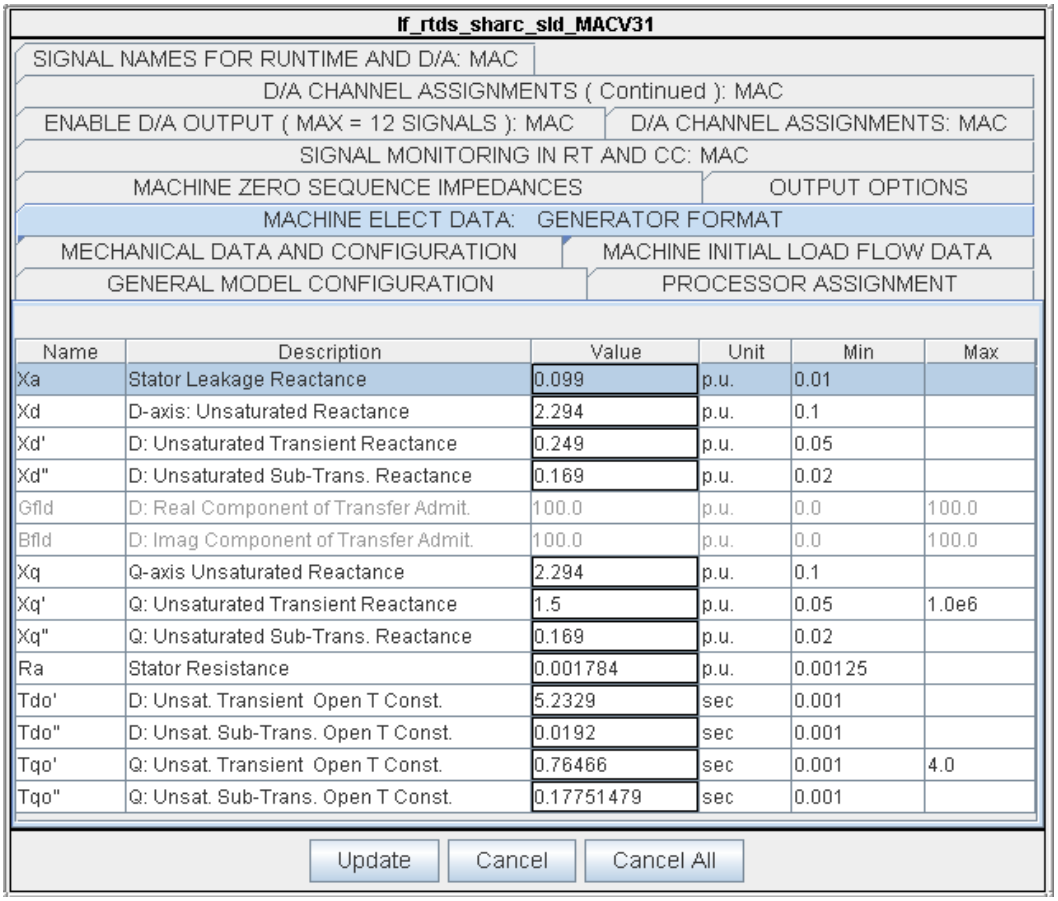

lf_rtds_sharc_sld_MACV31

SIGNAL NAMES FOR RUNTIME AND D/A: MAC | D/A CHANNEL ASSIGNMENTS (Continued): MAC | ENABLE D/A OUTPUT (MAX = 12 SIGNALS): MAC | D/A CHANNEL ASSIGNMENTS: MAC | SIGNAL MONITORING IN RT AND CC: MAC | MACHINE ZERO SEQUENCE IMPEDANCES | OUTPUT OPTIONS | MACHINE ELECT DATA: GENERATOR FORMAT | MECHANICAL DATA AND CONFIGURATION | MACHINE INITIAL LOAD FLOW DATA | GENERAL MODEL CONFIGURATION | PROCESSOR ASSIGNMENT

Name	Description	Value	Unit	Min	Max
Xa	Stator Leakage Reactance	0.099	p.u.	0.01	
Xd	D-axis: Unsaturated Reactance	2.294	p.u.	0.1	
Xd'	D: Unsaturated Transient Reactance	0.249	p.u.	0.05	
Xd"	D: Unsaturated Sub-Trans. Reactance	0.169	p.u.	0.02	
Gfld	D: Real Component of Transfer Admit.	100.0	p.u.	0.0	100.0
Bfld	D: Imag Component of Transfer Admit.	100.0	p.u.	0.0	100.0
Xq	Q-axis Unsaturated Reactance	2.294	p.u.	0.1	
Xq'	Q: Unsaturated Transient Reactance	1.5	p.u.	0.05	1.0e6
Xq"	Q: Unsaturated Sub-Trans. Reactance	0.169	p.u.	0.02	
Ra	Stator Resistance	0.001784	p.u.	0.00125	
Tdo'	D: Unsat. Transient Open T Const.	5.2329	sec	0.001	
Tdo"	D: Unsat. Sub-Trans. Open T Const.	0.0192	sec	0.001	
Tqo'	Q: Unsat. Transient Open T Const.	0.76466	sec	0.001	4.0
Tqo"	Q: Unsat. Sub-Trans. Open T Const.	0.17751479	sec	0.001	

Update | Cancel | Cancel All

Unit 6 – AVR Parameters

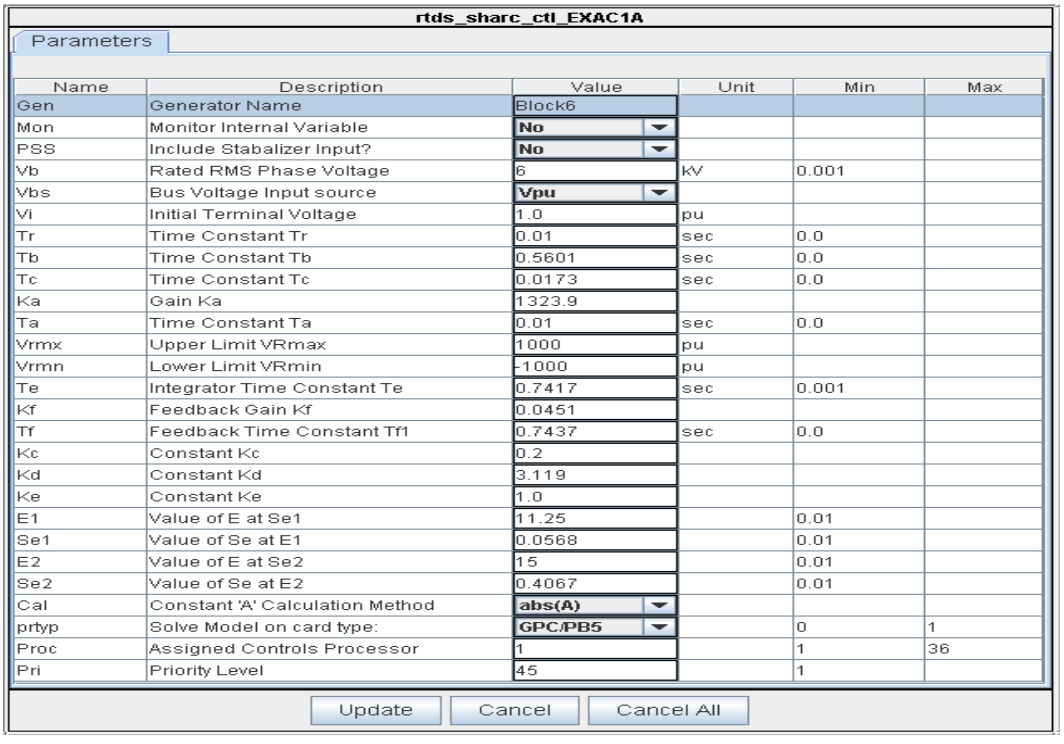

rtds_sharc_ctl_EXAC1A

Parameters

Name	Description	Value	Unit	Min	Max
Gen	Generator Name	Block6			
Mon	Monitor Internal Variable	No			
PSS	Include Stabalizer Input?	No			
Vb	Rated RMS Phase Voltage	6	kV	0.001	
Vbs	Bus Voltage Input source	Vpu			
Vi	Initial Terminal Voltage	1.0	pu		
Tr	Time Constant Tr	0.01	sec	0.0	
Tb	Time Constant Tb	0.5601	sec	0.0	
Tc	Time Constant Tc	0.0173	sec	0.0	
Ka	Gain Ka	1323.9			
Ta	Time Constant Ta	0.01	sec	0.0	
Vrmx	Upper Limit VRmax	1000	pu		
Vrmn	Lower Limit VRmin	-1000	pu		
Te	Integrator Time Constant Te	0.7417	sec	0.001	
Kf	Feedback Gain Kf	0.0451			
Tf	Feedback Time Constant Tf1	0.7437	sec	0.0	
Kc	Constant Kc	0.2			
Kd	Constant Kd	3.119			
Ke	Constant Ke	1.0			
E1	Value of E at Se1	11.25		0.01	
Se1	Value of Se at E1	0.0568		0.01	
E2	Value of E at Se2	15		0.01	
Se2	Value of Se at E2	0.4067		0.01	
Cal	Constant 'A' Calculation Method	abs(A)			
prtyp	Solve Model on card type:	GPC/PB5		0	1
Proc	Assigned Controls Processor	1		1	36
Pri	Priority Level	45		1	

Update | Cancel | Cancel All

Unit 6 – Governor Parameters

rtds_sharc_ctl_IEEEG1

CONFIGURATION | DATA

Name	Description	Value	Unit	Min	Max
K	Constant K	11			
T1	Time Constant T1	0.001	sec	0.001	
T2	Time Constant T2	0.01	sec	0.001	
T3	Time Constant T3	0.1	sec	0.001	
Uo	Upper Rate Limit	0.2	pu/sec		
Uc	Lower Rate Limit	-0.2	pu/sec		
Pmx	Upper Limit Pmax	1	pu		
Pmn	Lower Limit Pmin	0	pu		
T4	Time Constant T4	0.3	sec		
K1	Constant K1	1			
K2	Constant K2	0.0			
T5	Time Constant T5	0	sec		
K3	Constant K3	0.0			
K4	Constant K4	0.0			
T6	Time Constant T6	0	sec		
K5	Constant K5	0			
K6	Constant K6	0.0			
T7	Time Constant T7	0	sec		
K7	Constant K7	0			
K8	Constant K8	0.0			

Update | Cancel | Cancel All

Appendix C - Cross Rack Splitting Example

A very simple example of using the x-rack (splitting) transformer is provided. A small shunt capacitance is added to the transformer so it can be modelled with a travelling wave model and split between racks or subsystems.

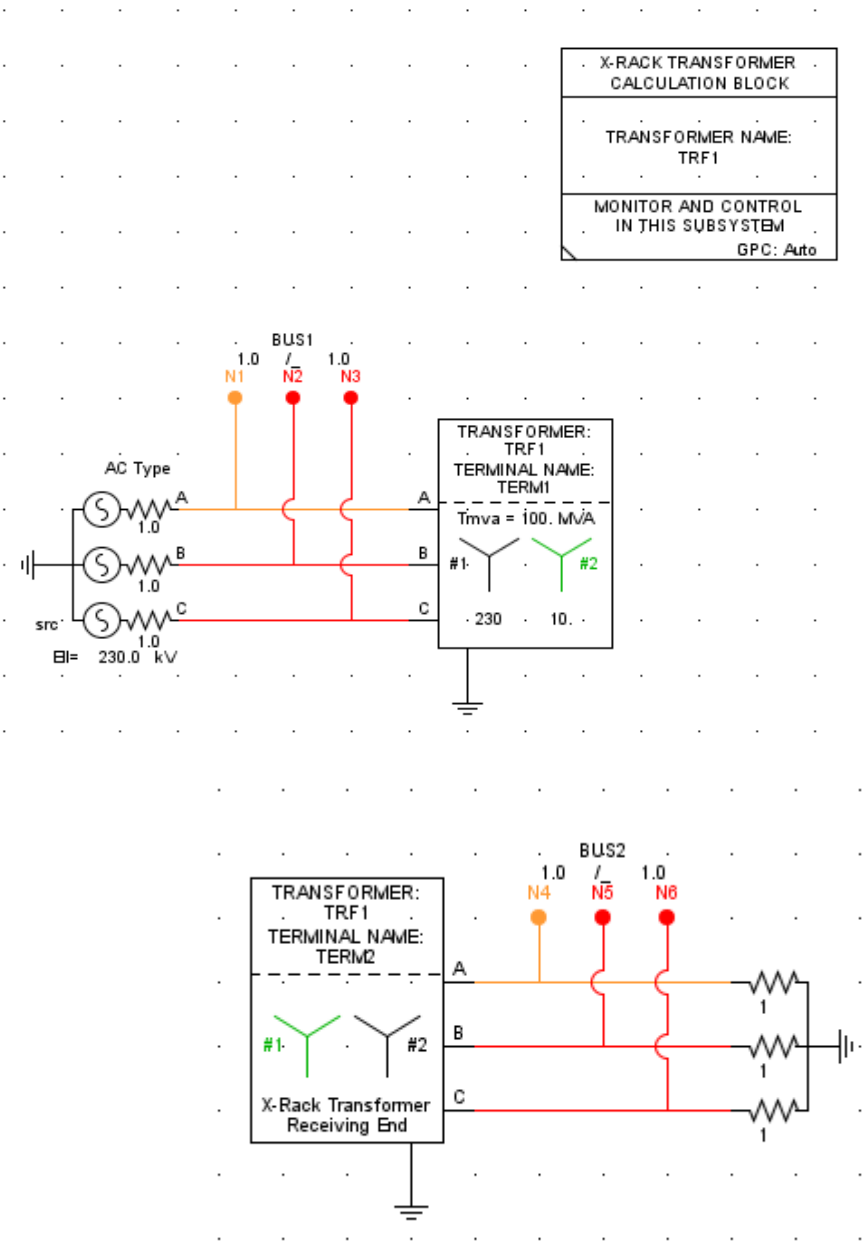

One of the features inherent in the x-rack transformer model is its ability to mathematically split the overall power system into so-called subsystems. The RTDS computes conditions in each subsystem using nodal analysis and hence a system conductance matrix is used. Splitting the overall system into subsystems keeps the conductance matrices within manageable dimensions. The mathematical splitting of the conductance matrix into subsystems using either travelling wave line and x-rack transformer models is therefore an important element in providing the real-time performance of the RTDS. When larger and larger power systems are to be studied, the simulation must be spread over many RTDS hardware racks. The nature of the RTDS hardware design is such that it conveniently mimics the layout of real power systems. The x-rack transformer or travelling wave line is one of the principle elements used to span between racks on the RTDS. Separate subsystems can be thought of as separate stations scattered around the power system with interconnection between stations (or racks) over x-rack transformer or transmission lines. In this way the mathematical solution within one subsystem (rack) can be performed independently from the conditions which exist in neighboring racks during the current time step. Please refer to reference [71] and [83] for more details on the concept of subsystems.

Appendix D - Modified IEEE 9-Bus System

Below is the characteristic of the modified IEEE 9-bus test system.

System characteristic	Value
Number of buses	9
Number of DGs	3
Number of loads	4
Number of transmission lines	8
Total generation	9.0 MW / 0.379 MVAr
Total load	9.0 MW / 0 MVAr

The IEEE standard type ST1 model is used for the steam turbine unit.

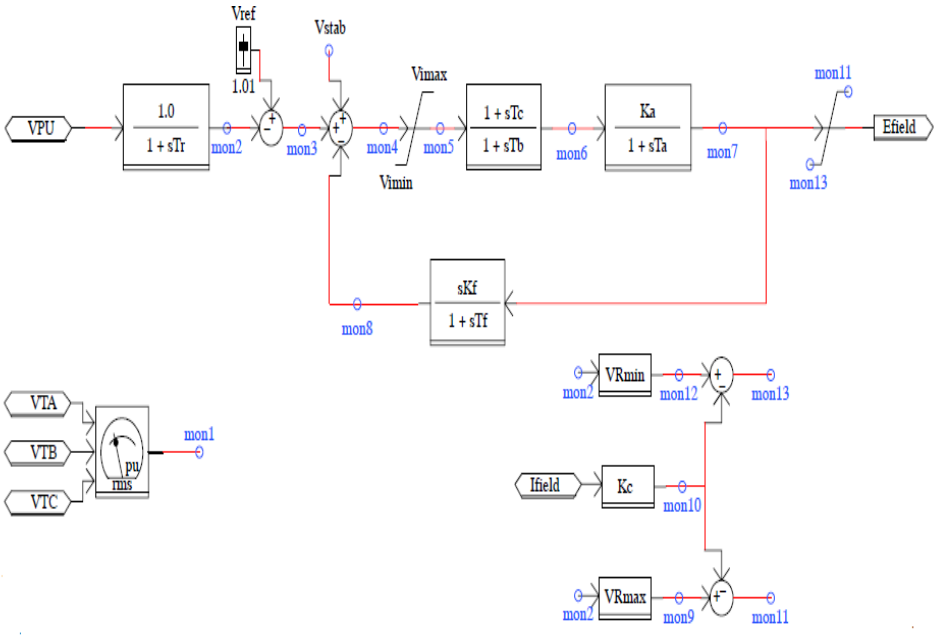

The IEEE standard type IEEEG1 governor model is applied in the speed governing system.

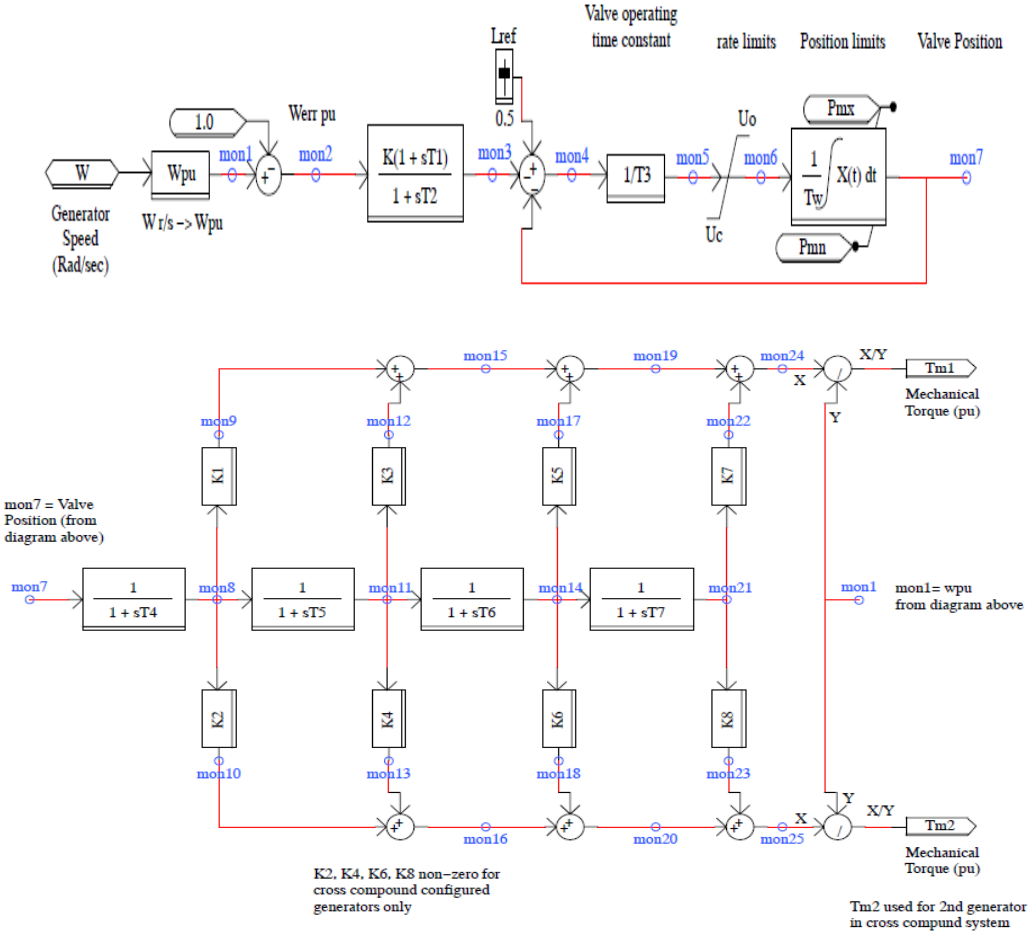

Parameter	Value	Parameter	Value
K	20	K2	0
T1	0.001	T5	5
T2	0.001	K3	0.7
T3	0.25	K4	0
U0	0.1	T6	0
Uc	-0.2	K5	0
Pmx	1	K6	0
Pmn	0	T7	0
T4	0.2	K7	0
K1	0.3	K8	0

The parameters used for the DG#1-3 and associated controls are listed in the following tables.

D/A CHANNEL ASSIGNMENTS (Continued): MAC
ENABLE D/A OUTPUT (MAX = 12 SIGNALS): MAC | D/A CHANNEL ASSIGNMENTS: MAC
SIGNAL MONITORING IN RT AND CC: MAC
MACHINE ZERO SEQUENCE IMPEDANCES | OUTPUT OPTIONS
MACHINE ELECT DATA: GENERATOR FORMAT
MECHANICAL DATA AND CONFIGURATION | MACHINE INITIAL LOAD FLOW DATA
GENERAL MODEL CONFIGURATION | PROCESSOR ASSIGNMENT

Name	Description	Value	Unit	Min	Max
Xa	Stator Leakage Reactance	0.100000	p.u.	0.01	
Xd	D-axis: Unsaturated Reactance	1.500000	p.u.	0.1	
Xd'	D: Unsaturated Transient Reactance	0.256000	p.u.	0.05	
Xd"	D: Unsaturated Sub-Trans. Reactance	0.168	p.u.	0.02	
Gfld	D: Real Component of Transfer Admit.	100.0	p.u.	0.0	100.0
Bfld	D: Imag Component of Transfer Admit.	100.0	p.u.	0.0	100.0
Xq	Q-axis Unsaturated Reactance	0.750000	p.u.	0.1	
Xq'	Q: Unsaturated Transient Reactance	0.176000	p.u.	0.05	1.0e6
Xq"	Q: Unsaturated Sub-Trans. Reactance	0.184	p.u.	0.02	
Ra	Stator Resistance	0.050400	p.u.	0.00125	
Tdo'	D: Unsat. Transient Open T Const.	3.105469	sec	0.001	
Tdo"	D: Unsat. Sub-Trans. Open T Const.	0.045714	sec	0.001	
Tqo'	Q: Unsat. Transient Open T Const.	0.122280	sec	0.001	4.0
Tqo"	Q: Unsat. Sub-Trans. Open T Const.	0.122283	sec	0.001	

rtds_sharc_ctl_EXST1

Parameters

Name	Description	Value	Unit	Min	Max
Gen	Generator Name	GEN1			
Mon	Monitor Internal Variable	No			
PSS	Include Stabalizer Input?	Yes			
Vbs	Bus Voltage Input source	Vpu			
Vb	Rated RMS Phase Voltage	6.350852961	kV	0.001	
Vi	Initial Terminal Voltage	-1	pu		
Tr	Time Constant Tr	0.000000	sec	0.0	
Vimx	Upper Limit VImax	1.000000	pu		
Vimn	Lower Limit VImin	-1.000000	pu		
Tc	Time Constant Tc	1.000000	sec	0.0	
Tb	Time Constant Tb	20.000000	sec	0.0	
Ka	Gain Ka	200.00000			
Ta	Time Constant Ta	0.020000	sec	0.0	
Vrmx	Upper Limit VRmax	5.700000	pu		
Vrmn	Lower Limit VRmin	-4.900000	pu		
Kc	Constant Kc	0.175000			
Kf	Feedback Gain Kf	0.000000			
Tf	Feedback Time Constant Tf1	1.000000	sec	0.0	
prtyp	Solve Model on card type:	GPC/PB5		0	1
Proc	Assigned Controls Processor	2		1	36
Pri	Priority Level	18		1	

rtds_sharc_ctl_IEEEG1

CONFIGURATION | DATA

Name	Description	Value	Unit	Min	Max
K	Constant K	20.000000			
T1	Time Constant T1	0.001	sec	0.001	
T2	Time Constant T2	0.001	sec	0.001	
T3	Time Constant T3	0.250000	sec	0.001	
Uo	Upper Rate Limit	0.100000	pu/sec		
Uc	Lower Rate Limit	-0.200000	pu/sec		
Pmx	Upper Limit Pmax	1.00	pu		
Pmn	Lower Limit Pmin	0.0000	pu		
T4	Time Constant T4	0.200000	sec		
K1	Constant K1	0.300000			
K2	Constant K2	0.000000			
T5	Time Constant T5	5.000000	sec		
K3	Constant K3	0.700000			
K4	Constant K4	0.000000			
T6	Time Constant T6	0.000000	sec		
K5	Constant K5	0.000000			
K6	Constant K6	0.000000			
T7	Time Constant T7	0.000000	sec		
K7	Constant K7	0.000000			
K8	Constant K8	0.000000			

Appendix E - PSO Algorithm

The PSO algorithm in the system is given following.

```
package pso;

//df(p1,p2,p3) = ()

// x = dP
// y = dq
// results = df
//
//The PSO problem is this case is
//to find an x and a y that minimize the function below:
//f(x, y) = (2.8125 - x + x * y^4)^2 + (2.25 - x + x * y^2)^2 + (1.5 - x +
x*y)^2
//where 1 <= x <= 4, and -1 <= y <= 1
// The PSO problem set for LFC is as follows:

//delta f = R_eq (P_sys- P_ref )
//delta f = R_eq *(P_sys- (Lref_G1*P_rated* CF_G1 + Lref_G2*P_rated*CF_G2 +
Lref_G3* P_rated*CF_G3))

//where
// Lref_G1 = ((P_sys-P_basetotal)*PF_G1 + Pbase_G1+(1/R1)*(f-fo))/(Srated);
// Lref_G2 = ((P_sys-P_basetotal)*PF_G2 + (1/R2)*(f-fo))/(Srated);
// Lref_G3 = ((P_sys-P_basetotal)*PF_G3 + Pbase_G1+(1/R3)*(f-fo))/(Srated);

// transforming to the typical PSO formulation of x, y and result

// let, x =  Lref_G2 and y = CF_G2 and result = delta f, -->

// result = R_eq (P_sys- P_ref )
// result = R_eq *(P_sys- ( (Lref_G1*P_rated * CF_G1) + (x*P_rated*y) +
(Lref_G3* P_rated*CF_G3)))


public class ProblemSet {
            public static final double LOC_X_LOW = 1;
            public static final double LOC_X_HIGH = 4;
            public static final double LOC_Y_LOW = -1;
            public static final double LOC_Y_HIGH = 1;
            public static final double VEL_LOW = -1;
            public static final double VEL_HIGH = 1;

            public static final double ERR_TOLERANCE = 1E-20; // the smaller
the tolerance, the more accurate the result,
                                                              // but the num-
ber of iteration is increased
```

```
            public static double evaluate(Location location) {

                        double R_eq = 0.1716;
                        double P_sys = 6;
                        double Lref_G1 = 0.3169;
                        double P_rated = 4.855;
                        double CF_G1 = 1;
                        double CF_G3 = 1;
                        double Lref_G3 = 0.3169;
                        double result = 0;
                        double x = location.getLoc()[0]; // the "x" part of
the location
                        double y = location.getLoc()[1]; // the "y" part of
the location

                        double pdg1=1.5;
                        double pdg2=1.5;
                        double pdg3=1.5;

                        double mdg1=4.85;
                        double mdg2=4.85;
                        double mdg3=4.85;


                        /*
                         pdg1=pdg2=pdg3=1.5;
                         mdg1=mdg2=mdg3=4.85;

                          */

                        double cdg1 = 1;
                        double cdg2 = 1;
                        double cdg3 = 1;

                        cdg1 = 1/(mdg1-cdg1);
                        cdg2 = 1/(mdg2-cdg2);
                        cdg3 = 1/(mdg3-cdg3);


                        /*
                         we assume min Î”T--> f(Î”Pi, Cost(dgi))

                         i.e., the optimization function minimizes the time
Î”T is takes to recover
                         the frequency devitation. deltaT is a function of
deltaP i.e., the active power
                         set point for each DG and costDGi i.e., the cost
factor for each DGi to
                         produce the the delta deltaPi.

                        for the calculation of optimization function we sup-
pose that:
                        results = Î”T
                        x = Î£ Î”Pi    (i=1,2,3...)
                        y = Î£ Cost(dgi)    (i=1,2,3...)
```

```
                        where Î”Pi = R_eq*(P_sys- ( (Lref_G1*P_rated * CF_G1)
+ (x*P_rated*y) + (Lref_G3* P_rated*CF_G3)));
                         */


                        result = R_eq*(P_sys- ( (Lref_G1*P_rated * CF_G1) +
(x*P_rated*y) + (Lref_G3* P_rated*CF_G3)))*(cdg1+cdg2+cdg3);




                        return result;
            }
}
```

www.elektro.dtu.dk/cee

Department of Electrical Engineering
Centre for Electric Power and Energy (CEE)
Technical University of Denmark
Elektrovej 325
DK-2800 Kgs. Lyngby
Denmark
Tel: (+45) 45 25 35 00
Fax: (+45) 45 88 61 11
E-mail: cet@elektro.dtu.dk

"ISBN 978-87-924658-66-5"